ANALYSIS AND DESIGN OF PAVEMENTS FOR HEAVY VEHICLES

Ph.D. THESIS

by

SANJAY SRIVASTAVA

DEPARTMENT OF CIVIL ENGINEERING
INDIAN INSTITUTE OF TECHNOLOGY ROORKEE
ROORKEE-247667 (INDIA)
JUNE, 2015

ANALYSIS AND DESIGN OF PAVEMENTS FOR HEAVY VEHICLES

A THESIS

Submitted in partial fulfilment of the
Requirements for the award of the degree
of

DOCTOR OF PHILOSOPHY

in

CIVIL ENGINEERING

by

SANJAY SRIVASTAVA

DEPARTMENT OF CIVIL ENGINEERING
INDIAN INSTITUTE OF TECHNOLOGY ROORKEE
ROORKEE-247667 (INDIA)
JUNE, 2015

INDIAN INSTITUTE OF TECHNOLOGY ROORKEE
ROORKEE

CANDIDATE'S DECLARATION

I hereby certify that the work which is being presented in the thesis entitled "**ANALYSIS AND DESIGN OF PAVEMENTS FOR HEAVY VEHICLES"** in partial fulfilment of the requirements for the award of the Degree of Doctor of Philosophy and submitted in the Department of Civil Engineering of the Indian Institute of Technology Roorkee, is an authentic record of my own work carried out during a period from August, 2008 to June, 2015 under the supervision of Dr. S.S. Jain, Professor, Transportation Engineering Group, Department of Civil Engineering, Indian Institute of Technology Roorkee and Dr. M.P.S. Chauhan, Associate Professor, Department of Civil Engineering, G.B. Pant Engineering College, Pauri Garwal, Pauri.

The matter presented in this thesis has not been submitted by me for the award of any other degree of this or any other Institute.

(SANJAY SRIVASTAVA)

This is to certify that the above statement made by the candidate is correct to the best of our knowledge.

(M.P.S. CHAUHAN)
Supervisor

(S.S. JAIN)
Supervisor

The Ph. D. Viva-Voce Examination of Sanjay Srivastava, Research Scholar has been held on.....

Chairman, SRC **Signature of External Examiner**

This is to certify that the student has made all the corrections in the thesis.

Signature of Supervisor (s) **Head of Department**

Dated:

ABSTRACT

The transportation by roads is most preferred mode of transportation by the people and industries due to maximum flexibility in speed of travel, direction, route and time. India, having roads network of over 4.2 million km of roads, is at second position after the U.S.A. in the world. To achieve higher economic growth there is need of efficient roads infrastructure. India having only 2% length of national highways of the total roads network carrying about 40% traffic. Because of lack of roads infrastructure, the goods and people do not reach the destination in time. To reach the destination in time is possible through efficient roads infrastructure network.

Realizing the need for efficient road infrastructure networks, the Govt. of India has launched most ambitious National Highway Development Plan (NHDP). NHDP consist of major projects like Golden Quadrilateral (GQ) (6000 km, phase-I), North-South and East-West Corridors (7300 km, phase-II), High Density Corridors of NH to give connection to ports and State capitals, (10,000 km, phase-III), All remaining NH to be made 2 lanes (Phase-IV), Expressways (1000 km, Phase-V), widening of G.Q roads project from 4 lane to 6 lane (Phase-VI), constructing by passes and bridges up to 2012 (Phase-VII). Therefore, it is quite clear from above discussion that we still need of large length of roads network.

Generally pavements are of two types on the basis of structural behavior. These are flexible pavements and rigid pavements. Construction of pavements cost about approximately 50% of the project cost. Therefore, careful right choice of pavement is necessary on some national basis. This will result in saving of enormous amount of money. From the recent studies by various researchers, it has been proved that rigid pavements are economical to flexible pavement. The initial construction cost of cement concrete roads are higher by 10 to 20% over flexible pavements but life cycle cost of cement concrete are lower than for the flexible pavements. Realizing the advantages of rigid pavements like smooth riding, saving in fuel, longer design life and less maintenance compared to flexible pavements etc., many developed countries have already constructed long stretches of concrete roads. Seeing the advantages of concrete pavements, about 30% length of new pavements of Golden

Quadrilateral under NHDP has been constructed with concrete pavements and about 15% in NSEW corridors. Delhi – Matura road, Mumbai Pune expressway, Indore bypass and Yamuna expressways have been constructed with cement concrete. Generally, in construction of all rigid pavements, the concrete of grades M30 or M40 have been used on a sub base of dry lean concrete. The pavements thickness range from 30 to 35 cm or oven more. With the invention of plasticizer and super plasticizer, the concretes of much higher strength are being developed. According to IS:456, the concrete strength equal to or greater than 60 MPa are known as high strength concrete. The interest in using high strength high performance concrete is continuously increasing. It is being used in the areas of buildings and bridges most frequently. Generally, HSHPC is being used for patch repair and damaged sections of rigid pavements. In India, HSHPC has not been used as full depth of pavements.

According to Henry Russel, ACI defines high performance concrete as concrete that meets special performance and uniformity requirements that cannot always be achieved routinely by using only conventional materials and normal mixing, placing and curing practices. The requirements may involve enhancement of placement and compaction without segregation, long term mechanical properties, early age strength, toughness, volume stability or service life in severe environments.

India comes under developing nation. Being developing nation, many infrastructure projects are under implementation and more infrastructure projects to be implemented in future. These infrastructure projects require the movement of people and goods from one place to another place as early as possible. Because of these infrastructure projects, to reach the goods and people to their destination with safety and economically, there is continuously growing number of heavy vehicles and also the size and weight of heavy vehicles. These heavy vehicles cause consumption of fatigue life of normal pavements and lead to early rehabilitation.

A heavy vehicle is a vehicle that has a gross vehicle mass (GVM) or aggregate trailer mass (ATM) of more than 45 kN and a combination that includes a vehicle with a GVM or ATM of more than 45 kN, as per Heavy Vehicle National law of Australia. As per Societe de i' Assurance Automobile du Quebec (SAAQ), Canada, any road vehicle or combination of road vehicles with a gross vehicle weight rating (GVWR) of 45 kN or more is considered a

heavy vehicles. The GVWR of vehicle include its maximum load capacity and net mass of vehicle as per manufacturer specifications.

GVWR = Net Mass of Vehicle + Maximum Load Capacity

By using HSHPC, it will not only reduce the design thickness of pavements compared to normal strength concrete but could also design the pavements for longer design period due to higher durability and impermeability. This will result in lower life cycle cost compared to flexible pavements. Today's need is concrete pavements of longer design life more than 40 years and should be durable. All the above goals could be achieved by using HSHPC in concrete pavements. The cost of HSHPC per m^3 is higher than the normal strength concrete. But due to thinning of the pavements and longer design life will offset the increase in cost. During the investigations, HSHPC of grade M60 with fly ash has been used.

Due to much higher load carrying capacity and high durability of HSHPC, the HSHPC pavement could be recommended for heavy duty pavement and longer design period. The flexural strength and fatigue properties of HSHPC are quite high, which are essential parameters from the point of pavement performance. Therefore, it is essential to examine the structural behavior of high strength high performance concrete pavement. Also the load at first crack, crack patterns, formation of cracks, crack propagation and crack width and ultimate load carrying capacity of HSHPC pavements under varying loads and loading positions needs to be studied. Therefore, the present experimental study on high strength high performance concrete (HSHPC) pavement has been carried out with the objective whether the existing theoretical methods of analysis could be used or there is need to develop a suitable design approach for the analysis of stresses and deflections in HSHPC pavements.

The local materials, which were used in development of mix design, were tested. Fine aggregate having F.M. 2.89, coarse aggregate having F.M. 6.7, 11% fly ash having fineness 3500 cm^2/gm and specific gravity 2.24, by weight of cement and 1.6% super plasticizer Sikament-N (modified naphthalene formaldehyde sulphonate) by weight of cement were used in development of design mix of grade M60 on trial basis.

Then the design mix of grade M60 was developed using fly ash on trial basis. Finally the design mix ratio came out as 1:1.1:1.9 (cement: F.A.: CA). The water cement ratio was 0.29. To assess suitability of HSHPC mixes for laying highway pavements, different tests were

carried out. For this purpose, cubes of dimensions 150 mm were prepared for finding out compressive strength, 150 mm diameter and 300 mm height cylindrical specimens for determination of modulus of elasticity and beams of dimensions 100 mm x 100 mm x 500 mm were prepared for determining flexural strength. All these specimens were prepared as per Indian Standard Code of practice and tested according to IS: 516 – 1959.

7 days and 28 days compressive strength were found to be 46.14 MPa and 70.4 MPa respectively. 7 days and 28 days flexural strength were found to be 4.82 and 6.4 MPa. Modulus of elasticity was found to be 41.7 GPa and slump was found to be 31.67 mm. Poisson's ratio 0.2 was used in the analysis for finding out stresses, strains and deflections.

The subgrade was prepared according to IRC: 15. The soil was compacted at optimum moisture content and dry density. Roorkee soil was classified as A-3 as per U.S.P.R.A. The optimum moisture content was found to be 11% and dry density was found to be 1.92 gm/cm^3. The modulus of subgrade reaction was found to be 0.0463 N/mm^3 (4.63kg/cm^3) and four days soaked CBR value of Roorkee soil was found to be 6%. The poisons ratio and modulus of elasticity of Roorkee soil had been taken for the analysis as 0.305 and 20.96 MPa respectively.

By using high strength high performance concrete mix developed in the lab of grade M60 having fly ash 11% and super plasticizer 1.6%, three concrete pavements of size 1800 mm x 1800 mm had been cast with varying thicknesses viz. 160 mm, 200 mm and 240 mm. All the pavements with different thicknesses were cast directly over the compacted subgrade having modulus of subgrade reaction 0.0463 N/mm^3 (4.63kg/cm^3).

To measure the deflections of pavement surface due to loading, mechanical dial gauges with least count 0.01 mm were used. Studs have been fixed with araldite on the surface of the pavement to measure the surface strain with Huggenberger mechanical deformometer.

The loading arrangement for applying a static load to the pavement consisted of a 250 kN capacity reaction frame fabricated with steel portal frame and steel girders. The reaction loading frame was mobile for carrying out the plate load test at any position along or across the test pit 2000 mm x 8000 mm in size. The testing was done in test hall of transportation engineering group. All concrete pavements slab were tested for corner, edge and central loading positions.

Wheel load stresses were calculated by Westergaard, Mayerhof's, Ghosh's and IRC-58 methods. For different thicknesses 160 mm, 200 mm and 240 mm pavements of dimensions 1800 mm x 1800 mm. the stresses, strains and deflections were also calculated by analytical technique i.e. Finite Element Method. Stresses calculated through different theories had been compared with the experimentally observed values and stresses obtained through analytical method i.e. FEM. It has been found that stresses obtained through existing theories and through analytical method i.e. FEM are in good agreement with the observed values and can be used successfully in designing of HSHPC pavements. The strains and deflections obtained through FEM are in good agreement with the observed values. Mayerhof's method can be used in designing of HSHPC pavements with factor of safety 2 to 3.

The load carrying capacities of HSHPC pavements at each position are sufficiently high at flexural strength when pavement was laid on compacted subgrade having modulus of subgrade reaction 4.63 kg/cm^3. With the increase in thickness, the load carrying capacity at each position increase. 200 mm thick pavement carry sufficiently high load of the order 230 kN at each positions.

The existing IRC-37 code could be used for design of flexible pavements for heavy vehicles. But design period should be reduced to corresponding to150 msa.

Economic analysis has been carried out and found that life cycle cost analyses of HSHPC pavements are lower than the flexible pavements.

From the above discussion, it is quite clear that the existing methods for designing of rigid pavements and analytical method i.e. FEM can be used in designing of thickness of HSHPC pavements. By using HSHPC, the thinner pavement can be designed for the same traffic. Thus there is lots of saving of natural aggregate that will result in less quarrying putting least impact on environment. Hoped that the methodology for the design of HSHPC Pavements and flexible pavements for heavy vehicles will cater the need of pavements where heavy vehicle movements is high, in industrial as well as for construction sites of irrigation structures like dams, power houses etc. and other sites too.

ACKNOWLEDGEMENT

I wish to express my most sincere gratitude to Dr. S. S. Jain, Professor, Department of Civil Engineering, Indian Institute of Technology Roorkee, for his guidance, valuable suggestions and all kind of support during the course of this study. His methodical approach provided overall direction to the research, steering the study to its logical conclusion. His tendering eased out the pressure while his critical observations significantly enhanced the overall quality of my work. I am grateful to him that in spite of his enormously busy calendar, he was always available for detailed discussions and guidance.

I am extremely grateful to Dr. M.P.S. Chauhan, Associate Professor, Department of Civil Engineering, G.B. Pant Engineering College, Pauri Garhwal,, for his overwhelming support, frank discussions and constant motivation throughout this research. I thank him from the bottom of my heart for sparing his valuable time in thoroughly reading the manuscript in spite of his extremely busy schedule.

I thank Prof. Pradipta Banerjee, Director, Indian Institute of Technology Rookee for all the institutional support during the course of this study. I also sincerely acknowledge the kind support of Prof. Vinod Kumar, Deputy Director of the Institute. I express my heartfelt thanks and gratitude to Prof. Deepak Kashyap, former Head, Department of Civil Engineering, IIT Roorkee. I thank Prof. Surendra Kumar, former Dean, Academic Research, for all the support. I am grateful to Prof. Pramod Agarwal, Dean, Academic Research, for all the support in completion of the Thesis work. I also wish to thank Dr. Ajay Kumar Sharma, Deputy Registrar (Academic Research), Ms. Sheeba Ramola, Assistant Registrar (Academic Research), and other staff of the Academic Research section for their support from time to time. I would also like to thank Prof. Satish Chandra and Prof. P. Bhargav, Chairman DRC, and Dr. Rajat Rastogi, Chairman SRC for their critical evaluation and advice on the progress of thesis. I thank Dr. S.R. Karade and Prof. Praveen Kumar for their valuable suggestions and feedback as member of SRC.

I would like to express my sincere thanks to Dr. M. Parida, Professor, Department of Civil Engineering, IIT, Roorkee, for all the enlightening discussions at various stages of my research work and for the motivations he instilled to give my full best for this research. His

all-time moral support made my research life smooth and rewarding. I pay my humble gratitude to Dr. Umesh Kumar Sharma, Dr. Anupam Chakraborty and Dr. Ashraf Iqbal for their encouraging words and support. Especial thanks are due to Er. Bibekanand Mandal, Research scholar, who helped me in carrying out Finite Element Analysis (FEM) using software, ABAQUS.

I am deeply obliged to Er. N.C. Sharma, Formerly Chief Engineer, I.R.I. and I.D.O. Roorkee and Er. A.K. Dinkar, Chief Engineer, Irrigation Department, Uttarakhand for all the organizational support during the course of this study. I also express my sincere gratitude to Er. K.N. Gupta, Formerly Superintending Engineer, Er. N.K. Sharma, Er. R.K. Gupta, Er. R. Chalisgaonkar and Dr. Subhash Mitra, Superintending Engineer, Irrigation Department, Uttarakhand for their moral support and encouragement. I also express my sincere thanks to Irrigation Department colleagues, Executive Engineers Er. Ajay Sharma, Er. V.K. Pandey, Er. P.K. Mall, Er. Kapil Kumar,Er. Rakesh Tiwari, Er. Subhash Pandey and Er. Sankar Kumar Saha for their kind moral support during the research work.

I would like to record my gratitude for Dr. L.R. Kadiyali, Chief Executive, Dr. L.R. Kadiyali and Associates, New Delhi. His research work was extremely inspirational. I also wish to thank all the researchers in the field of Highway and Pavement Engineering whose work enlightened me in carrying out this study. I acknowledge the contributions by Dr. R.M. Vasan, Dr. P. N. Kachroo , Dr. B. Prasad, Dr. A. Veeraragavan and Dr. Devesh Tiwari for useful research on Highway and Pavement Engineering.

I am thankful to Prof. S.P. Singh, Dr. B.R. Ambedkar, National Institute of Technology, Jalandhar, India and Prof. R.K. Dhir, Emeritus Professor, University of Dundee for interactive discussion during the proceedings of the international UKIERI Concrete Congress at Jalandhar in India. The guidance and direction of work derived from the published research work of Prof. T.F. Fwa, Prof. K.P. George, Prof. Waheed Uddin, and Prof. Arun Kumar in the field of Highway and Pavement Engineering is acknowledged.

I am thankful to my friends and colleagues at IIT Roorkee who have supported me in several ways during the research period. Thanks are due to Dr. Ankit Gupta, Dr. Kunal Jain, Dr. Yogesh Shah, Er. Bhupesh Jain, Er. Naveen, Er. (Ms.) Preetikana, Er. Ankit Kathuriya, Er. Vivek Singhal, Er. Shivani Sharma and Er. Amita Johar for providing motivation and

support. Thanks are also due to Shri Ram Kumar, Shri Sewa Ram, Shri Sanjay, Shri Surendar, Shri Anjesh, Shri Sonu, Shri Rajpal and others from the Department of Civil Engineering who have supported me during the course of this study. I convey my sincere thanks to Mr. Pradeep Singh, Laboratory Incharge of Transportation Engineering group and their staff and Sri Surendra Kumar Sharma, Incharge of Concrete Lab in Structural Engineering Group and their staff. I would like to thank Sri Yashpal for his assistance in the typing work and Sri Naveen Kumar for assistance in drawings. I would like to thank Sri Rakesh, Sri Randep Rana, and Sri Bhopal Singh who helped me in carrying out research work. I deeply thank Mr. Yogendra Singh, Librarian, Institute Central Library and Departmental Library for providing me the accessibility to its huge knowledge resource. I am grateful to the staff of the Department of Civil Engineering, Indian Institute of Technology Roorkee, Roorkee for all the administrative facilities and support.

My deepest gratitude goes to my family for their unflagging love, support and their belief in me in all my endeavors throughout my life. No words and no language are ever adequate to express my heartfelt admiration for my respected parents. I thank my father (Late) Dr. Harish Chandra and my mother Smt. Sarojini Devi for their invaluable constant motivation and care. Heartfelt thanks are also due to my father-in-law Shri Mukund Murari and mother-in-law Smt. Mohini Murari. I thank by heart to my sisters Dr. Anju Srivastava and Dr. Indu Srivastava for their moral support and inspiration. Special thanks are due to my brother-in-law Er. Harish Kumar Srivastava for his motivation and spiritual support. Thanks by heart to my elder brothers, brother in-laws and sister in-laws for being supportive and caring. I have no words to express my deep thanks with warm feelings to my nieces Nancy, Suchi, Mahima, Ruchika, Dakshyani, Padakshi, Shruti and Deepti for their continuous love, care and patience.

I would like to appreciate my wife Dr. Swati Murari and my lovely children Ishita and Prakhar for their love and persistent confidence in me, has made my Ph.D. comfortable. They always provided me a friendly, co-operative and encouraging environment after the study hours which became a major driving force behind me to achieve my destination.

Finally, I would like to thank everybody who was important to the successful realization of thesis. And to the rest, I am extremely thankful to those people, whose names have been unintentionally left.

Finally, I would love to dedicate my research work in the memory of my most revered father.

Even with all the available worldly advantages, fulfilment of this research work is due to the grace of Almighty and to Him, I offer my prayers. I acknowledge His presence in my life and Thank Him for everything with which I am blessed with.

(SANJAY SRIVASTAVA)

CONTENTS

LIST OF TABLES

LIST OF FIGURES

LIST OF PHOTOGRAPHS

ABBREVIATIONS

ACI	American Concrete Institute
FHWA	Federal Highway Administration
IRC	Indian Road Congress
NHDP	National Highway Development Programme
GQ	Golden Quadrilateral
NSEW	North South East West
HSHPC	High Strength High Performance Concrete
HPC	High Performance Concrete
GGBFS	Ground Granulated Blast Furnance Slag
w/b ratio	Water / Binder Ratio
w/c ratio	Water / Cement Ratio
FA /SF	Fly Ash / Silica Fume
SCC	Self – Compacting Concrete
CSF	Condensed Silica Fume
PLT	Plate Load Test
CBR	California Bearing Ratio
K	Modulus of Subgrade Reaction
SPT	Standard Penetration Test
LMC	Latex Modified Concrete
NH	National Highway
AASHTO	American Association of State Highway And Transportation Officials
ODRs	Other District Roads
VRs	Village Roads
GVM	Gross Vehicle Mass
ATM	Aggregate Trailer Mass
SAAQ	Societe De I' Assurance Automobile Du Quebec
GVWR	Gross Vehicle Weight Rating

CVPD	Commercial Vehicle Per Day
GSY	Google Search Year
FEM	Finite Element Method
SWA	Saturated Water Absorption
AAR	Alkali Aggregate Reaction
OPC	Ordinary Portland Cement
RCPT	Rapid Chloride Permeability Test
HVFA	High Volume Fly Ash
OMC	Optimum Moisture Content
Fig.	Figure
ESALs	Equivalent Standard Axle Loads
BC	Bituminous Concrete
SDBC	Semi-Dense Bituminous Concrete
DBM	Dense Bituminous Macadam
WMM	Wet Mix Macadam
GSB	Granular Sub-base
E	Modulus of Elasticity
μ	Poisson's Ratio
SR	Stress Ratio
FM	Fineness Modulus
LS	Lum-Sum
L	Litre

CHAPTER – 1

INTRODUCTION

1.1 GENERAL

American President, John F. Kennedy, has said that "It is not our wealth that built roads but roads that built our wealth".

The major modes of transportation are roadways and highways. The transportation by road is the most preferred mode of transport by the people due to maximum flexibility. With the vast roads network approximately 4.2 million km of roads as per MORTH, the India is at second place in the world after the U.S.A. The U.S.A having roads network of approximately 6.3 million Km. of roads. In the next twenty year, to have economy growth plan over 6%, it is essential to have efficient roads infrastructure. To meet the economic growth, large numbers of infrastructure projects are under implementation and more mega infrastructure projects to be implemented in future. Fast movement of goods and people with safety and economical cost is possible through efficient roads infrastructure. National highways are about 2% of the total roads network in country. This barely 2% national highway carry about 40% traffic. Realizing the need for efficient road infrastructure networks, the Govt. of India has launched most ambitious National Highway Development Plan (NHDP). NHDP consist of major projects like Golden Quadrilateral (GQ) (6000 km, phase-I), North-South and East-West Corridors (7300 km, phase-II), High Density Corridors of NH to give connection to ports and State capitals, (10,000 km, phase-III), All remaining NH to be made 2 lanes (Phase-IV), Expressways (1000 km, Phase-V), widening of G.Q roads project from 4 lane to 6 lane (Phase-VI), constructing by passes and bridges up to 2012 (Phase-VII).

From the above, it is quite clear that large length of roads network is still to be constructed. From the recent studies, it has been proved that rigid pavements are more economical than flexible pavements. Since, approximately more than 50% of highway project cost is being spent on pavements, therefore it is essential that a right choice of the pavement is

necessary on some rational basis. Right choice of pavement will result in economy of project that will result in saving of enormous amount of money in the interest of Nation [129].

1.2 TYPES OF PAVEMENTS

Broadly, based on structural behaviour, pavements are of two types:

(i) Flexible Pavements and

(ii) Rigid Pavements.

Being low in initial construction cost and feasibility of stage construction, flexible pavements have been preferred choice for the Engineers. Due to non-availability of cement and high initial construction cost, the rigid pavements were not preferred earlier. But now, with the availability of cement in plenty and rising prices of bitumen in international market, as the most of bitumen approximately 70% are being imported from the other countries, it would be wise decision to construct the cement concrete pavements. Recognizing the superiority of rigid pavements over flexible pavements, many developed countries have already constructed long stretches of concrete roads to meet the increasing passenger and freight traffic demand [133].

The initial construction cost of cement concrete road is more by about 10 to 20% over flexible pavement, but the life cycle cost of cement concrete road is low as compared to the flexible pavement.

Seeing the advantages of concrete pavements over flexible pavements and low life cycle cost, about 30% length of new pavements of Golden Quadrilateral under NHDP has been constructed with concrete pavements and about 15% in NSEW corridors.

Besides life cycle cost considerations, at some locations, due to climate / environmental conditions, the rigid pavement will have to be the preferred choice. Such locations are area of heavy rainfall, water logged area and subgrade with low CBR etc.

Cement concrete roads have made a come-back in India after a gap of many years. Delhi-Mathura road, the Mumbai-Pune Expressway and Indore Bypass have been constructed with cement concrete. With the construction of these projects and realizing the advantages of

cement concrete roads, we are mentally ready to adopt the rigid pavements. By now, approximately in all rigid pavement projects, the concrete grades of M30 or M40 have been used on a sub-base of dry-lean concrete. The design pavements thicknesses range from 30 to 35 cm and even more. With the invention of plasticizer and super plasticizer, it has now been possible to produce the concrete of much higher strength. Today, concrete of more than 100 MPa designed strength are being used in bridges construction. The interest in HSHPC has grown over the last decades of the 20th century. HSHPC concrete is being frequently used in high rise buildings and bridges deck. High strength high performance concrete (HSHPC) could also be used in highway rigid pavements. By the use of HSHPC, it will not only reduce the design thickness of pavements but could also design the pavements for longer design period due to higher durability and impermeability. Which will result in lower life cycle cost and economical compared to flexible pavements. In present investigations the HSHPC of grade M60 with fly ash has been used [147].

1.3 HEAVY VEHICLES

A heavy vehicle is a vehicle that has a gross vehicle mass (GVM) or aggregate trailer mass (ATM) of more than 45 kN and a combination that includes a vehicle with a GVM or ATM of more than 45 kN, as per Heavy Vehicle National law of Australia [184].

As per Societe de i' Assurance Automobile du Quebec (SAAQ), Canada, any road vehicle or combination of road vehicles with a gross vehicle weight rating (GVWR) of 45 kN or more is considered a heavy vehicles. The GVWR of vehicle include its maximum load capacity and net mass of vehicle as per manufacturer specifications [185].

GVWR = Net mass of Vehicle + Maximum Load Capacity

As per Notification S.O. 728 (E) dated 18th October, 1996, Ministry of Road Transport and Highways, Government of India (1996), the specifications of maximum gross vehicle weight and maximum safe axle weight are given in Table 1.1[109].

Table 1.1: Specification of Maximum Gross Vehicle Weight and Maximum Safe Axle Weight

Sl. No.	Transport vehicles category	Maximum gross vehicle weight in tonnes	Maximum safe axle weight
I. Rigid Vehicles			
(i)	Two Axle Two tyres on front axle Two tyres on rear axle	12.0	 6 tonnes on front axle 6 tonnes on rear axle
(ii)	Two Axle Two tyres on front axle, and Four tyres on rear axle	16.2	 6 tonnes on front axle 10.2 tonnes on rear axle
(iii)	Three Axle Two tyres on front axle, and Eight tyres on rear tandem axle	25.0	 6 tonnes on front axle 19 tonnes on rear tandem axle
(iv)	Four Axle Four tyres on front axle, and Eight tyres on rear tandem axle	31.0	 12 tonnes on two front axle 19 tonnes on rear tandem axle
II. Semi-Articulated Vehicles			
(i)	Two Axle Tractor 2 tyres on front axle 4 tyres on rear axle Single Axle Trailer 4 tyres on single axle	26.4	 6 tonnes on front axle 10.2 tonnes on rear axle 10.2 tonnes on single trailer axle
(ii)	Two Axle Tractor 2 tyres on front axle 4 tyres on rear axle Tandem Axle Trailer 8 tyres on tandem axle	35.2	 6 tonnes on front axle 10.2 tonnes on rear axle 19 tonnes on tandem axle
(iii)	Two Axle Tractor 2 tyres on front axle 4 tyres on rear axle Three Axle Trailer 12 tyres on 3 axle	40.2	 6 tonnes on front axle 10.2 tonnes on rear axle 24 tonnes on 3 axle

(iv)	Three Axle Tractor 2 tyres on front axle 8 tyres on tandem axle Tandem Axle Trailer 8 tyres on tandem axle	44.0	 6 tonnes on front axle 19 tonnes on rear tandem axle 19 tonnes on tandem axle
III. Truck-Trailer Combination			
(i)	Two Axle Truck 2 tyres on front axle 4 tyres on rear axle Two Axle Trailer 4 tyres on front axle 4 tyres on rear axle	36.6	 6 tonnes on front axle 10.2 tonnes on rear axle 10.2 tonnes on front axle 10.2 tonnes on rear axle
(ii)	Three Axle Truck 2 tyres on front axle 4 tyres on rear axle Three Axle Trailer 4 tyres on rear axle 8 tyres on rear tandem axle	45.4 (restricted to 44.0 tonnes)	 6 tonnes on front axle 10.2 tonnes on rear axle 10.2 tonnes on front axle 19.0 tonnes on rear tandem axle
(iii)	Three Axle Truck 2 tyres on front axle 8 tyres on rear tandem axle Three Axle Trailer 4 tyres on front axle 8 tyres on rear tandem axle	54.2 (restricted to 44.0 tonnes)	 6 tonnes on front axle 19 tonnes on rear tandem axle 10.2 tonnes on front axle 19.0 tonnes on rear tandem axle

1.4 HIGH STRENGTH HIGH PERFORMANCE CONCRETE (HSHPC)

According to P.K. Mehta, (2004) and Aitcin, high strength concrete during 1970s is now referred to as high performance concrete (HPC). [10, 103].

High performance concretes are developed for the specific requirements and applications under the prevailing environments and conditions. Some of the properties of HPC are high strength, high early strength, high modulus of elasticity, high abrasion resistance, high durability in severe environments, low permeability, resistance to chemical attack, high resistance to frost and de-icer, toughness and impact resistance, volume stability, ease of placement, compaction without segregation and inhibition of bacterial and mold growth etc..

According to Henry Russel (1999), ACI defines high performance concrete as concrete that meets special performance and uniformity requirements that cannot always be achieved routinely by using only conventional materials and normal mixing, placing and curing practices. The requirements may involve enhancement of placement and compaction without segregation, long term mechanical properties, early age strength, toughness, volume stability or service life in severe environments [140].

The strength of high performance concrete is usually higher than normal concrete. It is because of lower water-cement ratio, which is necessary for high strength, generally improving other properties also.

A major criticism presented by P.K. Mehta (2004) against the ACI definition of HPC is that durability of concrete is not mandatory. It is one of the options. It is generally assumed that high strength concrete is durable, but this may not so. There are many cases in which cracks and premature deterioration of HPC structures has taken place. Generally high strength concrete mix consist of high cement content, viz. 450-500 kg/m^3 portland or blended portland cement. It also contains a small amount of silica fume and fly ash or slag. Water/cement ratio is generally low for high strength concrete mix. When it is necessary to protect the concrete from cycles of freezing and thawing then air entraining agents is used. High strength concrete mixtures are prone to suffer early cracking from a variety of causes, such as a large thermal contraction due to high port-land cement content, a large autogeneous shrinkage due to low water-cement ratio and a high drying shrinkage due to the high cement paste aggregate ratio [104, 105, 106].

Aitcin (2003) defines HPC as a low water/binder concrete with an optimized aggregate to binder ratio to control its dimensional stability (i.e. drying shrinkage) and which receives an adequate water curing (to control autogenous shrinkage). This definition considers the durability of HPC concrete .The massive structural members may be subjected to thermal cracking. According to Mehta and Aitcin the term HPC should be applied to concrete mixtures possessing the three characteristics high workability, high strength and high durability [11, 105]. Comparison of compressive strength, flexural strength, modulus of elasticity and poisson's ratio for mix M40 and for HSHPC mix are given in Table 1.2.

Table 1.2: Comparison of Different Properties of Mix M40 and HSHPC Mix

Sl. No.	Properties	Values of M40 mix	Values of HSHPC
1	Compressive strength	55 MPa	70.4 MPa
2	Flexural strength	5.2 MPa	6.4 MPa
3	Modulus of elasticity	34 GPa	41.7 GPa
4	Poisson's ratio	0.15	0.2

1.5 APPLICATIONS AND ADVANTAGES OF HIGH STRENGTH HIGH PERFORMANCE CONCRETE IN PAVEMENTS AND BRIDGES

The performance of HSHPC is substantially higher than the normal concrete. It has been established by various researchers [25,134,146,158,159,179]. Generally, concrete pavements are designed for 20 to 25 years with low maintenance cost with normal concrete. With the understanding of the various advantages of concrete pavements, the concrete pavement has got wide acceptance all over the world. The various advantages of concrete pavements are long life, smooth riding quality, energy saving, lesser maintenance cost and low life cycle cost etc.. The key parameter for the design of concrete pavement is flexural strength. This is well-established fact that flexural strength increases with the increase in compressive strength. With increased flexural strength, thinner pavement could be designed. Recognizing the advantages of HSHPC, designers are continuously making effort in designing for thinner sections of pavement with better performance and long life. Currently HSHPC are being used in as overlay material for the rehabilitation of highway, surface layers on bridges and viaducts and patch repairs etc. Experience has shown that pavements in high volume traffic corridors need to be designed and constructed to provide longer service life because of the difficulties in performing effective repairs and rehabilitation activities [103,160]. Due to high durability and low permeability of HSHPC, the concrete pavement of HSHPC could serve the objectives for long life [91,146]. By virtue of its superior strength and fatigue characteristics, the HSHPC could be used as a layer for overlay and reduced depth of concrete pavement [158]. Because of very low maintenance and rehabilitation problem, there is much growing interest in using HSHPC in concrete pavement. Due to high modulus of elasticity, the HSHPC could be laid directly over the well compacted sub-grade. Since HSHPC could carry

much heavy load, potential to resist crack propagation and capacity to bear high stresses could be recommended for heavy duty pavement [35,194].

In 1993, the Federal Highway Administration (FHWA) initiated a national programme for the maximum use of HPC in bridges. Bridge decks, piers, girders and abutments were constructed with HPC. Nine bridges had been completed under this programme by the end of 1998. In U.S.A., numbers of states are using HPC under their own programmes. Longer span lengths of prestressed concrete girders, wider girder spacing or shallower sections could possible just because of the use of high strength high performance concrete [141]. Thus, seeing the advantages of use of HSHPC during the past decades in different fields, there is continuously increasing interest in using HSHPC for rigid pavements.

Some of the major advantages of using High strength High performance concrete in pavements are summarized below:

1. Flexural strength is key parameter in designing the concrete pavement. Due to significant increase in flexural strength of HSHPC, the thinner concrete pavement could be designed for the same traffic conditions. This will result in lots of saving in construction materials and consequent minor impact on natural environment.
2. HSHPC with fly ash and silica fumes have significant higher fatigue life than the normal concrete. Hence by the use of HSHPC, the fatigue life of concrete pavement could be increased.
3. Corrosion of reinforcing bars takes place usually due to Chloride ion penetration. The moisture and aggressive ion penetrates into the normal strength concrete easily. Since the permeability of HSHPC is very low, thus capable of preventing moisture and chloride ion penetration sufficiently.
4. HSHPC has high durability in severe environments and high resistance to chemical attacks. Therefore, by using HSHPC in pavements, the pavements could be constructed in severe environments too.
5. With the increase in strength of concrete the abrasion resistance also increases. Therefore, in abrasive environment, HSHPC is highly recommended. HSHPC with silica fume has high resistance to abrasion. Therefore silica-fume concrete is useful for the concrete pavements or concrete overlays subjected to heavy or abrasive traffic.

6. HSHPC has very low water cementing material ratio due to use of super plasticizer. HSHPC has high resistance to scaling and physical break-up due to freezing and thawing. Therefore, pavement of HSHPC could be constructed in the areas of low temperature.
7. Due to higher flexural strength, higher modulus of elasticity and higher resistance to crack propagation, a thinner pavement could carry much higher load. HSHPC therefore can be recommended for heavy duty full depth pavements and as well as overlay.
8. Being high strength and modulus of elasticity, HSHPC could be laid directly over well compacted subgrade.
9. Due to early gain in strength, the HSHPC pavement could be opened to the traffic earlier after the construction.
10. HSHPC concrete pavements require less maintenance and rehabilitation, almost nil. Thus, the life cycle cost is significantly reduced.

1.6 NEED OF THE STUDY

India is a developing nation and its economy is continuously growing. Large numbers of infrastructure projects are under construction and in future more mega infrastructure projects to be implemented. Because of these mega infrastructure projects there is continuously increasing number of heavy vehicles and also the size and weight of heavy vehicles. These heavy vehicles cause consumption of fatigue life of normal pavement and lead to early failure. Early failure of pavement leads to early rehabilitation and results in uneconomical. Therefore, we need a pavement which could cater the demand of heavy vehicles. For faster economic growth, it is essential we should have separate corridors of such heavy duty pavements for movement of heavy/commercial vehicles so that goods could reach its destination as early as possible with safety and economy.

In India, generally flexible pavements have been preferred choice due to its lower initial construction cost and feasible stage construction as per growth of the traffic. Rigid pavements had not been preferred in the past due to its high initial construction cost and also not availability of the cement in the country. It has been established that concrete pavements are much superior to flexible pavements. The life cycle cost analysis for rigid pavements are

low as compared to the flexible pavements. The advantages of rigid pavements are smooth in riding, saving in fuel, longer design life, less maintenance compared to flexible pavement, almost nil and can withstand in severe weather etc. Seeing the advantages of concrete roads over asphalt roads, concrete roads have got wide acceptance all over the world. With the availability of cement in abundant and realizing the advantages of concrete pavements over flexible pavements, we prefer the construction of concrete roads. Getting encouraged by the successful completion of Mumbai-Pune Expressway and Indore bypass concrete road projects, National Highway Authority of India has decided to construct some length of roads with concrete in country's highly ambitious road development plans like National Highway Development Programme (NHDP).

Generally, till today concrete roads in India are constructed with concrete mix of grade M30 to M40. According to Indian Standard Code of practice, the concrete having compressive strength equal to or more than 60 MPa is considered high strength concrete. Thus, so far concrete roads are being constructed with normal strength concrete. With normal strength concrete the pavement thickness range from 30 to 40 cm. This consumes lots of natural aggregate and high quarrying results in adverse impact on environment. Today's designers effort is to construct the pavement and other structures as economical as possible putting least impact on environment and must be durable. With the Invention of plasticizers and super plasticizers, it has now been possible to produce concrete of much higher strength and for specific performance requirements. For present study concrete of M60 grade using fly ash has been developed.

Due to much higher load carrying capacity and high durability of HSHPC, the HSHPC pavement could be recommended for heavy duty pavement and longer design period. Being higher abrasive resistance, dust is not produced in the environment. Due to non-production of dust, the visibility remains good for all time. Thus, by the use of HSHPC, a thinner concrete pavement with longer life could be designed. Various studies related to performance of HSHPC like as durability, permeability, compressive strength, flexural strength etc. have been carried out but there is almost negligible information is available about the physical performances of HSHPC pavements i.e. load carrying capacity under varying load positions. The flexural strength and fatigue properties of HSHPC are quite high. These are the essential

parameters from the point of pavement performance. Therefore, it is essential to examine the structural behaviour of high strength high performance concrete pavement. Also the load at first crack, crack patterns, formation of cracks, crack propagation, crack width and ultimate load carrying capacity of HSHPC pavements under varying loads and loading positions need to be studied.

From the above discussions, it is quite clear that there is need to develop a methodology for the analysis and design for HSHPC pavements, which may exhibit the results, obtained through analysis, closer to the experimental results.

1.7 OBJECTIVES OF THE STUDY

The objectives of the study are:

(i) To assess the suitability of HSHPC mixes for laying highway pavements over prepared subgrade.

(ii) To evolve a suitable design approach for the analysis of stresses and deflections in HSHPC rigid Pavement.

(iii) To develop a methodology for design thickness of high strength high performance concrete pavement for heavy axle loading.

(iv) To analyse and improvements in existing design methods of flexible pavements for heavy vehicles.

1.8 SCOPE OF THE STUDY

Scope of the study is limited to the design of rigid and flexible pavements. For this 62 cubes of size 150 mm were cast for compressive strength, 22 beams of size 100 mm x 100 mm x 500 mm were cast for flexural strength, 8 cylinders of size 100 mm diameter and 300 mm height were cast for modulus of elasticity. Three semi full scale HSHPC slabs of size 1800 mm x 1800 mm having thicknesses 160, 200 and 240 mm were laid on compacted subgrade. The slabs were tested for deflections, strains and load carrying capacity by applying loads at three positions (central, edge and corner). Stresses were determined by using existing theories and FEM analysis. CBR value of same soil for design of flexible pavements was determined after 4 days soaking. Life cycle cost of HSHPC pavements and flexible pavements were also found out.

1.9 ORGANIZATION OF THE THESIS

Objectives of the study, need of HSHPC pavements for heavy vehicles and scope of the study have been discussed in Chapter-1. Various studies conducted in India and abroad regarding the different properties of HSHPC and its applications in various fields like as in buildings, in bridges and in pavements have been discussed in Chapter-2. There are various theories which are used in designing of rigid and flexible pavements. Some of these are Westergaard's analysis, Mayerhof's theory, Ghosh's analysis, IRC-58 method, and IRC-37 method. Analytical method i.e. Finite Element Method has also been discussed. This method has been used in finding out for stresses, strains and deflections. All these things have been discussed in Chapter-3. In Chapter-4, experimental programme have been discussed. Development of HSHPC mix, preparation of subgrade and laying of HSHPC pavements of different thicknesses have been discussed. Plate load test on soil and testing of pavements at different positions have been discussed in Chapter-4. Analysis and discussion of the results for strains, deflections and wheel load stresses obtained through experiments, various methods and analytical method (FEM) have been made in Chapter-5. Also, the load carrying capacities at flexural strength, optimization of design thickness and economic analysis have been discussed in chapter-5. Some improvements in IRC-37 for heavy vehicles have also been discussed in Chapter-5. In Chapter-6, conclusions and recommendations for further studies have been discussed.

1.10 SUMMARY

In this chapter, the needs for roads infrastructure have been described for economic developments. Due to various infrastructure projects for economic developments, there are continuously increasing numbers of heavy vehicles. For these heavy vehicles, we need pavements. By using normal strength concrete the design thickness will be more. One of the options is to use HSHPC in pavement which will result in thinner section. The advantages of using HSHPC in pavements have been described. Therefore, there is need to develop the design methodology in designing of HSHPC pavements for heavy vehicles. In Chapter-2 broad research survey has been discussed regarding the properties of HSHPC concrete and its applications in various fields.

CHAPTER – 2

RESEARCH SURVEY

2.1 GENERAL

Various design parameter's like as gradation of aggregate, water binder ratio, types of cement and admixtures which affect the strength of concrete mix, have now been well understood. As a result of vast research carried out, it is well known fact that concrete strength increases as water binder ratio decreases. With the invention of plasticizers and super plasticizers, the water binder ratio could be reduced to a great extent and hence concrete of high strength could be produced easily. With the advancement in concrete technology, the concrete of strength upto 120 MPa are being produced commercially. High rise buildings and large span bridges could possible, just because of development of high strength concrete. High strength high performance concrete is being used in these areas very frequently. Generally, HSHPC has not been used in design of full depth pavements for traffic.

In designing of rigid pavements, the key factor is flexural strength. Other factors are fatigue life, toughness, impact, durability and modulus of elasticity etc. Various researchers have established that all the above factors are superior in high strength high performance concrete than the normal strength concrete. By the use of HSHPC in pavement, the thinner pavement with longer design life and higher durability could be designed for the same traffic conditions than the normal strength concrete [55]. It is estimated that HSHPC can carry much higher load (stress) than normal strength concrete, therefore, HSHPC pavement could be recommended for heavy duty pavement [156]. Also durability, the crack arrest, abrasion resistance properties of HSHPC is much more superior to normal strength concrete. Being high durability, HSHPC pavements could be constructed in severe environment too. Due to thinner pavements of HSHPC section, there are lots of saving in natural aggregates which in turn put less impact on natural resources and environment.

Because of the above properties of HSHPC, there is much growing interest in using HSHPC in highway pavements. The pavements where traffic volumes are very high, the

problem of frequent repairs and rehabilitation is much-much difficult. During the repair the traffic has to be diverted or interrupted. The public get irritated due to frequent closure. Realising these problems, there is necessity to design the concrete pavement for longer life. Today's needs are concrete pavements of longer design life more than 40 years and should be durable. By using HSHPC in pavements, all the above goals could be achieved. Being high flexural strength and durability, the HSHPC could be easily use in highway pavements [20, 123]. No doubt, the cost of HSHPC per m^3 is higher than the normal strength concrete, but due to thinning of the pavements and longer design life (more than 40 years) will offset the increase in cost. HSHPC are being used on patch repair and rehabilitation of damaged pavements. It is being used on bridge deck overlays most frequently [112].

Various studies regarding the properties of HSHPC done in India and abroad are as follows:

2.2 STUDIES CONDUCTED IN INDIA

2.2.1 Workability

Many researchers have tried to define term 'Workability'. But, the workability signifies much wider properties and qualities of concrete. It does not project any particular meaning. Road Research Laboratory, U.K., define workability as 'The property of concrete which determines the amount of useful internal work necessary to produce full compaction'. Another definition which covers a wider meaning is 'ease with which concrete can be compacted hundred percent having regard to mode of compaction and place of deposition'.

Sinha (2012) observed in their experiment that if cement is replaced by 30% flyash, the slump increases from 70 mm of reference mix to 80 mm. As the percentage of fly ash is decreased along with increase in percentage of silica fume, the slump gradually decreases from 80 mm to 43 mm at 30% silica fume. The same pattern is observed if ground granulate blast furnace stage (GGBFS) is used in place of silica fume. At 30% GGBFS the slump is 55 mm, a similar pattern was also observed in case of meta-Kaolin, if it is used along with fly ash. At 30% replacement of cement by meta-Kaolin, the slump observed is 47 mm. From the above discussions, it is quite clear that except fly ash, SF, GGBFS and metakaolin reduce the workability of concrete [152].

Perumal and Sunderarajan (2004) developed the mix of grade M60, M70 and M110 in the lab with replacement of silica fume. They found optimum dose of silica fume 10%. They carried out the test for workability such as compaction factor test, slump test and vee-bee consistometer test with 3% super plasticizer dosage. They observed that workability of concrete decrease as the percentage of silica fume increase [123].

Nazeer and Reddy (2009) et al., developed mix of grade M70 with varying content of silica fume at 8%, 10% and 12% by mass of cements. The water binder ratio kept 0.3 for all mixes. They observed that, there is reduction in slump with the addition of silica fume. To enhance the workability, it is necessary to use high range water reducer. As the replacement level of silica fume increase, higher dosage of super plasticizer is required to maintain the workability [115, 137].

Shrivastava and Bajaj (2012) developed high volume fly ash concrete mixes of grade M20, M50 and M70 with replacement of 35%, 50% and 70% fly ash. They found that with the increase of fly ash, bleeding of concrete keep on decrease and slump increase at constant w/c ratio [148].

Arediwala and Jamnu (2012) conducted study for the relationship between workability and compressive strength of the self-compacting concrete. Mixes contained constant binder content of 500 kg/m^3 and 550 kg/m^3 having water binder ratio of 0.4 and 0.5 respectively. The percentage of fly ash was 15%. Super plasticizer used was based on carboxylic with fly ash. They found that mixes having constant ingredients and dosage of super plasticizers have higher workability with fly ash. There exists a linear relationship between workability and compressive strength. Knowing the workability, the compressive strength could be predicted [15].

2.2.2 Compressive Strength

The strength of concrete is specified by its compressive strength of cubes at 28 days. It is characteristic strength of concrete as given in IS-456 [76].

The characteristic strength is the strength below which not more than 5% of the test results are expected to fall.

During 1950s, the concrete mix was just prepared by adding aggregate, cement and water. To make workable concrete, the water usually added in large quantity i.e. w/c ratio was nearly 0.6 to 0.7. The strength was in the range of 20 to 40 MPa. During 1970s, it could possible to reduce the w/c ratio from 0.6 to 0.45 with the introduction of water reducing agent and strength was developed between 60 to 70 MPa.

Further, with the introduction of high range water reducer, it could possible to reduce the w/c ratio to 0.25 and hence higher strength i.e. more than 100 MPa has been developed [25]. There is no literature available about the using HSHPC concrete in pavement in India. But HSHPC has been used in high rise buildings and bridges most frequently. During fifties, in India, number of prestressed concrete bridges was constructed with the concrete having strength ranging from 35 MPa to 45 MPa. Assam Rail link at Siliguri was the first prestressed concrete bridge constructed in 1949. High rise buildings in Mumbai and Delhi have been constructed with concrete of grade M45 to M60. First time in India, the J.J. Flyover at Mumbai has been constructed by using high strength high performance concrete of grade M75 in 2002. M60 grade of concrete with silica fume has been used in construction of Containment Dome at Kaiga Power Project [147].

Vinayagam (2012) has developed M80 and M100 high performance concrete and found that cement could be replaced by silica fume about 10% without affecting the strength. Also he showed that flexural strength, split tensile strength and elastic modulus is maximum [179].

Arunachalam and Gopalkrishnan (2004) has conducted study on high performance fly ash concrete in normal and aggressive environment and found that concrete with 25% ash fly shows continuously increase in strength in normal as well as aggressive environment at 28 days and 60 days than the concrete without fly ash, which showed reduction in strength in aggressive environment. Split tensile strength of concrete with fly ash showed increase in strength in both environments i.e. normal and aggressive. But split tensile strength of concrete without fly ash, almost maintains the same strength without any improvement, in aggressive environment at 28 days and 60 days [16].

Bhikshma (2009) et al., carried out study on mechanical properties of high strength silica fume concrete and demonstrated that the compressive strength and split tensile strength of M40 and M50 mixes increase up to optimum level of 12% silica fume. Beyond 12%, replacement of cement with silica fume, there is reduction of strength take place. The compressive strength for M40 and M50 mix is increased by 16.37% and 20.20% respectively and split tensile strength by 36.06% and 20–63% respectively. Also there is increase in young's modulus as silica fume increase up to 12%. The young's modulus (E) at this replacement level is 32.19 GPa for M40 grade concrete which is 28 .06% higher than conventional concrete [22].

Shrivastava and Bajaj (2012) showed in the laboratory that compressive strength, modulus of elasticity and toughness increase with increase in fly ash upto 35% with respect to reference mix [148].

Suryawanshi (2007) in their study showed that ascending linear part remain upto 90% of peak stress of HPC whereas normal strength (lower strength) concrete shows very low or negligible linear part. The non-linear part in ascending branch and post-peak softening part are low indicating the brittleness of high performance concrete. But if it is confined by reinforcement or lateral compression, the high performance concrete become ductile [159].

Ghorpade (2010) found that 1% glass fiber volume and 10% silica fume give maximum compressive strength at any age. The percentage increase is 14% over plain concrete without silica-fume and fiber content. Split tensile strength is also optimum at 1% glass fiber along with 10% silica fume replacement. It is 18% over plain concrete without glass fiber and silica fume [47].

Reddy Sekhar (2013) et al., showed that combination percentage replacement of mineral admixtures i.e. 20% fly ash and 10% meta Kaolin give optimum compressive strength 79.90 MPa after 180 days curing period and under same condition maximum split tensile strength of M70 grade is 5.58 MPa [137].

Agrawal (2012) et al., studied the fly ash concrete for pavement and found that in all mixes, with increase in replacement level of fly ash, the compressive strength decrease but

from 28 days to 90 days rate of development of compressive strength is more than for the initial period up to 28 days [9].

Sinha (2012) found in their experiment that if cement is replaced with 15% fly ash and 15% meta kaoline give more compressive strength by 31.5% and 10.76% than the reference mix for 28 days and 90 days. Similarly, if cement is replaced by 10% fly ash and 20% silica fumes give more compressive strength by 21.61% and 20.4% than the reference mix for 28 days and 90 days. Similarly if cement is replaced with 10% fly ash and 20% GGBFS give compressive strength more by 9.17% and 16.71% than the reference mix for 28 days and 90 days [152].

2.2.3 Flexural Strength

Flexural strength increases with increase in compressive strength. It is a measure of tensile strength of unreinforced concrete beam in bending. Modulus of rupture represents the flexural strength. It is a key parameter in designing rigid pavements. Flexural strength is determined by standard test with third point loading as per IS: 516–1959 [77].

Arunachalam and Gopalkrishnan (2004) demonstrated that flexural strength increases from 28 days to 60 days for control concrete (without fly ash) and concrete with fly ash. He also demonstrated that concrete with fly ash (25% and 50%) show increase in flexural strength in aggressive environment too while concrete without fly ash almost maintain the same strength without any improvement at 28 days and 60 days. Flexural strength with 25% fly ash show better increase in strength than concrete without fly ash at 28 days and 60 days [16].

Sunkurwar and Patil (2011) showed through his study that addition of silica fume and fly ash improve tensile strength and other mechanical properties of high strength prestressed concrete like as compressive strength, flexural strength, reduction in expansion due to alkali aggregate reaction and durability etc. [157].

Suresh Kumar (2012) et al., carried out fatigue analysis of high performance cement concrete and inferred that addition of fly ash and silica fume (SF) improve the fatigue performance of concrete by 48% and 83% at a stress level of 0.75 [158].

Bhikshma (2009) et al., through their study showed that up to 12% SF replacement, there is increase in flexural strength at 28 days for M40 and M50 concrete by 16.4% and 15.61% respectively to the concrete without silica fume. Beyond 12% replacement with silica fume, there is decrease in 28 days flexural strength [22].

Shrivastava and Bajaj (2012) found that there is increase in flexural strength upto 35% replacement of cement with fly ash [148].

Solanki et al., studied the steel fiber reinforced concrete pavement and found that it delay and control the tensile cracking of the composite material. The advantages of any fiber reinforcement in cement bound road base are that it improves the fatigue life of the base and also develop the resistance for the reflective cracking of the asphalt. Study also demonstrated that flexural strength of steel fiber reinforced cement concrete are remarkably better than those of conventional reinforced cement concrete. Steel fiber reinforced concrete has been mostly used as overlay in roads, air field pavements and bridge decks [153].

Ghorphade (2010) found through his experiment that flexural strength increases up to 1% of fiber volume and then after strength decreases. With the replacement of silica fume by 10%, the mix show optimum increase in flexural strength and beyond 10% silica fume flexural strength decreases. When silica fume (10%) and fiber (1%) in combination is used then flexural strength observed is 10.89 MPa [47].

Agrawal (2012) et al., studied the fly ash concrete for pavement and found that the rate of development of flexural strength is more in comparison for compressive strength of fly ash concrete mixes [9].

Ram Kumar (2012) et al., found that replacement of cement by silica fume up to 10% shows increase in flexural strength by 8.93% [132].

Sinha (2012) showed that if cement is replaced with 15% fly ash and 15% meta Kaoline then flexural strength observed is more by 45.14% and 21.71% than the reference mix for 28 days and 90 days respectively. Similarly if cement is replaced by 10% fly ash and 20% silica fume the flexural strength is more by 51.39% and 31.62% than the reference mix for 28 days and 90 days. Similarly if cement is replaced with 10% fly ash and 20% GGBFS then

flexural strength is more by 36.81% and 21.03% than the reference mix for 28 days and 90 days [152].

2.2.4 Durability

According to ACI 201.2R durability of concrete is expressed as ability to resist weathering action, chemical attack, abrasion or any other process of deterioration. Deterioration process includes freezing and thawing, alkali-aggregate reaction (AAR) and corrosion of embedded metals etc.

Buenfeld and Newman (1984) studied the mix containing varying percentage of fly ash in enhanced salt concentration approximately eight times of average salt concentration (2g/l) of sea water. He observed that for 40% fly ash replacement there is 5% reduction in strength for all grade OPC 33, 43 & 53, while without fly ash concrete showed 8% reduction in strength. This proves that partial replacement of cement with fly ash improves the durability when exposed to sulphate environment. Due to formation of calcium silicate hydrate, it fills the pores of cement paste reducing the permeability. When loss is compared among the three grade of cement i.e. 33, 43 and 53 grades, it is found that there is much loss in case of 53 grade cement [26].

Marthong and Agrawal (2012) also found that fly ash decreases the shrinkage due to low water demand [100].

Bendapudi and Saha (2011) presented overview on fly ash as supplementary material in mortar. Supplementary cementing material fly ash is mostly used in production of high strength high performance concrete. By using fly ash, it improves properties like water requirement, workability, setting time, compressive strength and durability etc. significantly. First time fly ash approximately 30% by weight of cement was used in construction of Hungry Horse Dam. In construction of Canyon and Ferry dams also the fly ash was used. In India, in construction of Rihand Dam approximately 15% fly ash by weight of cement had been used. [20].

According to Mehta (2004) it is possible to produce sustainable high performance concrete mixture with 50% or more replacement by fly ash that has high workability, high

ultimate strength and high durability. Due to water reducing property of fly ash, fly ash could be advantageously used for reducing drying shrinkage and thermal cracking of the concrete. According to Mehta, when high volume fly ash concrete is properly cured, it provides excellent water-tightness and durability. Due to water tightness, the resistance to corrosion, resistance to sulphate and chemical attacks and resistance to alkali aggregate expansion are enhanced [103].

Agarwal (2010) et al., through literature review found that by using fly ash in concrete, there are number of benefits like higher ultimate strength, improved workability, reduced bleeding, reduced heat of hydration, reduced permeability, increased resistance to sulphate attack, lower cost, reduced shrinkage and high durability etc. Generally 15 to 20% fly ash by mass of total cementitious materials is used. Good workability and cost economy could be achieved by using such small percentage of fly ash [8].

Reddy (2012) et al., developed M80 and M90 grade of concrete using fly ash, silica fume, metakaoline and blast furnace slag and carried out acid attack test, alkaline attack test and sulphate attack test. They found that for M80 concrete, in case of acid attack test, there is 2.5% loss in weight and 34% loss in compressive strength with the replacement of 20% fly ash and 13.23% metakaoline and 2.38% minimum loss in weight and 32.8% loss in compressive strength with the replacement of 20% fly ash and 13.23% blast furnace slag. In case of alkaline attack test, the loss in weight and compressive strength are 3.8% and 24.3% respectively with replacement of 20% fly ash and 13.23% blast furnace slag and minimum loss in weight and compressive strength are 3.55% and 23.2% respectively with replacement of 20% fly ash and 13.23% silica fume. In case of sulphate attack test, loss in compressive strength is 12.65% with 20% fly ash and 13.23% blast furnance slag replacement and minimum percentage loss in compressive strength is 12.4% with 33% fly ash and 15.13% metakaoline. For M90, they found, in case of acid attack test, maximum loss in weights and compressive strength are 1.8% and 30% respectively with replacement of 33% fly ash and 15.13% of metakaoline and minimum percentage loss in weight and compressive strength are 1.42% and 27.2% respectively with replacement of 33% fly ash and 15.13% blast furnace slag. In case of alkaline attack test maximum 2.5% loss in weight and 19% loss in compressive strength with replacement of 33% fly ash and 15.13% metakaoline and minimum

1.89% loss in weight and 15.9% loss in compressive strength with replacement of 33% fly ash and 15.13% blast furnace slag have been observed. In case of sulphate attack test, maximum loss in compressive strength is 14.9% with replacement of 33% fly ash and 15.13% blast furnace slag and minimum loss in compressive strength is 13.2% with 33% fly ash and 15.13% metakaoline have been observed [138].

Perumal and Sunderarajan (2004) developed the concrete strength of grade 60 MPa, 70 MPa and 110 MPa at 28 days with the replacement of silica fume at 10% and compared with the mixes without silica fume. To assess the durability they carried out saturated water absorption (SWA) test, porosity test, sorptivity test, permeability test, acid resistance test, sea water resistance test, erosion resistance test and impact resistance test. They observed that at 10% SF, there is minimum SWA, porosity and sorptivity. Mixes containing SF have lower SWA, porosity and sorptivity than the mixes without SF. Mixes containing SF have lower or negligible water penetration while the mixes without SF have more water penetration depth. Thus mixes having SF and low w/b ratio are almost impermeable concrete. Acid resistance and sea water resistance was found more for mixes M60, M70 and M110 containing SF than the mixes without SF. Mixes containing SF have more abrasion and impact resistance than the concrete mixes without SF. This is due to the formation of stable C-S-H gel [123].

Magudeaswaran and Eswaramoorthi (2013) conducted study on durability characteristics of high performance concrete. They replaced cement with 25% fly ash and 12.5% SF, 30% fly ash and 15% SF and 35% fly ash and 17.5% SF. They kept the water cement ratio constant for all mixes. They observed that the pH value of concrete have decreased by 5.47% and the rate of absorption of concrete have reduced by 0.24%. Thus by the use of fly ash and silica fume an acceptable durability characteristics could be achieved [95].

Amudhavalli and Mathew (2012) developed M35 grade concrete with partial replacement of silica fume by 0, 5, 10, 15 and 20% and carried out acid attack test for durability. They found that loss in compressive strength was 7.69% for concrete mix with replacement of 10% SF and 11.91% was for concrete mix not having silica fume. Thus concrete mixes having silica fume have better durability property [14].

Nazeer (2009) et al., conducted the study of chloride diffusion characteristics by Simple Immersion Test and Rapid Chloride Permeability (RCP) Test. The concrete mixes of target mean strength 70 MPa was prepared with the replacement of silica fume at 8%, 10% and 12% by the mass of cement. The water binder ratio kept 0.3 for all mixes. The mixes were examined for both strength development and chloride penetration resistance. Simple immersion test indicate that 7 days curing make concrete mixes containing silica fume more impermeable. The total charge passed through the specimen in RCPT decreases with increase in silica fume content. This optimum replacement is 10% of silica fume. There is linear relationship between total charge passed and the initial current in RCP test. Higher silica fume content and prolonged curing both enhance the chloride penetration resistance of mixes [115].

2.3 STUDIES CONDUCTED ABROAD

In different part of the world, the following studies related to high performance concrete have been carried out.

2.3.1 Workability

Zhang and Li (2012) found that with the addition of silica fume and increase in content, gradually decrease the slump and increase the drying shrinkage strain gradually of concrete composites containing fly ash [193].

Memon (2013) et al., observed that with the addition of silica fume as partial replacement of fly ash, the workability of geopolymer concrete decreases. The addition of silica fume 10% by weight of fly ash, there is reduction of 4.3% slump [107].

Yijin (2009) et al., carried out study to understand the effect of fly ash on the fluidity of cement paste, mortar and concrete. They found that with increase in fineness of ultra-fine fly ash, there is reduction in water demand. The water reduction rate increases with the level of fly ash replacement. Addition of the ultra-fine fly ash decreases the slump loss and also prolongs the setting time [189].

Zhang and Li (2012) carried out study to see the combined effect of polypropylene fiber and silica fume on workability and carbonation resistance of concrete composite containing fly ash. They found that with the addition of fly ash, the workability of concrete

composite become good. But the addition of silica fume and polypropylene fiber reduce the workability [190].

Turkel and Altunas (2009) studied the effect of lime-stone powder, fly ash and silica fume on the properties of self-compacting repair mortars. They found that use of silica fume increase the dose of super plasticizer due to its high surface area. They showed that limestone powder change the workability at constant super plasticizer dose and 30% mineral additives. They also found that some combination of fly ash, silica fume and lime powder can improve the workability in better way than that of using individually [171].

Panjehpour (2011) et al., concluded from their experiment that by addition of silica fume, the workability and consistency of concrete decreases. However consistency could be increased by using silence treated silica fume. Sound absorption ability of concrete is increased by the addition of silica fume and stiffness is also reduced. Therefore, such concrete could be used as noise barriers [121].

Osci and Jackson (2012) during investigation found that by using natural clay pozzolana, the workability get reduce. As the content of natural pozzolana is increased, the workability keep on reduce [118].

Bouzoubaa (2011) et al., in their study maintained the slump in the range 100 to 150 mm by maintaining the dosage of super plasticizer. The dosage of super plasticizer was in the range of 0.9 to 3.6 L/m^3 of concrete. Air content in the concrete was in range of 5 to 7% by maintaining the dosage of air-entraining admixture. It has been observed significant loss of slump and air content with passage of time. By the use of high volume fly ash cement, there is appreciable reduction in bleeding. The bleed water was in the range of 0.004 to 0.032 ml/cm^2. High volume fly ash concrete setting time was 3 to 5 hours higher than those of control concrete. By the use of blended cement in high volume fly ash concrete, there is reduction in initial and final setting time by 30 to 40 minutes [23].

Thomas (2010) carried out study to optimise the fly ash content for sustainability, durability and constructability. They found that optimum level of fly ash depends on

properties of fly ash, performance requirements for fresh and hardened concrete, climatic conditions etc. In mostly cases the optimum level of fly ash may be 40% or more [164].

2.3.2 Compressive Strength

Memon (2013) et al., during his investigation on fly ash based self-compacting geo-polymer concrete found that with the addition of silica fume at 10% by weight of fly ash, showed that there is increase in compressive strength by 6.9% [107].

Turkel and Altunas (2009) conducted study on twelve samples of self-compacting repair mortar having different proportions of fly ash, limestone powder and silica fume. They found 28 days compressive strength in the range of 33.7 to 70.3 MPa. The highest 28 days compressive strength correspond to the mixes having 30% silica fume and lowest correspond to mixes containing 30% limestone powder of cement. This shows that limestone powder has no effect on mechanical properties [171].

Panjehpour (2011) et al., showed that addition of silica fume increases the compressive strength. Many researchers have shown that addition of silica fume to concrete mix increase the strength of mix by between 30% and 100% depending on the ingredients proportions. Modulus of elasticity does not show the same trend as that of tensile strength. There is slight increase in modulus of elasticity compared to compressive strength of concrete [121].

Osci and Jackson (2012) investigated the effect of natural clay pozzolana as a partial replacement of cement at 0%, 10%, 20%, 30%, 40% and 50% by mass. Then they tested the specimen at 7, 14, 21 and 28 days. They found that at 30% replacement by mass, the compressive strength is always high at all ages. At 28 days, there is 19% increase in compressive strength for 30% replacement level. Thus natural clay pozzolana can be used in production of concrete without compromising strength [118].

Turk (2013) et al., found that self-compacting concrete (SCC) with fly ash and silica fume have lower compressive strength than the plain self-compacting cement concrete at 3 days. They further found that SCC with silica fume has highest compressive strength at 7, 28 and 130 days. SCC with 40% fly ash has highest compressive strength 59.04 MPa after a period of 130 days [169].

Ismeik (2009) observed in their study that addition of silica fume increases the compressive strength. High percentage of silica fume does not increase compressive strength. Beyond 15%, the benefits decrease rapidly. A 10% replacement of silica fume, almost for all w/c ratios, increases the compressive strength keeping composition parameters constant. The optimum replacement of silica fume is not unique. It varies from 7.5% to 12.5%. It is a function of mix w/c ratio. The rate of gain of strength is higher in silica fume concrete than the normal concrete. Isemeik also investigated the effect of fly ash on compressive strength. At 15% fly ash replacement by weight of cement and w/c ratio 0.35, the maximum 60 MPa 28 days compressive strength has been observed.

The minimum compressive strength 35 MPa has been observed at 25% fly ash replacement by weight of cement. They observed gain in strength after 90 days. At earlier stage, no advantages have been observed at any replacement level of fly ash. High percentage replacement level of fly ash reduces the strength. It has been observed that benefits are increased as the age of fly ash concrete increases. Keeping mix composition parameters constant, the optimum level of fly ash replacement is approximate 15% at 90 days. They also observed that by the addition of silica fume and fly ash, the 28 days compressive strength increases for lower w/c ratio. In their study, he found maximum compressive strength 52 MPa at 10% silica fume and 20% fly ash replacement for w/b ratio of 0.30. Keeping the mix composition parameters constant, the optimum mineral admixture percentage is above 10% silica fume and 20% fly ash [79].

Langan (2002) et al., studied the effect of silica fume and fly ash on heat of hydration of Portland Cement. In their study, they found that fly ash at high w/c ratio retards the hydration of cement very significantly while silica fume accelerates the hydration of cement significantly and retards the hydration of cement at low w/c ratio. When silica fume and fly ash are used in combination, the hydration of cement is significantly reduced [93].

Yazici and Arel (2012) carried out study to find out the effects of fly ash fineness on mechanical properties of concrete. They used the fly ash having fineness 2351 cm^2/g, 3849 cm^2/g and 5239 cm^2/g. They found that long term and short term mechanical properties are affected by fineness of fly ash. As the fineness of fly ash increases, the compressive and split

tensile strength increases. Through their study they concluded that fly ash having fineness more than 3849 cm^2/g have positive effect on mechanical properties of concrete. The fly ash with fineness 5235 cm^2/g has remarkably impact on compressive and split tensile strength [188].

Elsayed (2011) investigated the effect of fly ash, superpozz, silica fume and high slag cement on water permeability and strength of concrete. He added 5%, 10% and 15% silica fume and 10%, 20% and 30% fly ash or superpozz by weight of cement keeping w/c ratio 0.4. Results showed lowest water permeability for 10% superpozz and 10% silica fume or 20% fly ash mixes. The lowest permeability leads to greater durability of concrete. The highest compressive strength was obtained for 10% silica fume replacement of cement. As the other mineral admixture is added the compressive strength gets reduce [39].

Bouzoubaa (2011) et al., carried out the study on mechanical properties and durability of concrete made with a high volume fly ash blended cement using a coarse fly ash that does not meet the fineness requirement of ASTM C618. They tested the specimen at 7, 14, 28 and 91 days and compared the results with that of other concrete mixes. There was significant increase in compressive strength of concrete made with blended high-volume fly ash. The increase in compressive strength was 30% at 91 days and 45% at 7 days. Modulus of elasticity at 28 days for control concrete and for blended concrete was 30.3 and 33.0 GPa and at 91 days, it were 31.6 GPa and 32.5 GPa respectively. These data shows that the modulus of elasticity for high volume fly ash concrete is generally higher than those of the normal Portland cement concrete [23].

Turk (2010) et al., in his study showed that self-compacting concrete (SCC) specimen has higher compressive and tensile strength when silica fume and fly ash is added than those of normal concrete. They observed that for 3 days there is decrease in compressive strength of SCC specimen as there is increase in content of fly ash and silica fume. The highest compressive and tensile strength observed was 73.87 and 5.489 MPa respectively at 130 days for 15% replacement with silica fume of cement. The modulus of elasticity was highest in SCC specimen with silica fume while there was lowest modulus of elasticity for SCC specimen with fly ash [169].

2.3.3 Flexural Strength

Memon (2013) et al., investigated the effect of silica fume on fly ash based self-compacting geo-polymer concrete. The silica fume used was 0%, 5%, 10% and 15% by weight of fly ash. They observed that for 10% silica fume by weight of fly ash, there is increase in tensile strength by 12.8% and flexural strength by 11.5% [107, 144].

Turkel and Altunas (2009) investigated the effect of limestone powder, fly ash and silica fume on properties of self-compacting repair mortars. They prepared the twelve samples having different proportions of fly ash, limestone powder and silica fume. They found the 28 days flexural strength in the range of 7.1 to 12.2 MPa. The highest 28 days flexural strength was obtained for the mix having 20% fly ash and 10% silica fume and lowest for the mix having 30% limestone powder of cement. This shows that limestone powder has no impact on mechanical properties [171].

Panjehpour (2011) et al., through their experiment found that for silica fume concrete there is same relationship between tensile, flexural and compressive strength as in case of ordinary strength concrete. Increase in compressive strength is accompanied by increase in tensile and flexural strength. Increase in tensile strength, cause reduction of tensile members, leading to the reduction of weight of members and cost [121].

Isemeik (2009) investigated in his study that in case of silica fume, when w/c ratio decreases, the flexural strength increases for all percentage of silica fume. They observed that the mixes having replacement levels of 5%, 7.5%, 10%, 12.5% and 15% silica fume have higher flexural strength than the control mix for all w/c ratio. 10 MPa, the highest value of flexural strength has been observed for mixes having 15% silica fume replacement level and w/c ratio of 0.30. It has been observed that as the silica fume replacement level increases, the flexural strength also increases. It has been observed that silica fume has more effect on flexural strength than that of compressive strength. Very high percentage of silica fume, improve the flexural strength significantly than that of compressive strength. Flexural strength does not follow the same trend as that of compressive strength [79].

Zhang and Li (2013) carried out study the effect of polypropylene fiber on concrete containing fly ash and silica fume. They found the effect of polypropylene fiber on fracture

properties of concrete. By addition of polypropylene fiber in concrete containing 15% fly ash and 6% silica fume, the fracture properties like as fracture toughness, fracture energy, effective crack length, maximum mid span deflection, the critical crack opening displacement and the maximum crack opening displacement of three-point bending beam specimen has greatly improved. As the fiber volume fraction increases from 0 to 0.12%, the fracture parameters increase gradually. The resistance to crack propagation of concrete containing 15% fly ash and 6% silica fume become stronger and stronger with the increase of polypropylene fiber volume fraction but not beyond 0.12% [191].

Bouzoubaa (2011) et al., in their study used the blended high-volume fly ash cement to determine the flexural strength and splitting-tensile strength of concrete. They found that HVFA blended cement improves the flexural and splitting tensile strength of concrete at 28 days [23].

Sabir (1997) in their study noted that 5 to 10% replacement of OPC with silica fume increase the strength of concrete. From results, it is evident that there is significant increase in compressive strength at 7 days and 28 days irrespective of whether air entrained concrete or non-air entrained concrete. The trend of flexural strength is similar as that of compressive strength. He found 28 days flexural strength is higher than that of control concrete [143].

Atan and Awang (2011) carried out study to find out the effect of raw rice husk ash on compressive and flexural strength of self-compacting concrete. By using 15% raw rice husk ash as cement replacement produces 40 MPa concrete. 30% cement replacement using raw rice husk ash combined with lime stone and 45% cement replacement combined with raw rice husk ash, lime stone and silica fume produce comparable compressive strength to normal concrete and improved flexural strength [18].

2.3.4 Durability

Zhang and Li (2012) studied the effect of silica fume on concrete composite containing fly ash. Silica fume content used were at 3%, 6%, 9% and 12%. Results showed that the durability has been improved to great extent with the addition of silica fume. Properties like, water permeability, carbonation resistance and freeze-thaw resistance have greatly improved the concrete composites containing fly ash. With the increase in content of silica fume, the

relative dynamic elastic modulus increase, the carbonation depth decrease and reduce the permeability of concrete [193].

Zhang and Li (2012) found that addition of fly ash reduces the carbonation resistance of concrete composite while addition of silica fume enhance the carbonation resistance of concrete composite containing fly ash. Further the carbonation resistance of concrete composite increase with the addition of polypropylene fibers as the fiber volume fraction is below 0.12% [190].

Jalal (2012) et al., conducted the study related to durability on high performance self-compacting concrete containing nano silica and silica fume. He replaced the cement with micro silica, nano silica and blend of micro and nano silica at different percentage levels as 10%, 2% and 10% + 2% respectively. He observed that there is reduction in water absorption, capillary absorption and Cl ion percentage. The reduction was more in case of blend of micro and nano silica. Resistivity of self-compacting concrete increases which leads to reduction of corrosion [80].

Zhang and Li (2013) carried out study freezing and thawing durability of fly ash concrete composites containing silica fume and polypropylene fiber. Study revealed that by the addition of fly ash and increase in content enhance the freezing and thawing durability. By the addition of silica fume and polypropylene fiber, they enhance the freezing and thawing durability to great extent of composite concrete containing fly ash. There is gradual increase in freezing and thawing durability as the content of silica fume and fiber volume fraction increases. This is optimum at fiber volume fraction 0.08%. Beyond this percentage, reduction in durability has been observed [192].

Turkel and Altunas (2009) studied that total water absorption are reduced by the addition of silica fume. They found lowest total and capillary water absorption at 24 hours for the mixes having fly ash 20%, limestone powder 5% and silica fume 5%. They also noted that highest total and capillary water absorption for mixes having fly ash 20% and lime powder 10%. From the above discussion, it could be inferred that silica fume has reducing effect while fly ash and limestone powder have no such effect. Therefore for capillary block, limestone powder and fly ash could not be recommended [171].

Panjehpour (2011) et al., through literature found that addition of silica fume reduces the efflorescence and enhances the corrosion resistance. It also enhances the chemical attack resistance, whether the chemical is acid, chloride and sulphate. Addition of silica fume also reduces permeability.

Also through literature he found that for equal strength and any concrete strength below 40 MPa, carbonation is higher in silica fume concretes. Silica fume concrete is utilized normally when the compressive strength is above 70 MPa. Bleeding is also significantly reduced when silica fume is used. By the use of silica fume, the freeze- thaw durability increases and also permeability to chloride ion reduces. There is reduction in water absorption also [121].

Naik (1995) et al., carried out study on abrasion resistance of high strength concrete made with class C fly ash. They replaced cement with class C fly ash at levels 15%, 30%, 40%, 50% and 70%. A reference concrete of 28 days compressive strength 41 MPa without fly ash has been developed. The concrete specimens were tested for abrasion as per ASTMC-944 test method. An accelerated test method was used to evaluate abrasion resistance of high strength concrete. Accelerated test results showed that 30% class C fly ash replacement have same abrasion resistance as that of reference concrete. Beyond 30% fly ash replacement, the concrete show lower abrasion resistance than that of reference concrete [113].

Assas (2012) found in his investigation that the concrete containing silica fume show better resistance to chloride ion permeability and water penetration compared to fly ash concrete [17].

Khan (2010) carried out investigation regarding the resistance to chloride of high performance concrete. He found that in binary system, silica fume up to 10% reduces significantly chloride permeability. Further addition of pulverized fuel ash resulted in further reduction of chloride permeability to a negligible level [91].

Folagbade and Olufemi (2012) carried out study the effect of fly ash and silica fume on the sorptivity of concrete and found that at equal w/c ratio, concrete containing fly ash have poor resistance against sorption and as the content of fly increases the resistance against

sorption reduces. But with the passage of time, the resistance against sorption become good than that of plane concrete. The resistance against sorption becomes good by the addition of silica fume at early and later stage. Sorptivity is affected by strength. As the strength increases, sorptivity reduces. The cement combination concretes have lower sorptivity than that of plane concrete [41].

Turk (2010) et al., found that self-compacting concrete (SCC) containing silica fume has lowest sorptivity values than that of SCC with Portland Cement and SCC with fly ash. As silica fume content is increased from 5% to 20%, the sorptivity of SCC containing silica fume is decreased. The resistance against carbonation is low in self-compacting concrete containing fly ash. From statistical evaluations, it had been found that dosage of silica fume had insignificant effect except for 24 hours on the carbonation resistance of SCC [170].

Kathuda (2010) et al., investigated the effect of micro silica and water proofer on the concrete to the resistance of phosphoric acid. For this purpose keeping w/c ratio constant, three specimen of micro silica replacement at levels of 10%, 15% and 20% by weight of cement and three mixes of 0.4, 0.6 and 0.8 L of water proofer were prepared. Durability of concrete to phosphoric acid attack after 15 cycles of wetting and drying in phosphoric solution, compressive strength and modulus of rupture were tested. Study showed that there was no significant loss of compressive strength and modulus of rupture of concrete. Further, the combined effect of micro silica and water proofer improved the durability of concrete to freezing-thawing and to phosphoric acid attack [87].

Marriaga and Yepez (2010) in his study found that addition of silica fume reduces chloride ion permeability. Due to reduction of chloride ion permeability, there is less threat to corrosion of steel [99].

Hooton (2010) et al., taken out cores, four concrete cores from bridge decks in New York State and one in Ohio. More four cores were taken from four parking garage decks located in Wisconsin, Utahand 2 in Ohio. All the concrete structures were 6 and 15 year old when cored. The cores were tested for chloride penetration. The results showed that all the concrete cores have high resistance to chloride penetration. Using the life-365 program, the residual life came out between 30 and 61 years for silica fume concrete [57].

Bouzoubaa (2011) et al., investigated the abrasion resistance of blended high volume fly ash concrete. They measured the abrasion of concrete ranged from 1.3 to 1.6 mm after 20 minutes of testing. The lowest value was for the concrete made with HVFA blended cement and higher value was for the concrete in which the unground fly ash and the LPC had been added separately to the concrete mixer. Abrasion resistance is function of compressive strength of concrete.

The test results show that blended cement concrete has very good resistance to freezing and thawing. The durability factor ranges from 95 to 102.

The slab made with blended cement concrete show severe scaling than those of control concrete. Thus concrete made with blended cement show low resistance to De-icing salt scaling [23]

2.4 CALIFORNIA BEARING RATIO (CBR)

California Division of Highways in the U.S.A., developed CBR method for pavement design in 1928. California bearing ratio test method is used to classify and evaluate the soil sub-grade and base course materials for flexible pavements. U.S. Corps of Engineer adopted the CBR test in designing the base course for air field pavements after World War-II. The test is empirical and cannot be related to fundamental properties of the materials. CBR is a measure of strength of soil and base materials. Higher is the CBR better is the materials.

Tomar and Maallick (2011) in their study "A study on variation of test conditions on CBR determination" found that the value of CBR decreases from one day to 4^{th} day of soaking. The loss of CBR value is gradual. There is significant loss of CBR value from un-soaked condition to soaked condition. It has been observed that there is not much change in moisture content from first day of soaking to fourth day of soaking. They found that four days soaked CBR may not good for all kind of soil. For non-expansive soil, since there is not much difference in soaked CBR after one day, therefore, it is not recommended being soaked for shorter period. Shorter period will result in higher CBR leading to smaller thickness of pavement. However there is need of more studies for variety of soils [168].

California Bearing Ratio of sub-grade is basis for designing of flexible pavements. For this only a limited numbers of CBR test being performed over the length which do not reveal the detailed variation of CBR values. These tests are time consuming and high cost. For such cases CBR could be determined on the basis of some tests which are cheap, less time consuming and quick. By considering this aspect a number of investigators in the past have developed different methods to determine CBR value.

Roy (2010) et al., in their study has tried to validate the predicted CBR determined by different methods as per guidelines of IRC:SP: 72 – 2007 [139].

Joseph and Vipulanandan (2010) in their study have developed the correlation between California Bearing Ratio and soil parameters. He used laboratory and field compacted soil samples (CL, CH and SC). There was non-linear relationship between CBR and undrained shear strength of soil [82].

Nugroho (2012) et al., have developed the correlation between Index Properties and California Bearing Ratio for soaked and unsoaked conditions. CBR is a measure of soil strength. In their research, they have made comparison between CBR soaked test results and CBR un-soaked results in some variation of clay content. On the basis of soil properties, comparisons have been made between CBR soaked and un-soaked conditions. Knowing the soil properties and un-soaked CBR value, the soaked CBR value can be predicted. The results showed that there were linear correlations between soaked and un-soaked CBR values. This relationship is also influenced by the properties of soil [117].

Keshav and Mangaiar (2012) carried out study the effect of fly ash on an expansive soil for flexible pavement design. The objective of this study was to use fly ash effectively to reduce the quantity of lime in stabilizing the soil and also to reduce the construction cost. Various index properties of expansive soil were studied initially and then different proportions of fly ash were added. CBR and unconfined compressive strength tests for different proportions of fly ash were conducted and optimum percentage of fly ash was found. Improvement in strength of soil has been observed with the addition of fly ash. California Bearing Ratio was increased 1.64 times of the initial strength of soil. By using lime fly ash in stabilization of soil, there could be saved rupees from 1.7 lakhs to 2.0 lakhs per km. The

construction cost could be saved by an amount from rupees 2.85 lakhs to 5.3 lakhs per km when compared with lime stabilization [88].

Singh (2011) et al., for their study prepared hundred samples in laboratory. Four different compaction levels 50, 56, 65, 75 and five different moisture contents on dry and wet sides of optimum moisture content were used. Soaked and unsoaked CBR tests were conducted on each sample. Different independent parameters like as index properties of soils, degree of compaction and moisture content were considered in development of Regression Model. The validity of model was tested using the soil which was not used in development phase of models. The results showed that the models give reasonable estimate of CBR values. During the study, it has been observed that there is significant impact on soaked and unsoaked CBR by variation in moisture content and compaction effort [149].

Bagui (2012) carried out study to design the pavement for low to medium volume traffic using cement and lime treated base. There are no guidelines for pavement design having cement / lime treated base. Therefore, the aim is to develop a design chart using cement and lime stabilized base for rural roads with light to medium traffic. The study shows that for given resilient modulus of stabilized base and CBR of sub-grade, with the increase in number of repetition, the thickness of base treated with cement and lime increases. As the modulus of sub-grade treated with lime and cement increases, the thickness of base decreases for the given number of repetition. For each modulus of soil- cement base and soil-lime base, as the CBR is increased, the thickness of base treated with lime and cement decrease significantly [19].

2.5 MODULUS OF SUBGRADE REACTION (K)

Modulus of subgrade reaction is defined as pressure sustained per unit deformation of sub-grade at specified deformation or pressure level using specified plate size. The standard size of plate for finding K-value is 75 cm diameter. But in some tests a smaller plate of 30 cm diameter is also used. Modulus of sub-grade reaction [K] depends on shape and size of plate, depth of embedment and the type of soil [Terzaghi (1955)].

Dey (2011) et al., carried out study, the distribution of subgrade modulus beneath beams on reinforced elastic foundations. The study shows that type of loading significantly

affects the contact pressure and subgrade modulus of profiles along the length of beam. While during the calculations we assume uniform modulus of sub-grade reaction. There is variation of 45 to 50% in non-dimensional flexural responses when considered varying modulus of subgrade reaction compared to the results obtained by considering uniform subgrade modulus along the length of footing [36].

Moayed and Nacini (2006) carried out study evaluation of modulus of subgrade reaction in gravely soils based on Standard Penetration Test (SPT) results. It is most popular test and economical means to get the information of sub-surface. SPT and Plate Load Test (PLT) were carried out on gravely soils. They found that SPT and PLT could be correlated in medium to dense gravely soils. They found that modulus of subgrade reaction increase with increasing the corrected SPT blows counts $(N_1)_{60}$ for medium to dense gravely soil [111].

Ping and Sheng (2013) investigated the resilient modulus and modulus of subgrade reaction for Florida Pavement subgrade. AASHTO pavement design guide (1993) suggested a theoretical relationship between modulus of subgrade reaction and resilient modulus of subgrade based on assumptions that the subgrade materials are linear elastic. This was not evaluated by experimental work. They carried out extensive field and laboratory test to study the load-deformation and resilient modulus characteristics of the granular sub-grade soils. In addition, laboratory cyclic biaxial test were performed to evaluate the resilient modulus characteristics of subgrade materials. On the basis of experimental results, correlation relationships were developed between the subgrade soil resilient modulus and modulus of subgrade reaction to calibrate the AASHTO theoretical relationship. It has been found that the calibrated relationship was close to the AASHTO theoretical relationship with difference around 10% [126].

Moayed and Janbaz (2008) investigated the effect of foundation size on modulus of subgrade reaction in clayey soil. The modulus of subgrade reaction is dependent on parameters like as soil type, size, shape, depth and types of foundation etc. The modulus of sub-grade reaction is generally determined by plate load test. Generally Terzaghi Equation is used for determining the modulus of subgrade reaction. By using the finite element method, the effect of size of foundation on subgrade reaction has been determined and then compared

with modulus of subgrade reaction determined by Terzaghi equation. The results show that the modulus of subgrade reaction values obtained from Terzaghi's equation for prototype footing has lower value than from 3-D finite element analysis [110].

Janbaz and Janbaz (2011) investigated the effect of foundation size on modulus of subgrade reaction on sandy soil and found that as the side dimensions of footing (B) increased the modulus of subgrade reaction (K) decreased. The modulus of subgrade reaction that obtained from Terzaghi's equation for prototype footing has lower value than that of finite element analysis [81].

2.6 APPLICATIONS OF HIGH STRENGTH HIGH PERFORMANCE CONCRETE (HSHPC)

Understanding the potential advantages of HSHPC due to its ease of placement and consolidation, long term mechanical properties, higher toughness, higher abrasion resistance, higher volume stability, extended life in severe environment, its use is increasing day by day. HSHPC is being increasingly used in all kind of civil engineering structures like as tall buildings, bridges, tunnels and highways etc.

2.6.1 In Buildings

Today's such high-rise buildings are possible due to development of advancement in concrete technology. High strength high performance concretes are in use in columns of high rise buildings since long back. Due to high strength and high modulus of elasticity, the sizes of members are reduced leading to the reduction of dead weight. This will results in lighter foundation. Due to reduction in size of members, the usable area increases. High strength concrete were used in high rise buildings first time in U.S.A. Ingalls Building in Cincinnati, Ohio, is the first high rise reinforced concrete building. It is fifteen story building and was completed in 1903. It is still in use.

There are plenty of examples of high-rise buildings in America. Pacific First Centre, which is 44 story and Two Union Square, which is 62 stories, situated at Seattle in Washington are notable examples of high-rise buildings. Concrete of grade 115 MPa compressive strength and modulus of elasticity 50,000 MPa have been used. Two Prudential

Plaza and 311 South Wacker Drive buildings, whose heights are 281 m and 295 m respectively, are another example of high-rise buildings. The concrete used were of compressive strength 83 MPa. 50 MPa concrete was used in Lake Point Tower in Chicago, constructed in 1965, the 79 story Water Tower Placed in Chicago contain 60 MPa concrete columns. Scotia Plaza Building in Toronto has been constructed by using 90 MPa concrete [94].

In Malaysia, the Petronas Tower linked by a sky bridge at mid height, situated at Kuala Lumpur, is good example of high-rise building. The concrete of compressive strength 60 and 80 MPa has been used. 60 MPa concrete has been used in foundations and 80 MPa has been used in core walls and columns. Other projects where high strength concrete has been used are Wisma Consplant, KTP Flyover Bridge, Port Klang Wharf of and Menara Public Bank in Johor Bahru. 55 MPa concrete has been used in Wisma Consplant, 50 MPa concrete has been used in KTM Fly Over Bridge and Port Klang Wharf, 60 MPa and 65 MPa concrete have been used in Menara Public Bank, Johor Bahru [53].

In Germany, 'Trianon' 186 m high rise building situated in Frankfurt, first time 85 MPa concrete was used. Another high rise building 'Taunustor' in Frankfurt, high strength concrete of grade 105 MPa was used first time for flexural and shear stressed members. There are various projects in Germany where strength up to 115 MPa concrete have been used [25].

Other various notable high rise buildings are Burj Khalifa (828 m high) in Dubai, Makkah Clock Royal Tower (601 m high) in Makkah, Trump International Hotel and Tower (415 m high) in Chicago, Taipei 101 (509 m high) in Taipei, Shanghai World Financial Centre (492 m high) in Shanghai, International Commerce Centre (Union Square, 484 m high) in Hong Kong, Wills Tower (442 m high) in Chicago, Jin Mao Tower (421 m high) in Shanghai, Two International Finance Centre (415 m high) in Hong-Kong, Princess Tower (414 m high) in Dubai etc. have been constructed with high strength high performance concrete.

In India concrete of varying strength from 45 to 60 MPa has been used in high rise buildings in Delhi and Mumbai. Mostly high rise buildings have been constructed in Mumbai and New Delhi [147].

2.6.2 In Bridges

By using HSHPC, long span bridges with thinner sections and longer life can be constructed. Thinner sections cause to reduction in dead weight and lead to lighter foundation, which in turn results in economical. HSHPC reduce deflection and maintenance. Due to such advantages, the HSHPC in bridges and fly over are being in use extensively. High strength high performance concrete bridges are mostly in U.S.A., Japan, Canada, France and Norway.

In Japan, in 1973, three high strength concrete bridges were built for Japan Nation Railway. The 2nd Ayaragigawa post tensioned bridge was constructed using 60 MPa concrete. Iwahana first prestressed concrete truss bridge in Japan has been constructed by using 80 MPa concrete. The bridge is 45 m span. A 24 m Howe Truss, Ootanabe railway bridge has been constructed with 80 MPa concrete. The other bridges in Japan constructed with HSC are Nitta Highway Bridge (30 m span, 59 MPa), Kaminoshima Highway Bridge (86 m span, 59 MPa), Akkagawa Railway Bridge (46 m span, 79 MPa) etc.

In France, various bridges as Sylans Viaduct (60 MPa), Re Island Bridge (60 MPa), Pont du Joigny (46 m span, 60 MPa), Pont due Pertuiset etc. have been constructed by using HSHPC.

In Norway, bridges constructed with high strength concrete are as Giske (52 m span, 55 MPa), Sandhomeya (154 m span, 55 MPa), Bokna Sundet (190 m span, 60 MPa), Helgelandsbrua (425 m span, 65 MPa) etc. Other high strength concrete bridges are Tower Road Bridge (49 m span, 62 MPa) in Washington, East Huntington Bridge (274 m span, 55 MPa) in W. Virginia, Kwung Tong By Pass (65 MPa) in Hong-Kong, Braker Lane Bridges Austin (60 MPa) in Texas, Portneuf Bridge Quebec (60 MPa) in Canada etc. [1].

In India, the first prestressed concrete bridge was built in 1949 for the Assam Rail Link at Silliguri. Numbers of presstressed concrete bridges were constructed during fifty's using concrete 35 MPa to 40 MPa compressive strength. More than 35 MPa compressive strength was used in Konkan Railway Project. Vidya Sagar Setu at Kolkata where longest cable stayed bridge (in India) was built using high strength concrete. J.J. Fly Over at Mumbai where high-strength high-performance concrete 75 MPa was used for the first time in India (2002) [147].

2.6.3 In Pavements

The interest is continuously increasing in use of high strength high performance concrete in highway pavements. This is due to increased resistance to freeze-thaw, increased abrasion resistance, high durability, low permeability, low maintenance and longer life. Longer lives, low maintenance of pavements result in lower life cycle cost.

Concrete paving industry in Iowa has developed fast track concrete. Fast Track concrete is nothing but it gain high strength at early age and is durable. By using Fast Track Concrete for repair of pavement, the traffic can be open in 4-5 hours. This technology is being used all over country (U.S.A.). This technology has been introduced in U.K. in July 1990.

Field studies of special rapid-strength-gain cements such as MPC (Magnesium Phosphate Cement) used for patching [Sheera et al., 1993] and PBC (Pyrament Blended Cement) used for full depth pavement replacement [Ozyildirim, 1994] have also been carried out and very satisfactory results have been obtained.

High strength high performance concrete has been used for rehabilitation of Bridge decks. In Washington, twelve bridges decks were rehabilitated with latex modified concrete. But the results were not satisfactory. In Virginia, the bridge decks were rehabilitated with silica fume (7% to 10%) concrete. The results showed that silica fume concrete can be used as an alternative to LMC [119, 154].

In Oregon, the bridges decks were rehabilitated using micro silica modified concrete [Miller, 1991]. The overlay met two design objectives of their three after one year in service. They were adding strength to the deck and providing a smooth and durable wearing surface. Because of cracks, they could not retard the intrusion of chlorides to the underlying deck. Sprinkel studied the polymer concrete overlay. He suggested polymer concrete constructed with epoxy, methacrylate and polyster styrene binders and graded silica and basalt aggregate can provide skid resistance and protection against chloride intrusion for 1 to 20 years [154].

High performance concrete can be employed as thin overlays of concrete by 100 mm over old flexible pavements. This is called white-topping. This technique is being adopted by U.S.A. and some North-West European countries. This technique was also in use earlier

decades of twenty century. An international review of HPC applied as white toppings around the world are given in Table 2.1.

In Norway, to overcome the increased wear resistance of steel studded tires, high strength concrete has been used in highway pavements. 18 cm thick pavement was laid by using 90 MPa concrete in 1989. After 4 years of service pavement did perform as per expectation to meet the wear resistance of HSC. But some longitudinal cracks have been observed, near to the some of joints. This problem is probably due to insufficient thickness of pavement and also due to fatigue. In Sweden and Norway, there are many cases of using high strength, high performance concrete for highway pavements to improve the abrasion resistance [1].

Table 2.1: Details of White Topping over Flexible Pavements*

Year	Place	Compressive strength (MPa)	Flexural strength (MPa)	Notes
1990	Northampton Country, Virginia, U.S.A	18 hrs 25.0 24 hrs 28.8 7 days 39.3 28 days 47.5	28 days 5.6	Opened to traffic after 58 hours amount of 240 equivalent single axle load per day
1991	Dallas country, Iowa, USA	28 days 27.5	28 days 4.7	
1996	Tijuana BC, Mexico		28 days 5.1	Urban street, 2100 vehicles for mixed traffic per hour
1997	Sao Paulo State Highway SP-280 Brazil	28 days achieved in laboratory, 56, 28 days measured from field cores: 41	28 days design strength 5	
1991	Suzukuisimati Japan	24 hr : 30	24 hr : 3.5	
1991	Sin-Jo-i, Japan	24 Hr: 30	24 hr : 3.6	
1992	Aomori, Japan	24 hr : 30	24 hr : 3.5	
1990	Missouri R67, USA	18 hr : 24.1		
1991	Kanas City U.S.A	24 hr : 20.7		
1990	Virginia R13, U.S.A	24 hr : 24.1		

*****Source- Applications of High Performance Concrete for Ultra-Thin Pavement Overlays (Whitetopping) By J. T. Balbo

2.7 SUMMARY

In this chapter, broad research surveys have been discussed regarding the properties of HSHPC concrete mix. HSHPC mix has been used in the present investigations. Studies conducted in India regarding the various properties workability, compressive strength, flexural strength and durability and abroad have been discussed. The essential parameters for designing of rigid pavements are load carrying capacity, the flexural strength, flexural impact, toughness and fatigue. All these parameters are superior in HSHPC concrete mix to the normal strength concrete. Therefore, on the basis of these properties, the HSHPC mix could be used in pavements for heavy vehicles.

The frequent use of HSHPC mixes in high rise buildings and bridges have also been discussed. HSHPC mix, also, has been used in pavements for patch repair, damaged sections and white toppings. But not has been used as full depth pavements. Therefore, on the basis of research survey, the efforts have been made to use HSHPC mix in heavy duty pavements.

To design HSHPC pavements for heavy vehicles, the existing design methods and analytical method i.e. Finite Element Method (FEM) for rigid and flexible pavements are discussed in Chapter-3.

CHAPTER – 3

PAVEMENT DESIGN

3.1 GENERAL

Civil Engineering fraternity in India has so far preferred the construction of flexible pavements. This is due to its initial lower cost, feasibility to stage construction and scarcity of cement. But now, the country has launched the highly ambitiousroad modernization programme which includes the construction of expressways and four laning projects to fulfill its need of road networks for infrastructure development. Therefore we need a re-appraisal of the past strategies. The country's road system has got a fillipand boost due to recently introduced National Highway Development Programme (NHDP) provoking a profound paradigmatic shift towards the construction of concrete roads due to abundant availability of cement in the country. In this context, cement concrete roads have a major role to play. Many four laning projects, expressways and many other district roads (ODRs) and village roads (VRs) are being constructed of concrete. World Bank States that "A technical option that has not been sufficiently explored in developing countries, particularly in the humid tropics, is the use of Portland Cement Concrete Pavements". It is now well established fact that ifconcrete roads are properly designed and constructed could last long with negligible maintenance during design life. Although, initial construction cost are high but life cycle cost are low [133].

On the basis of structural behavior, the pavements are generally classified into two categories:

1. Flexible pavements
2. Rigid pavements.

3.1.1 Flexible Pavements

These pavements have negligible flexural strength. The deformation of the lower layer reflects on to the surface of layers. Thus if the lower layer of the pavements or soil subgrade is undulated, the flexible pavement surface also gets undulated. The flexible pavements layer transmits the vertical or compressive stresses to the lower layers by grain to grain transfer

through the points of contact in granular structure. A well compacted layer will transmit the load through a wider area and thus forms a good flexible layer.

3.1.2 Rigid Pavements

These pavements have significant flexural strength depending on the strength of concrete used for the pavements. The rigid pavement has the slab action and is capable of transmitting the load stresses through a wider area below. The main point of difference in the structural behaviour of rigid pavement as compared to flexible pavement is that the critical condition of stresses in rigid pavement are the maximum flexural stresses occurring in the slab due to wheel load and the temperature changes whereas in the flexible pavement, it is the distribution of compressive stresses. Due to bending of the slab under wheel load and temperature variation, the tensile stresses are developed in cement concrete pavement. Thus the types of stresses developed in cement concrete pavement are quite different as compared to the flexible pavement. The rigid pavement does not get deform to the shape of the lower surface as it can bridge over the minor variations of lower layer.

3.2 HEAVY VEHICLES

In India, mainly three types of vehicles having rear axle load of 10.2 tonnes, 19.0 tonnes and 24.0 tones are used. Up to a load of 10.2 tonnes, normal truck having four wheel in the rear axle, between load 10.2 to 19 tonnes, 2 axle of four wheel each either in single or tandem combination and beyond the load 19.0 tonnes and up to 24.0 tonnes load, there are three single axle or one single one tandem or one tridem axles are used. These are shown in Figure 3.1 . Beyond 24.0 tonnes load various combinations of single, tandem and tridem axles are used.

Front axle Rear axle

Rear single axle of 10.2 tonnes

Front axle Rear axle

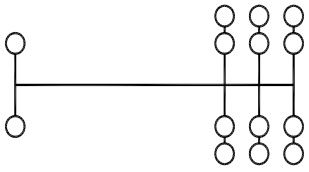

Rear tridemaxle of 24 tonnes

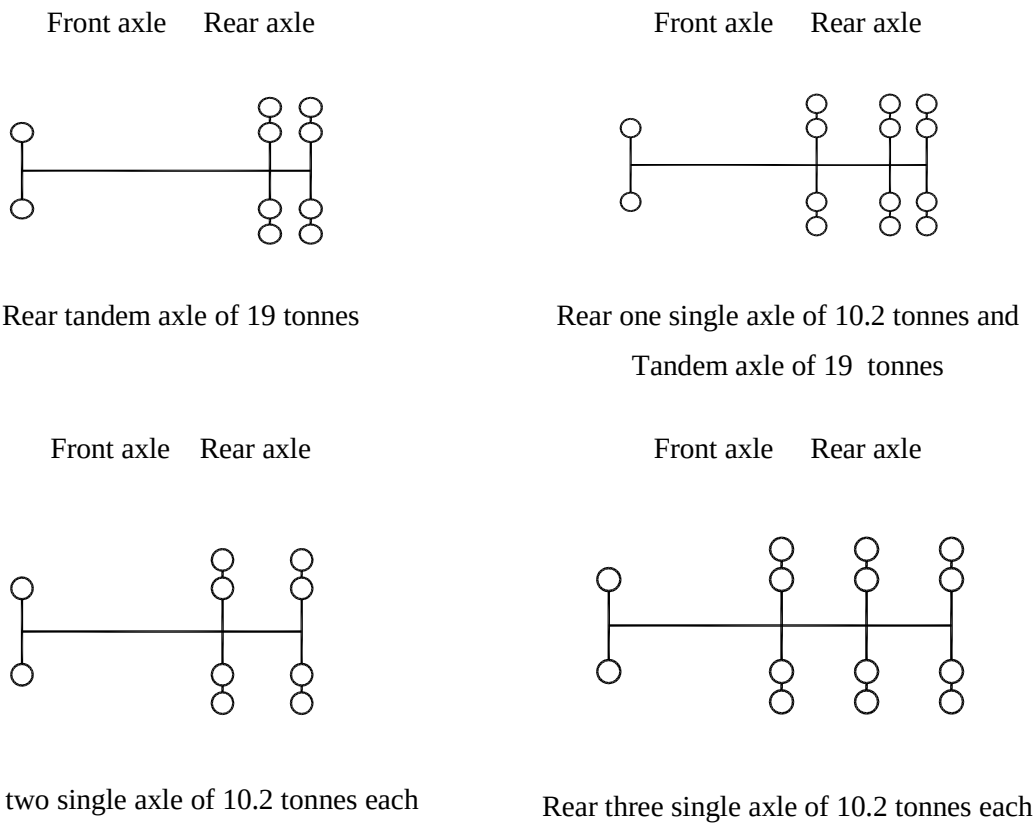

Fig. 3.1: Details of Types of Heavy Vehicles

Flexible pavements are designed for total numbers of equivalent standard axle loads of 80 kN for their design period. But due to commercial activities, the heavy vehicles are also using the existing flexible pavement system. Because of these heavy vehicles, the pavement will achieve earlier total numbers of equivalent standard axle loads and pavement will fail earlier.

Therefore, while designing the flexible pavements, the considerations should be given to these heavy vehicles. To consider the effect of heavy vehicles average daily traffic data should be collected for different types of vehicles. Axles weight distribution and configuration data are also collected. Then these heavy vehicles of any axle configuration and weight are converted to equivalent standard axle of loads 80 kN by using load equivalency factors suggested by AASHTO (1993). During design period, the total numbers of design ESALs is calculated due to heavy and normal vehicles. These total numbers of ESALs are used in the design of flexible pavement.

Considering the case of 4500 heavy vehicles having composition of traffic as type-I vehicles 2000, type-II vehicles 1500 and type-III vehicles 1000 as shown in Figure 3.2. The VDF would be calculated as given in Table 3.1.

1. Type – I: Rear standard axle with dual wheel of 10.2 tonnes

Front axle Rear axle

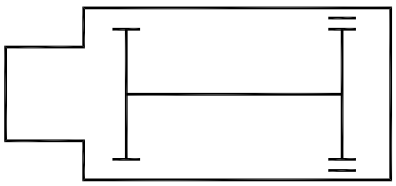

Axle load 6.0 tonnes 10.2 tonnes

Total number of vehicles = 2000

Weight of vehicle = 16.2 tonnes

2. Type – II: Rear tandem axles of 19 tonnes

Front axle Rear axle

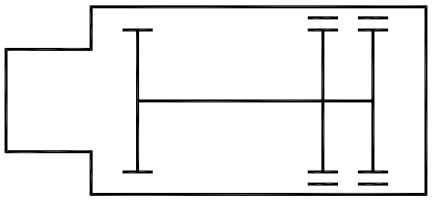

Axle load 6.0 tonnes 19.0 tonnes

Total number of vehicles = 1500

Weight of vehicle = 25.0 tonnes

Types-II vehicle in terms of type-I standard vehicle = (25 / 16.2) = 1.543

3. Type – III: Rear tridem axle of 24 tonnes

Front axle Rear axle

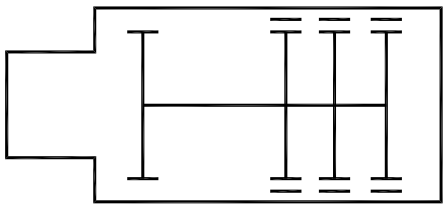

Axle load	6.0 tonnes	24.0 tonnes
Total number of vehicles	= 1000	
Total weight	= 30.0 tonnes	

Types-III vehicle in terms of type-I standard vehicle = (30 / 16.2) = 1.852

Fig. 3.2Different Axle Configurations of Heavy Vehicles

Total number of vehicles in terms of type-I standard vehicles would be equal to the sum of type-I, type-II and type-III.

Type-II vehicles =1.543×1500 = 2315 Type-I vehicles

Type-IIIvehicles =1.852×1000 = 1852 Type-I vehicles

Thus total number of vehicles in terms of Type-I vehicles = 2000 + 2315 + 1852

= 6167.

Vehicle damage factor of 10.2 tonne axle in terms of 8.2 tonne axle = $(10.2 / 8.2)^4$

= 2.394

Table 3.1: Calculationof VDFfor Heavy Vehicles

Sl. No.	Vehicle details	Heavy vehicles types		
		Type-I	Type-II	Type- III
		Standard axle of 10.2 tonnes	Tandem axle of 19.0 tonnes	Tridem axle of 24.0 tonnes
1.	Number of vehicles	2000	1500	1000
2.	Numbers of vehicles in terms of standard axles of 10.2 tonnes	2000	2315	1852
3.	Actual VDF values in terms of 10.2 tonnes vehicle	1	1.543	1.852
4.	Combined VDF value in terms of 8.2 tonnes	2.394		

(Veeraragavan et al., www.h-a-d.hr/pubfile.php?id.709)

Total ESLAs during design (N) life 15 years would be calculated as

$$N = \frac{365 \text{ x } A \text{ x } \{(1+r)^n - 1\}}{r} \text{ x } D \text{ x } F$$

Where,

N = cumulative number of standard axles during the design period

A = initial number of axles per day in the year when the road is operational

r = annual rate of growth of commercial traffic

n = design period in years.

D = lane distribution factor.

F = vehicle damage factor

For 4500 heavy vehicles, total number of equivalent standard axles during the design period would be

$$N = \frac{365 \text{ x } 6167 \times \{(1+0.075)^{15} - 1)\}}{0.075} \text{ x } 0.75 \text{ x } 2.394$$

$$= 105.6 \text{ msa}$$

$$\text{Say} \quad = 106 \text{ msa}$$

Now for total ESALs, for 15 years design period, 106 msa traffic corresponding to 4500 heavy vehicles, the total design pavement thickness would be found out using IRC-37 method for given CBR value of subgrade.

3.3 DESIGN OF FLEXIBLE PAVEMENTS

3.3.1 General Principle

Flexible pavement generally consists of number of elastic layers. Each layer consists of material characterized by modulus of elasticity, the resilient modulus and poisson's ratio. Soil subgrade is assumed infinite in both directions i.e. horizontally and vertically and layers are finite in vertical direction and infinite in horizontal direction. During design, it is to be ensured that under application of load none of the layer is over stressed. This means that at any instance no section of the pavement structure is subjected to excessive deformation to form a localized depression or settlement. The maximum intensity of stresses occurs in the top layer of the pavement. The magnitude of load stresses reduces at lower layer. Hence the high quality materials are used in top layers of flexible pavements.

For design of flexible pavements, yet it has not been possible to have a rational design methods wherein design process and service behaviour of pavement can be expressed or predicted by mathematical laws. Accordingly, the flexible pavement design methods are empirical, semi empirical and theoretical. There are numerous design methods of flexible pavements. Some of the methods are as given below:

(1) Group Index Method
(2) Triaxial Test Method
(3) McLeod Method
(4) Burmister Method
(5) Indian Road Congress Method (IRC-37)

(6) Road Note Number 29 Method

3.3.2 IRC: 37 Method

As per IRC: 37, "Guidelines for the Design of Flexible Pavements", using the following input parameters, appropriate design thicknesses could be chosen from the plates for the given traffic and soil strength:

(i) Design traffic in terms of cumulative number of standard axles and

(ii) CBR value of soil subgrade.

The procedure for estimating design traffic and assessing the CBR value of subgrade soil is described below [59, 60].

3.3.2.1 Design traffic

IRC-37 method considers design traffic in terms of cumulative number of standard axles (80 kN) to be carried by pavement during the design life. Following information is needed for estimating design traffic.

Assessment of the present day average traffic should be based on seven days 24 hour count made in accordance with IRC: 9-1972 "Traffic Census on Non-Urban Roads". Only the number of commercial vehicles having gross vehicle weight of 30 kN or more and their axle-loading is considered for the purpose of design of pavement. Traffic growth rate during the design life in percentage should be analyzed by the study. If the data for the annual growth rate of commercial vehicles is not available, a growth rate of 7.5 percent should be used as per IRC: SP: 84-2009 [64, 65].

3.3.2.2Design life

The design life is defined in terms of cumulative number of standard axles in msa that can be carried by a pavement before a major strengthening, rehabilitation, or capacity augmentation of the pavement is necessary.

A minimum design life for national highway and state highway is 15 years. Expressways and Urban Roads may be designed for a longer life of 20 years or higher using innovative design adopting high fatigue bituminous mixes. For other categories of roads, a design life of 10 to 15 years may be adopted.

3.3.2.3 Vehicle damage factor (VDF)

The Vehicle Damage Factor (VDF) is a multiplier to convert the number of commercial vehicles of different axle loads and axle configurations into the number of repetitions of standard axle load of magnitude 80 kN. It is defined as equivalent number of standard axles per commercial vehicle. The VDF varies with the vehicle axle configuration and axle loading.

Since the VDF values in AASHTO Road Test for flexible and rigid pavement are not much different, for heavy duty pavements, the computed VDF values are assumed to be same for bituminous pavements with cemented and granular bases. The equations for computing equivalency factors for single, tandem and tridem axles are given below should be used for converting different axle load repetitions into equivalent standard axle load repetitions.

$$\text{Single axle with single wheel on either side} = \left[\frac{\text{Axle load in kN}}{65}\right]^4 \quad (3.1)$$

$$\text{Single axle with dual wheels on either side} = \left[\frac{\text{Axle load in kN}}{80}\right]^4 \quad (3.2)$$

$$\text{Tandem axle with dual wheels on either side} = \left[\frac{\text{Axle load in kN}}{148}\right]^4 \quad (3.3)$$

$$\text{Tridem axles with dual wheels on either side} = \left[\frac{\text{Axle load in kN}}{224}\right]^4 \quad (3.4)$$

Axle load survey should be carried out without any bias, for loaded or unloaded vehicles. On some sections, there may be significant difference in axle loading in two directions of traffic. In such situations VDF should be evaluated direction wise. VDF should be arrived at carefully by carrying out specific axle load survey on the existing roads.

3.3.2.4 Distribution of commercial traffic over the carriageway

Distribution of commercial traffic in each direction and in each lane is required for determining the total equivalent standard axle load applications to be considered in the design [136]. In the absence of adequate and conclusive data, the following distribution may be assumed until more reliable data on placement of commercial vehicles on the carriageway lanes are available:

(i) Single-lane Roads

Traffic tends to be more channelized on single-lane roads than two-lane roads and to allow for this concentration of wheel load repetitions, the design should be based on total number of commercial vehicles in both directions.

(ii) Two-lane single carriageway roads

The design should be based on 75 percent of the total number of commercial vehicles in both directions. If vehicle damage factor in one direction is higher then the traffic in the direction of higher VDF is recommended for design.

(iii)**Four-lane single carriageway roads**

The design should be based on 40 percent of the total number of commercial vehicles in both directions.

(iv)**Dual carriageway roads**

The design of dual two-lane carriageway roads should be based on 75 percent of the number of commercial vehicles in each direction. For dual three-lane carriageways and dual four lane-carriageways, the distribution factor will be 60 percent and 45 percent respectively.

Where there is no significant difference between traffic in each of the two directions, the design traffic for each direction may be assumed as half of the sum of traffic in both directions. Where significant difference between the two streams exists, pavement thickness in each direction can be different and designed accordingly.

For two way two lane roads, pavement thickness should be same for both the lanes even if VDF values are different in different directions and designed for higher VDF. For divided carriageways, each direction may have different thickness of pavementlayer if the axle load patterns are significantly different.

3.3.2.5Subgrade

The top 500 mm of subgrade should be well compacted to limit the scope of rutting in pavement due to additional densification during the service life of the pavement. Subgrade shall be compacted to a minimum of 97 percent of laboratory dry density achieved with heavy compaction as per IS:2720 (Part 8) for Expressways, National Highways, State Highways, Major District Roads and other heavily trafficked roads [73].

For high category roads, like Expressways, National Highways and State Highways, the material used for subgrade construction should have the dry density of not less than 1.75 gm/cc.

For design, the subgrade strength is assessed in terms of the CBR of the subgrade soil in both fill and cut sections at the most critical moisture conditions likely to ocur in-situ. As a general practice, the worst field moisture is simulated by soaking the specimens in water for four days.

For determining the CBR value, the standard test procedure should be strictly adhered to. IS: 2720 (Part-16) "Methods of Test for Soils; Laboratory Determination of CBR" should be used. The test must always be performed on remoulded samples of soils in laboratory. Wherever possible the test specimens should be prepared by static compaction but if not so possible, dynamic method may be used as an alternative [74].

3.3.2.6Pavement design catalogues

In IRC-37, different combinations of traffic and material properties have been considered for which pavement compositions have been suggested in the form of design charts presented in plates 1 and 2. The design thicknesses have been proposed in these plates. In present study,the combination of Granular Base and Granular Subbase has been used [60].

As per IRC-37, the design thickness for different traffic and CBR value is given in Fig. 3.3.

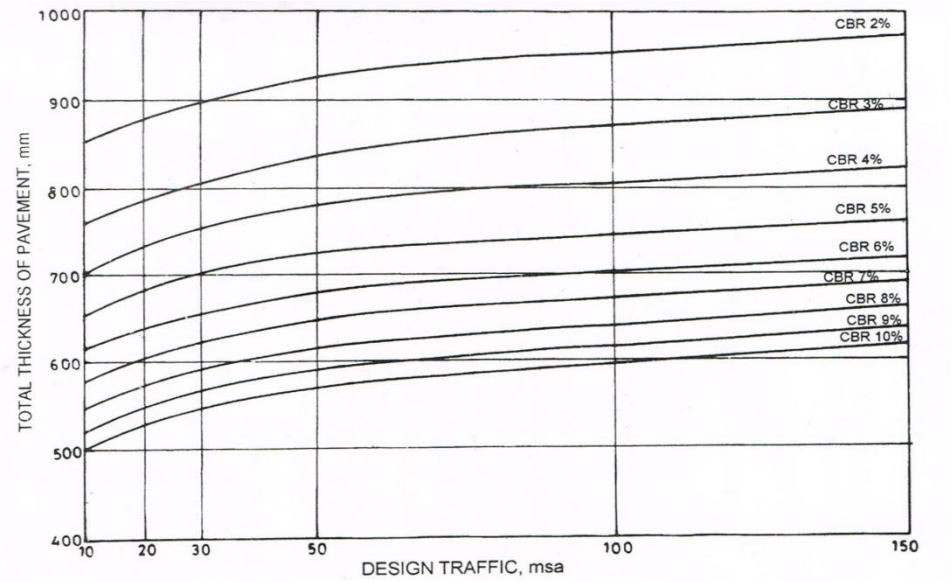

Fig. 3.3: Pavement Thickness Design Chart for Traffic 10-150 msa

3.4 DESIGN CALCULATIONS OF FLEXIBLE PAVEMENTS USING IRC-37 METHOD

In India, the design of flexible pavements isdone by IRC-37 method. The design thickness of flexible pavements depends on CBR values of soil subgrade. Lower the CBR value, higher the thickness of flexible pavement. The total pavement thicknesses with three cases of traffic volumeswith different CBR are given in following Table 3.2.

Table 3.2: Total Design Thicknesses for Different Traffic for Different CBR Values

Sl. No.	CBR value (percent)	Total pavement thickness for traffic (mm)		
		5 msa	50 msa	150 mas
1	2	795	925	975
2	6	535	660	700
3	10	475	585	625

From Table 3.2, it is evident that for the same CBR value, the total pavement thickness increases as the traffic increases. But from 50 msa traffic to 150 msa traffic the increase in total pavement thickness is very less.

For experimentally obtained 6% CBR, traffic growth rate 7.5% and design life 15 years, the following three cases have been considered for the design of two lane single carriage way flexible pavements.

(i) For 200 heavy vehicles and vehicle damage factor (VDF) 3.5, the cumulative number of standard axles to be carried for two lane single carriage way during the design life is 5 msa.

(ii) For 1550 heavy vehicles and VDF 4.5, the cumulative number of standard axles to be carried for two lane single carriage way during the design life is 50 msa.

(iii) For 4500 heavy vehicles and VDF 4.5, the cumulative number of standard axles to be carried for two lane single carriage way during the design life is 150 msa.

The composition of design thicknesses for 5 msa, 50 msa and 150 msa traffic and for CBR 6% is given in Table 3.3.

Table 3.3Composition of Design Thicknesses for 5 msa, 50 msa and 150 msa for 6% CBR

Sl. No.	Traffic msa	Total pavement thickness (mm)	Composition of Pavement Thickness			
			Wearing course (mm)	Binder course (mm)	Base (mm)	Sub-base (mm)
1	5	535	SDBC = 25	DBM = 50	WMM = 250	GSB = 210
2	50	660	BC = 40	DBM = 110	WMM = 250	GSB = 260
3	150	700	BC = 50	DBM = 140	WMM = 250	GSB = 260

As the numbers of heavy vehicle increase, the cumulative numbers of standard axles to be carried during design life will exceed the limit of 150 msa. Considering the case 6000 heavy vehicles and VDF 4.5 for two lane single carriage way, the cumulative numbers of standard axles come out as 193 msa for design period 15 years, traffic growth rate 7.5%. For 6000 heavy vehicles, CBR 6%, traffic growth rate 7.5% and vehicle damage factor (VDF) 4.5, the composition of flexible pavements thicknesses for different design periods 5, 10 and 13 years are given in the following Table 3.4.

Table 3.4: The Design of Flexible Pavement for 6000 Heavy Vehicles and 6% CBR for Different Design Life

Sl. No.	Design Life	Traffic msa	Composition of pavement thicknesses				
			Wearing course (mm)	Binder course (mm)	Base (mm)	Sub base (mm)	Total pavement thickness (mm)
1	5	43	40	108	250	260	658
2	10	105	50	127	250	260	687
3	13	150	50	140	250	260	700

From the above Table 3.4, it is clear that for 6000 heavy vehicles, as the design life 13 years is attained, the maximum numbers of cumulative standard axles i.e. 150 msa the maximum limit prescribed by IRC-37 is achieved. If the same flexible pavement thickness is used for 15 years design period, for which cumulative numbers of standard axles is 193 msa, which exceeds 150 msa, in such case the pavement will fail earlier and require early rehabilitation. IRC - 37 does not recommend design thickness beyond 150 msa.

In such case, the options are either the design period should be reduced to corresponding to 150 msa traffic or design curves for more than 150 msa traffic should be developed.

3.5 FACTORS GOVERNING THE DESIGN OF RIGID PAVEMENTS

The main design parameters which govern the design of concrete pavements are design period, design commercial traffic volume, composition of commercial traffic in terms of single, tandem, tridem and multi-axles, axle load spectrum, tyre pressure of commercial vehicles, lateral placement characteristics of commercial vehicles, directional distribution of commercial vehicles, composition and strength of foundation and climatic considerations [62, 63].

3.5.1 Axle Load Characteristics and Tyre Pressure

Legal axle load limits in India are 10.2 tonnes (100 kN) for single axle, 19 tonnes (186 kN) for tandem, and 24 tonnes (235 kN) for tridem axles. But the actual axle loads operating

on highways in India are much higher than the prescribed limits due to lack of enforcement of laws. It is essential to collect the data of axle load spectrum of commercial vehicles i.e. single, tandem and tridem axles in each direction during the design period. Minimum percentage of commercial vehicles to be weighed should be 10 percent for volume of commercial vehicles per day (CVPD) exceeding 6000, 15 percent for CVPD for 3000 to 6000 and 20 percent for CVPD less than 3000. Axle load survey should be conducted for a continuously 48 hour period. To avoid biasness, the vehicles surveyed should be randomly selected. If the spacing of the consecutive axles is more than 2.4 m, each axle may be considered as a single axle.

Generally, tyre inflation pressure of heavy commercial vehicles may range from about 0.7 MPa to 1.0 MPa. It has been noticed that for the slabs of thickness 200 mm or more, the variation in tyre inflation pressure has little effect on flexural stress in pavement slabs.

3.5.2 Design Period

Generally cement concrete roads are designed for a life span of 30 years or more. However, the design engineer should use his judgment about design period taking into various considerations such as uncertainty of traffic growth rate, traffic volume, the capacity of roads and the possibility of augmentation of capacity by widening.

3.5.3 Design Traffic

The lane carrying the maximum number of heavy commercial vehicles is termed as design lane. Each lane of a two-way two-lane highway and the outer lane of multi-lane highways are generally considered as design lanes.

Assessment of average traffic should normally be based on seven days 24-hour count made in accordance with IRC: 9 “Traffic Census on Non-Urban Roads” [64]. The actual value of growth rate ‘r’ of heavy commercial vehicles should be determined. However, if actual data is not available an average annual growth rate of 7.5% may be adopted. The wheels of commercial vehicles travelling along the edge or tangentially of the outer lane, cause critical stress condition. A very low percentage of vehicles meet this condition for both two-way two-lane and four-lane divided highways. As per some research, 25 percent of the total two-lane two-way commercial vehicles are considered as design traffic. For four-lane and multi-lane

divided highways, 25 percent of the total traffic in the predominant direction is considered as design traffic. In case of new highway, where no traffic data is available, data from roads of similar classification and importance may be used to predict the design traffic. The above mentioned percentage of design traffic is very conservative estimate. Portland Cement Association considers only 6% of the traffic for thickness design. The cumulative number of repetitions of axles during the design period may be computed from the following formula:

$$N = \frac{365 \text{ x } \{(1+r)^n - 1\}}{r} \text{ x } A \times D \text{ x } F \qquad (3.5)$$

Where,

N = cumulative number of axles during the design period

A = initial number of axles per day in the year when the road is operational

r = annual rate of growth of commercial traffic

n = design period in years

D = lane distribution factor

F = vehicle damage factor (VDF).

3.5.4 Temperature Considerations

3.5.4.1 Westergaard's concept for temperature stresses

Temperature stresses are developed in cement concrete pavements due to variation in slab temperature. The variation in temperature across the depth of slab is caused by daily variation, which produces warping stresses whereas frictional stresses are caused by an overall increase or decrease in slab temperature is caused by seasonal variation in temperature.

Thus due to variation in temperature, two types of stresses are developed:

(1) Warping Stresses

(2) Frictional Stresses

3.5.4.1.1 Warping stresses

Whenever the top and bottom surfaces of a concrete pavement simultaneously posses different temperatures, the slab tend to warp downwards or upwards inducing warping stresses. Warping stresses are caused due to variation in daily temperature.

If surface temperature is t_1 degree and the bottom temperature is $t_2$degree, the difference of temperature between top and bottom surfaces is equal to $(t_1 – t_2) = t$ degrees.

Assuming straight line variations of temperature across the pavement depth, the average temperature of the slab would be $(t_1 + t_2) / 2$.

If the slab has no restraint, then unit elongation of the top fibres and also unit contraction of the bottom fibres due to relative temperature condition, each would be equal to Eet/2, where ‘e’ is the thermal coefficient of concrete. Westergaard worked out the stresses, due to warping of concrete slab. Later, introducing the effect of poison’sratio,Bradberry developed a chart to find out the warping stresses at critical locations i.e.Edge,Corner and Centre [92].

3.5.4.1.2 Frictional stresses

Due to uniform temperature rise and fall in the cement concrete slab, there is an overall expansion and contraction of the slab. Since the slab is in contact with the soil sub-grade or sub-base, the slab movements are restrained due to the friction between the bottom layer of pavement and soil layer. This frictional resistance therefore tends to prevent the movements, thereby, inducing the frictional stress in bottom fibres of the cement concrete pavement. Stresses in the slabs, resulting due to this phenomenon, vary with slab length. In short slab, stresses induced due to this is negligibly small whereas in long slabs, which would undergo movements of more than 0.15 cm, the higher amount of frictional stresses are developed.

IRC guidelines use Bradbury’s equations which are based on assumptions such as (i) linear temperature variation through the depth of slab (ii) slab resting on winkler foundation (iii) full contact between the pavement slab and the subgrade.

The difference of temperature between top and bottom fibres of concrete pavements causes the concrete slab to curl, giving rise to stresses. The temperature differential is a

function of solar radiation received by the pavement surface, wind velocity, thermal diffusivity of concrete, latitude, longitude and elevation of the place and is thus affected by the geographical features of the pavement location. As far as possible, values of actually anticipated temperature differentials at the location of the pavement should be adopted for pavement design. In the absence of any local data, the maximum temperature differential values given in IRC-58-2012 may be adopted for pavement design.

3.5.4.2 Thomlinson's temperature stress analysis

J. Thomlison in 1940 provided an analytical approach for temperature stress computations. From actual measurement of temperature in cement concrete pavements using thermocouples, it has been observed that the temperature gradient across the slab thickness is curvilinear as against the assumption of straight line variation by Westergaard. Thomlinsondeveloped an analysis which yields results closer to the experimental data and lower than Westergaard's equations [33, 34, 120, and 165].

3.6 CHARACTERISTICS OF SUBGRADE AND SUBBASE

3.6.1 Subgrade

The main function of the subgrade is to provide adequate support to the pavement from beneath. For this, the subgrade should possess sufficient stability under adverse climate and loading conditions. The formation of waves, corrugations, rutting and showing in black top pavements and the phenomenon of pumping, blowing and consequent cracking of cement concrete pavements are generally attributed due to the poor subgrade conditions. Therefore, soil should possess adequate stability or resistance to permanent deformation under loads and should possess resistance to weathering, thus retaining the desired subgrade support. Minimum variation in volume will ensure minimum variation in differential expansion and strength values. Good drainage is essential to avoid excessive moisture retention and to reducethe potential frost action. Ease of compaction ensures higher dry density and strength under particular type and amount of compaction [92].

The strength of subgrade is expressed in terms of modulus of subgrade reaction K, which is defined as pressure per unit deflection of the foundation as determined by Plate Bearing Test. The deflection level is taken 0.125 cm. If p is the pressure sustained in $kg/cm^2$by

the rigid plate of diameter 75 cm at a deflection (Δ) = 0.125 cm, the modulus of subgrade reaction 'K' is given by

$$K = \frac{P}{\Delta} = \frac{P}{0.125} \text{ kg / cm}^3 \quad (3.6)$$

3.6.2 Subbase

The main purpose of the subbase is to provide a uniform, stable and permanent support to the concrete slab laid over it. It must have sufficient strength so that it is not subjected to disintegration and erosion under heavy traffic and adverse environmental conditions such as excessive moisture, freezing and thawing. Therefore, to meet these requirements, subbase of Dry Lean Concrete (DLC) having 7days average compressive strength of 10 MPa should be used. This should be determined as per IRC-SP: 49. Minimum recommended thickness of DLC for major highways is 150 mm [62, 63].

3.7 CHARACTERISTICS OF CONCRETE

3.7.1 Design Strength

Concrete pavement design is based on flexural strength, since concrete pavements fail due to bending stress. For the pavement construction, the concrete mix should be designed as per the specified flexural strength.Flexural strength should be determined by modulus of rupture test under third point loading. The test should be conducted as per IS: 516 [77].

Alternatively, the flexural strength can be derived from the characteristic compressive strength of concrete as per IS: 456-2000 using the following relationship:

$$F_{cr} = 0.7\sqrt{f_{ck}} \quad (3.7)$$

F_{cr} = flexural strength (modulus of rupture),MPa.

f_{ck} = characteristic compressive strength of concrete, MPa.

The Elastic Modulus (E) increases with increase in strength and Poisson's Ratio (μ) decreases with increase in modulus of elasticity. These values should be determined

experimentally since these depend on concrete mix. A 25 percent variation in E and μ values does not have any significant effect on the flexural stresses in the concrete pavement.

As per IS: 456-2000, the modulus of elasticity is determined by the following relation:

$$E = 5000\sqrt{f_{ck}} \tag{3.8}$$

E = short term static modulus of elasticity in N/mm^2

f_{ck} = characteristic compressive strength in MPa.

3.7.2 Fatigue Behavior of Cement Concrete

Due to repeated applications of flexural stresses by the traffic loads, the progressive fatigue damage take place due to development of micro-cracks especially when ratio between the applied flexural stress and the flexural strength of concrete is high. This ratio is termed as stress ratio (SR). If the SR is less than 0.45, the concrete is expected to sustain infinite number of repetitions. As the stress ratio increases the number of load repetitions required to cause cracking decreases. The relation between fatigue life (N)and stress ratio (SR) is given as

$$N = \text{unlimited for } SR < 0.45 \tag{3.9}$$

$$N = \left[\frac{4.2577}{SR - 0.4325}\right]^{3.268} \quad \text{when } 0.45 \le SR \le 0.55 \tag{3.10}$$

$$\log_{10} N = \frac{0.9718 - SR}{0.0828} \quad \text{for } SR > 0.55 \tag{3.11}$$

Use of fatigue criteria is made on the basis of Miner's hypothesis. Fatigue resistance not consumed by repetitions of one load is available for repetitions of other loads.

3.8 DIFFERENT THEORIES FOR THE ANALYSIS OF STRESSES IN RIGID PAVEMENTS

Westergaards formulae is being used for the analysis and design of cement concrete pavements, wherein the foundation is Winkler type [182, 183] or the stress analysis advanced by Westergaard, Picket, Hall and Hogg [54, 56 , 125], in which subgrade is treated as elastic continum. The design based on elastic theory, is based on working stresses [27, 28, 29],

Mayerhof's and Ghosh's [48, 101] analysis is based on ultimate strength or yield line theory. The stresses in rigid pavements are very close to the flexural strength, therefore Ghosh suggested that rigid pavement should be designed based on breaking load reduced by a suitable load factor. In India, highway pavements are designed in accordance with IRC-58 'GuideLines for the Design of Plain Jointed Rigid Pavements for Highways'. The load stresses in critical edge region may be obtained as per Westergaard analysis, modified by Teller and Sutherland [161, 162]. The load stresses in the corner region may be obtained as per Westergaard's analysis, modified by Kelly [89].

Cement concrete pavements represent the group of rigid pavement. There are many theories for the analysis of stresses in rigid pavements. Some of these are:

(i) Westergaard's Analysis
(ii) Mayerhof'sAnalysis
(iii)Ghosh'sAnalysis
(iv)IRC-58 Method.

Pavement could be designed more rationally by using analytical method like Finite Element Method (FEM).

3.8.1 Westergaard's Analysis

Load carrying capacity of cement concrete pavements is due to high rigidity and high modulus of elasticity of concrete slab i.e. slabaction. In 1926, H.M. Westergaard provided the rational formulae for calculations of stresses in concrete pavements. Westergaard used classical bending theory for the analysis of stresses. The following assumptions are made in the analysis:

(i) Concrete slab is thin elastic plate of uniform thickness.
(ii) Subgrade soil is like an elastic dense liquid and upward reaction is proportional to the deflection.
(iii)The wheel load is uniformly distributed over a circular contact area.
(iv)The slab is fully in contact with subgrade.
(v) The load at the edge of the slab is distributed uniformly over semi-circular contact area, the diameter of semi-circle being along the edge of slab.

3.8.1.1 Modulus of subgrade reaction (K)

Since subgrade is elastic dense liquid, the vertical upward reaction (p) is proportional to the deflection (Δ).

$P = K\Delta$ where K is modulus of subgrade reaction.

$$K = \frac{p}{\Delta}$$

Where $\Delta = 0.125$ cm

p = pressure sustained in kg/cm^2 by the rigid plate of diameter 75 cm.

$$K = \frac{p}{0.125} = \frac{Kg}{cm^3} \qquad (3.12)$$

3.8.1.2 Relativestiffness of slab to subgrade (*l*)

Deflection of the slab depends upon the stiffness or pressure deformation properties of the subgrade material and also its flexural strength. The resultant deflection of the slab is a direct measure of subgrade pressure. The pressure deformation characteristics of rigid pavement are thus a function of relative stiffness of slab to that of subgrade. Westergaard defined this term as radius of relative stiffness (l):

$$l = \left[\frac{Eh^3}{12K(1-\mu^2)}\right]^{1/4} \qquad (3.13)$$

Where,

l = radius of relative stiffness, cm

E = modulus of elasticity of cement concrete, kg/cm^2

μ = poisson's ratio for concrete

h = slab thickness in cm.

K = subgrade modulus or modulus of subgrade reaction, kg/cm^3.

3.8.1.3 Critical load condition

Since pavement slab has finite length and width, the maximum stress induced by the application of load is dependent on the location on pavement surface. Three critical loading locations are interior, edge and corner. At these locations different conditions of slab continuity exist.

3.8.1.4 Equivalent radius of resisting section

According to Westergaard, the equivalent radius of resisting section is approximated in terms of radius of load distribution and slab thickness,

$$b = \sqrt{1.6\,a^2 + h^2} - 0.675\,h \qquad (3.14)$$

b = equivalent radius of resisting section, cm, when a < 1.724 h.

a = radius of wheel load distribution, cm

h = slab thickness, cm

when a > 1.724 h, then b = a.

3.8.1.5 Westergaard's stress analysis for wheel loads

The critical stresses S_i, S_e and S_c at interior, edge and corner region of cement concrete pavement slab are given as

$$S_i = \frac{0.316\,P}{h^2}\,[4\log_{10}(l/b) + 1.069] \qquad (3.15)$$

$$S_e = \frac{0.572\,P}{h^2}\,[4\log_{10}(l/b) + 0.359] \qquad (3.16)$$

$$S_c = \frac{3P}{h^2}\left[1 - \left(\frac{a\sqrt{2}}{l}\right)^{0.6}\right] \qquad (3.17)$$

S_i,S_e, S_c = maximum stress at interior, edge and corner loading respectively, kg/cm^2

h = slab thickness, cm

P = wheel load, kg

a = radius of wheel load distribution, cm

l = radius of relative stiffness, cm

b = radius of resisting section, cm.

3.8.2 Mayerhof's Theory

Rankine yield condition is being used by Mayerhof to evaluate the ultimate load carrying capacity of rigid pavement slabs for centre, edge and corner positions. According to Mayerhof, as the load increases, the flexural stress directly below the point of loading increases and become equal to the flexural strength of concrete used for casting the slab. The slab begins to yield, leading to the formation of radial tensile cracks in the bottom of the slab and with an increasing load the radial cracks increase in length until the flexural stress at the top of the slab becomes equal to the flexural strength of concrete mass, which is known as the Rankine yield condition at this stage. A circumferential crack appears on the slab surface and the slab fails completely under breaking load. The following equations are used to evaluate the collapse loads at different positions.

3.8.2.1 Centralloading

Collapse loads are computed from the following equations:

$$P_o = 2\pi M_o \text{ for } a = 0 \qquad (3.18)$$

$$P_o = \frac{4\pi M_o}{1 - \frac{a}{3l}} \quad \text{for} \quad \frac{a}{l} > 0.2 \qquad (3.19)$$

P_o= ultimate load in kg

M_o = maximum elastic or yield moment of resistance of slab per unit length

$$= \frac{h^2}{6}\sigma_b$$

l = radius of relative stiffness

$$= \left[\frac{E h^3}{12 k (1 - \mu^2)}\right]^{1/4}$$

σ_b = flexural strength of concrete, kg / cm^2

h = thickness of slab, cm

a = the contact radius, cm

E = modulus of elasticity of concrete, kg/cm^2

μ = poisson's ratio of concrete

K = modulus of subgrade reaction, kg/cm^3

3.8.2.2 Edgeloading

Collapse loads are computed from the following equations

$$P_o = \left[2 + \frac{\pi}{2}\right] M_o \qquad \text{for a = 0} \qquad (3.20)$$

$$P_o = \frac{(\pi + 4)\, M_o}{1 - \frac{2a}{3l}} \qquad \text{for} \frac{a}{l} > 0.2 \qquad (3.21)$$

All notations are having the same meaning as in central loading.

3.8.2.3 Cornerloading

Collapse load are computed from the following equations:

$$P_0 = \frac{4\, M_o}{\left(1 - \frac{a}{l}\right)} \quad \text{for } \frac{a}{l} > 0.2 \qquad (3.22)$$

$P_o = 2\, M_o$ for a = 0

All notations are having the same meaning as in central loading.

3.8.3 Ghosh's Analysis

Ghoshand Dinkaran(1970) presented analysis to determine the breaking load of pavement slab taking the effect of both load (centrally placed) and temperature independently and assuming transverse yield line under the load to devote the failure. Here the effect of temperature is not considered. Effect of wheel load is calculatedonly.

According to Ghoshand Dinkaran(1970) the yield line of slab at breaking under wheel load may be predicted by considering that as the slab passes strength beyond the elastic limit, an elasto-plastic region is formed and the rigidity of slab changes resulting in redistribution of the foundation reaction and the moment set-up in the slab. For the slab of large dimensions subjected to a concentrated load, the failure is most probably through formation of a circular and cone like plastic hinge. In case of slabs of limited width, as are normally used in pavement, the yield is more likely to occur along a line hinge over the width of the slab. The assumption of a line plastic hinge ratherthan a circular one at breaking load appears to be

more rational. This is also borne out from field experience; structural cracks near the centre or edge of slab are mostly in the transverse direction (i.e. along the width of the slab).

The breaking load is calculated from the following equation

$$P_o = \frac{2\pi M_o}{1 - \frac{a}{6l}} \qquad (3.23)$$

P_o = breaking load,kg

a = radius of the equivalent circle of the load contact, cm

M_o = maximum elastic or yield moment of resistance of the slab per unit length, kg-cm

$$= \frac{h^2}{6}\sigma_b$$

σ_b= flexural strength of concrete (kg / cm^2).

3.8.4 IRC-58 Method

The stresses for critical positions i.e. for edge position and corner position are obtained as below:

3.8.4.1 For edge position

The stresses may be obtained as per Weteraard analysis modified by Teller and Sutherland from the following equation.

$$\sigma_e = \frac{0.529\,P}{h^2}(1 + 0.54\,\mu)\left[4\log_{10}\left(\frac{l}{b}\right) + \log_{10} b - 0.4048\right] \qquad (3.24)$$

where

σ_e = load stress in edge region, kg/cm^2

P = design wheel load, kg

= half of single axle load.

= one-fourth of the tandem axle load.

h = pavement thickness, cm

μ = poisson's ratio for concrete.

K = modulus of subgrade reaction, kg/cm^3

l = radius of relative stiffness in cm

b = radius of equivalent resisting section, cm

a = radius of load contact area, assumed circular, cm.

3.8.4.2 For Corner position

Stress may be obtained by Wetergaard's analysis, modified by Kelly from the following equation:

$$S_c = \frac{3P}{h^2}\left[1 - \left(\frac{a\sqrt{2}}{l}\right)^{1.2}\right] \qquad (3.25)$$

Where

S_c = stress in corner region, other notations remaining the same as in the case of edge load stress formula, kg/cm^2

P = wheel load in kg

a = radius of equivalent circular contact area in cm.

The temperature stress in corner region is negligible, as the corners are relatively free to warp and, therefore, may be ignored.

3.8.5 Finite Element Method (FEM) Analysis

Engineers, Physicists and Mathematicians have developed finite element method independently. In 1943 Courant made an effort to use piecewise continuous functions defined over triangular domain.

After that it took nearly a decade to use this distribution idea. In fifties renewed interest in this field was shown by various researchers. They introduced the concept of applying energy principles to the formation of structural analysis problem in 1960. In the same year Clough introduced the word 'Finite Element Method. [21].

This is a numerical technique. This analysis gives approximate results. The problem having varying shapes, boundary conditions and complex loading conditions could be solved

rationally. Due to slash in cost of computer, these techniques becoming more popular, being the computerbasic need for this techniques.

The methods discussed so far are being used in the analysis of rigid pavements. To simplify the analysis, these methods are based on some assumptions and restrictions. These methods are not applicable under all circumstances. Basic need of structural design of rigid pavement is that no parts of pavement should be over stressed under the traffic load. For this, there is need of analysis for stresses, deflections and strains for the layered pavement systems having different characteristic properties of materials in the layers under complex loading and varying boundary conditions. To solve such problem with actual boundary conditions, material characteristics such as modulus of elasticity, poisson's ratio, the finite element is a powerful technique. In the present study ABAQUS, finite element software, has been used to find out stresses, strains and deflections for edge position. While the finite element analysis can also be used for central, corner and with discontinuities like joints and cracks for the analysis of stresses, strains and deflections. During the analysis, the foundation has been assumed elastic. A3-D finite element analysis for edge position has been done for concrete pavement [40].

The general procedure for obtaining the critical stresses are as:

1. The global nodal displacements $\{\delta\}_G$ are obtained by solving the governing equations. [K] is the global stiffness matrix. The global nodal force vector is {F}.

$$[K]\{\delta\}_G = \{F\} \quad (3.26)$$

2. The local element displacement vector $\{\delta\}_e$ can be selected from $\{\delta\}_G$. The displacement [U] at any point in the element can be determined by assumed shape function [N].

$$[U] = [N]\{\delta\}_e \quad (3.27)$$

3. Strains [ε] are calculated by the linear geometrical equations in the theory of elasticity.

$$[\varepsilon] = [B]\ \{\delta\} \quad (3.28)$$

[B] is the strain displacement matrix.

4. Stresses [σ]are calculated by Hooks law. [D] is the stress-strain matrix.

$$[\sigma] = [D]\ \{\in\} \quad (3.29)$$

3.8.5.1 Shape functions of the 3-D eight linear noded brick element

3-D Eight nodedlinear brick element and its local coordinates are shown in Figure-3.4. Whole pavement system i.e. pavement and soil has been divided into many such elements. These shape functions represent the variation of deflections within an element. Discritisation of the pavement model is shown in Figures 3.5 to 3.7.

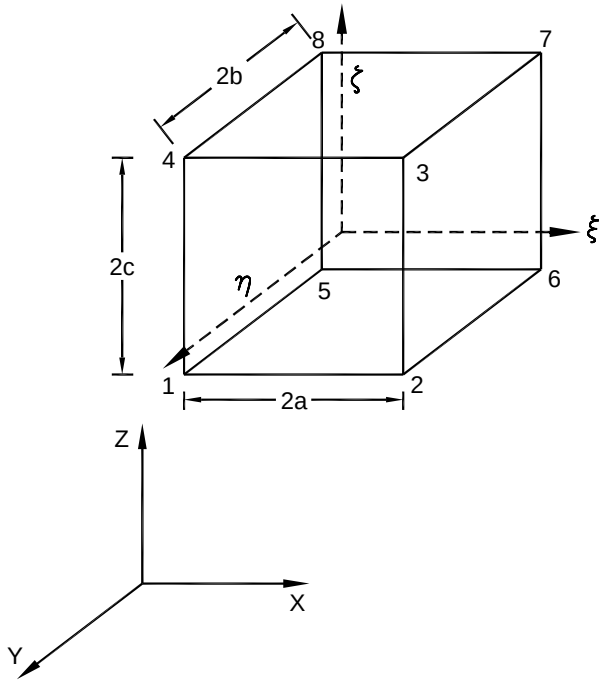

Fig. 3.43-D Eight Noded Linear Brick Element

$$N_1 = \frac{1}{8}(\xi + 1)\ (\eta - 1)(\zeta - 1) \tag{3.30}$$

$$N_2 = -\frac{1}{8}(\xi + 1)\ (\eta + 1)(\zeta - 1) \tag{3.31}$$

$$N_3 = \frac{1}{8}(\xi + 1)\ (\eta + 1)(\zeta + 1) \tag{3.32}$$

$$N_4 = -\frac{1}{8}(\xi + 1)\ (\eta - 1)(\zeta + 1) \tag{3.33}$$

$$N_5 = -\frac{1}{8}(\xi - 1)\ (\eta - 1)(\zeta - 1) \tag{3.34}$$

$$N_6 = \frac{1}{8}(\xi - 1)\ (\eta + 1)(\zeta - 1) \tag{3.35}$$

$$N_7 = -\frac{1}{8}(\xi - 1)\ (\eta + 1)(\zeta + 1) \tag{3.36}$$

$$N_8 = \frac{1}{8}(\xi - 1)\ (\eta - 1)(\zeta + 1) \tag{3.37}$$

In general

$\xi = \frac{x}{a}; \eta = \frac{y}{b}; \zeta = \frac{z}{c}$ andthe natural coordinate range from [-1, 1] for the element.

The stiffness matrix $[K]_e$ of the element with respect to nodal displacement $\{\delta\}$ is evaluated from the principle of virtual work by equalizing the internal virtual work done to the external work associated with the virtual displacements.

$$[K]_e = \int_{vol} [B]^T [D] [B].dv \tag{3.38}$$

The stiffness matrix $[K]_e$ is evaluated by numerical integration with the help of Gaussian Quadrature formula.

3.9 PROBLEM FORMULATION

The accuracy of FEM analysis depends on the selection of element and discritisation of the structure. As the number of nodes and order of element increases, the accuracy of

results increases. The same is true, if finer discritisation of the structure is done. For the present analysis, 3-D eight noded linear brick element has been considered for the analysis. A quadratic brick elements i.e. twentynoded has also been tried but the results obtained are approximately same as that for eightnoded linear brick element. This was verified by analysis done for 100 kN load at edge position. At 100 kN load, the deflection was 4.13 mm by twentynoded quadratic brick element as compared to the deflection 4.10 mm obtaionedby considering eight noded linear brick element. Also, the computation time was also high for 20 noded quadratic brick element. Therefore, it was decided to carry out analysis considering eight noded linear brick element.

Amrit Singh (1976) has shown in his analysis that effect of load in vertical direction i.e. depth wise beyond the eight times of the radius of loaded area is negligible and in the horizontal direction beyond four times the radius of loaded area is negligible. This criteria of analysis has also been used by Vasan, goyal and Kacharoo [52, 83, 177]. On this basis, the depth of soil is taken as 2.0 m and horizontal length 6.0 m, which are more than the above mentioned criteria. The model is shown in Figures 3.5 to 3.7. During the analysis by FEM, the half of the slab, line passing through the centre of test plate has been considered due to symmetry. This lead to significant reduction of computation time.

By using FEM analysis, the performance of HSHPC pavements of any thicknesses can be carried out.

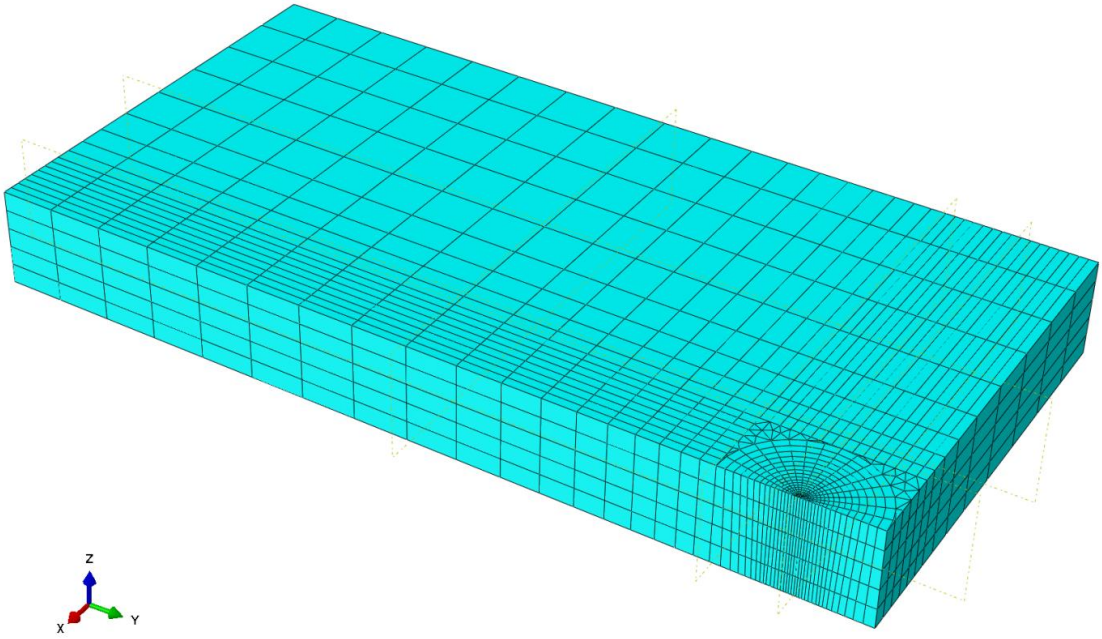

Fig. 3.5Discritisation of the Slab - 3-D Eight Noded Linear Brick Element

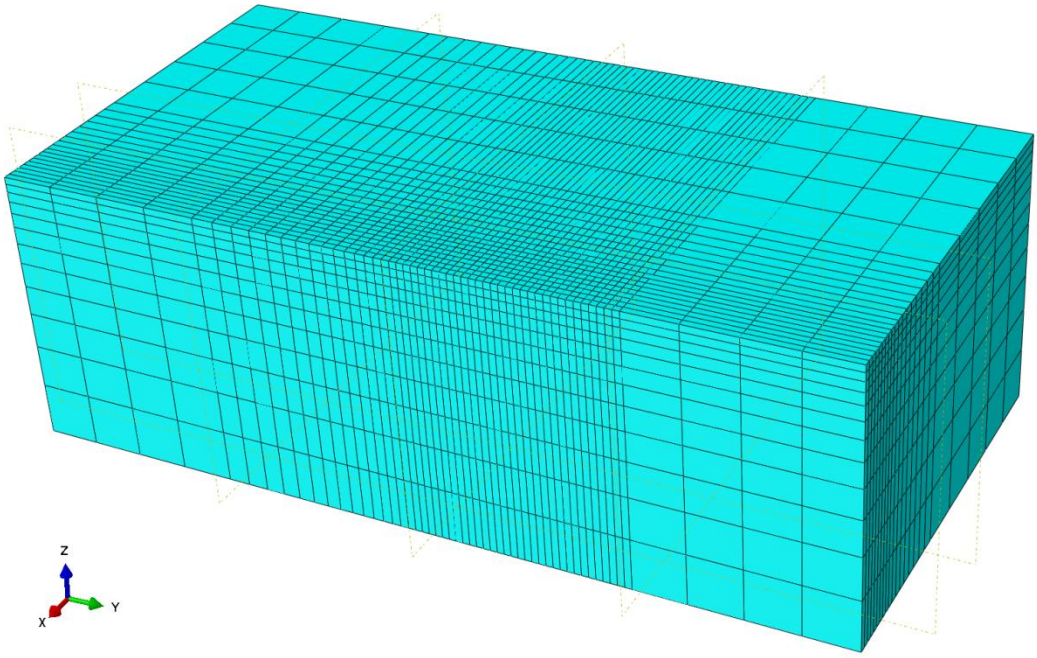

Fig. 3.6Discritisation of the Soil - 3-D Eight Noded Linear Brick Element

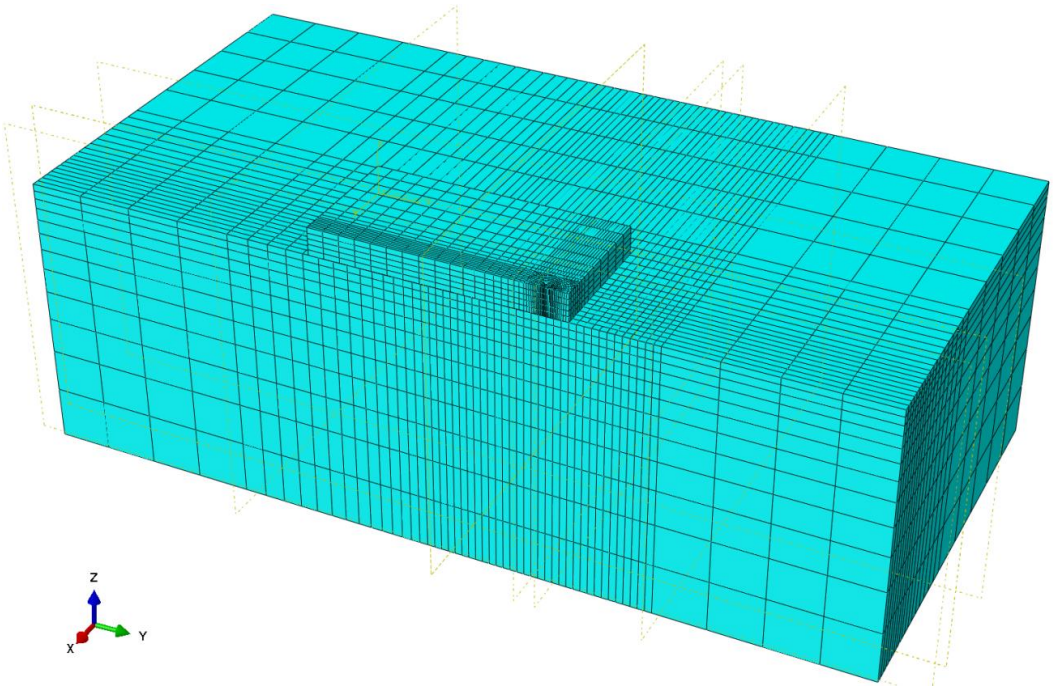

Fig. 3.7Discritisation of the Slab and Soil Together - 3-D Eight Noded Linear Brick Element

3.10 FACTOR OF SAFETY (F.O.S)

According to Mayerhof, the collapse load under central loading condition for large plain concrete slab is roughly twice the load at which yielding begins or first crack is formed. For edge load also, the collapse load is roughly twice the corresponding yield load and is somewhat greater than one half of that of a central loading condition. For corner loading condition, the collapse load is of the same order as the yield load. The collapse load is somewhat greater than one quarter of that of a centrally loaded large slab and somewhat greater than one half of that of an edge loaded slab.

It is applied to the nominal flexural strength to avoid cracking. Factor of safety (FOS) is determined by dividing the modulus of rupture by a working stress at designed wheel load. It generally varies between 1.3 to 2.0 for the theoretical yield load depending upon the design methods. The FOS is low for the structures designed on the basis of limit state of

serviceability and is high for the structures designed on the basis of Limit State of Collapse. According to Frank, the safety factor applied to the collapse load should be greater than that applied to yield load and suggested a value of 2 to 3. Concrete pavement designed on the basis of IRC-58 orWestergaard method, a factor of safety of the order of 1.1 to 1.2 is adequate.

3.11 SUMMARY

In this chapter, various theories for the design of flexible pavements and rigid pavements have been discussed. Design factors for flexible and rigid pavements have also been discussed. There are various methods for design of flexible pavements, but IRC-37 methods have been described in detail. Using existing IRC-37 method, the design of flexible pavements have been done for heavy vehicles. To design HSHPC pavements, the methods for design of rigid pavement, Westergaard analysis, Mayerhof analysis, Ghosh analysis and IRC-58 method have been described. Analytical method i.e. Finite Element Method (FEM) has also been described. Formulation of the problem has also been discussed.

On the basis of these theories for the design of flexible and HSHPC pavements, the various experiments have been planned, which has been discussed in Chapter-4.

CHAPTER – 4

EXPERIMENTAL PROGRAMME

4.1 GENERAL

The present experimental study on high strength high performance concrete (HSHPC) pavement has been carried out with the objective whether the existing theoretical methods of analysis could be used or there is need to develop a suitable design approach for the analysis of stresses and deflections in HSHPC pavements.

To date there is no information regarding the structural behavior of HSHPC pavements under different loading positions i.e. central, edge and corner loading. Various researchers through their investigations have established that the load carrying capacity, the flexural strength, the flexural impact and the toughness and the fatigue properties of HSHPC are much superior to the normal strength concrete. Also the crack arrest property of HSHPC is much superior to the normal strength concrete. All these properties are of much significant for the rigid pavements. It is, therefore, important to investigate the load carrying capacity of HSHPC pavement, their cracking behavior and crack patterns. Therefore, following test programme had been planned to evaluate the different properties of materials in the design of pavements and the structural behaviour of HSHPC pavements:

(1) Laboratory testing of materials to be used in high strength high performance concrete mix design.
(2) Design of high strength high performance concrete mix of grade M60 using fly ash.
(3) Laboratory testing for the evaluation of strength characteristics of high strength high performance concrete mix i.e. compressive strength, flexural strength and modulus of elasticity.
(4) Plate load test on soil subgrade for the evaluation of modulus of subgrade reaction.
(5) Laying of different thicknesses of high strength high performance concrete (HSHPC) pavements in pavement testing hall for testing under different loading positions.

4.2 MATERIALS

The characteristics of the different materials used in the present investigations i.e. cement, coarse aggregate, fine aggregate, water, fly ash and super plasticizer are as follows:

4.2.1 Coarse Aggregate

Locally available crushed stone coarse aggregate of maximum size 20 mm confirming to IS: 383-1970 was used. The gradation of coarse aggregate used and other properties are given in Table 4.1. The fineness modulus of coarse aggregate in the study was 6.7 [72, 75].

Table 4.1: Grading and other Physical Properties of Coarse Aggregate

1. Sieve Analysis				
IS. Sieve Size	Weight retained in gm.	Percentage weight retained	Cumulative percentage weight retained	Percentage passing
20 mm	126	2.52	2.52	97.48
10 mm	3224	64.48	67.00	23.00
4.75 mm	1572	31.44	98.44	1.56
2.36 mm	78	1.56	100.00	0
1.18 mm	0	0	100.00	0
600 µ	0	0	100.00	0
300 µ	0	0	100.00	0
150 µ	0	0	100.00	0
Total			667.96	-
Fineness Modulus			6.70	
2. Specific Gravity			2.656	
3. Aggregate crushing value in %			10.81	
4. Soundness Test in Na_2SO_4 saturated solution			Negligible loss of weight	
5. Water absorption in %			0.20	
6. Unit weight in kg/m^3			1631.72	

4.2.2 Fine Aggregate

Locally available fine aggregate confirming to IS: 383-1970 was used. The fineness modulus of the aggregate in the study used was 2.89. The gradation of the aggregate and other properties are given in Table 4.2 [75].

Table 4.2: Grading and other Physical Properties of Coarse Sand

1. Sieve Analysis				
IS Sieve Size	Weight retained in gm.	Percentage weight retained	Cumulative percentage weight retained	Percentage passing
4.75 mm	310	15.50	15.50	84.50
2.36 mm	106	5.30	20.80	79.20
1.18 mm	199	9.95	30.75	69.25
600 µ	228	11.40	42.15	57.85
300 µ	841	42.05	84.20	15.80
150 µ	226	11.30	95.50	4.50
Total			288.90	-
Fineness Modulus			2.89	
2. Specific Gravity			2.69	
3. Moisture content in %			2.30	
4. Unit weight in kg/m^3			1834.24	

4.2.3 Cement

Ordinary Portland Cement, Grade-43, confirming to IS: 8112-1989 was used throughout the investigations. The cement used in the experiment has the following properties as given in Table 4.3 [68].

Table 4.3: Tests for Physical Properties of Cement

Type and Brand - OPC- 43 Grade, Jay Pee Cement

Colour of Cement- Grey

Sl. No.	Name of tests	Test Results	Specified as per IS : 8112-1989
1.	Standard Consistency percentage mixing water by weight of cement	30	30%
2.	Fineness specific surface by blain's air permeability method (M^2/kg)	290	Not less than 225 M^2/kg
3.	Soundness Expansion by Le-Chatelier method (mm)	1.0	Not more than 10 mm
4.	Specific Gravity	3.15	3.15
5.	Setting Time (minutes)		
	(a) Initial	65	Not less than 30 minutes
	(b) Final	158	Not more than 600 minutes
6.	Compressive Strength (MPa)		
	(a) 72 ± 1 hour (3 days)	28.3	Not less than 23 MPa
	(b) 168 ± 2 hour (7 days)	35.5	Not less than 33 MPa
	(c) 672 ± 4 hour (28 days)	43.8	Not less than 43 MPa

4.2.4 Fly Ash

Fly ash is the finely divided residue that results from the combustion of pulverized coal and is transported from the combustion chamber by exhaust gases.

India has ninety six coal based thermal power stations producing in excess of 100 million tones of fly ash annually. Generally, the fly ash produced at all the thermal power stations is of low calcium fly ash with calcium content less than 5% in most of the cases. For the present study, fly ash was procured from Delhi region (Dadri), the nearest thermal power

station. The calcium content of the fly ash was found to be 0.49% only. The physical and chemical properties are given in Table 4.4 [67].

Table 4.4: Properties of Fly Ash

Sl. No.	Properties	Values
1.	Fineness, cm^2/gm	3500
2.	Specific gravity	2.24
3.	Percentage coarser than 45 μm	5.60
4.	Average particle size, μm	10.10
5.	Silicon dioxide, SiO2, percent by mass	57.50
6.	$Al_2O_3 + Fe_2O_3$, percent by mass	33.50
7	Loss on ignition, percent by mass	0.57

4.2.5 Super Plasticizer

Super plasticizer used in this study was Sikament-170. It is modified naphthalene formaldehyde sulphonate type. It is dark in brown and specific gravity is around 1.16 to 1.20. It complies with IS: 9103, ASTMC 494 Type-F and BS: 5075 Part-3.

4.2.6 Water

Water used for mixing and curing should be free from injurious and deleterious materials. Throughout the investigations potable water was used.

4.3 DESIGN OF HIGH STRENGTH HIGH PERFORMANCE CONCRETE MIX

Mix design can be defined as the process of selecting suitable ingredients of concrete and determining their relative proportions with the objective of producing concrete of certain minimum strength and durability as economically as possible. The purpose of designing mix is two-fold. The first objective is to achieve the stipulated minimum strength and durability. The second objective is to make the concrete in the most economical manner. Since main cost governing material is cement, therefore, much attention is given to the use of cement as little as possible consistent with strength and durability.

Concrete is generally classified as Normal Strength Concrete (NSC), High Strength Concrete (HSC) and Ultra High Strength Concrete (UHSC). Indian Standard recommends that concrete having strength 60 MPa or more are high strength concrete [147].

Typically, these mixtures are composed of high cement content viz. 450-500 kg/m^3 Portland or blended Port land cement containing relatively small amount of silica fume and fly ash or slag, a low water/cement ratio of the order of 0.3 (with the help of super plasticizer admixture) and an air entraining agent when it is necessary to protect the concrete from cycles of freezing and thawing [134].

According to Aitcin (1993) et al., high strength concrete differs from normal strength concrete in that it invariably contains a high range water reducer (or super plasticizer), while normal strength concrete contains it only sometimes. All the other basic ingredients are the same namely, Portland cement, aggregate, water and admixture. As far as other ingredients are concerned such as retarders, fly ash, blast furnace slag and silica fume, they may or may not be present in either type of concrete [12].

From the above statement, it is evident that ingredients are same for production of high strength concrete as that for production of normal strength concrete except that quality of materials being used for production of high strength concrete should be high. Therefore, there is need of great skill in selection of ingredients. To achieve high strength concretes, optimum proportions must be selected, considering the cement and fly ash characteristics, aggregate quality, admixture type and dosage rate and mixing [5,6,7,61,71,78,96,187].

4.3.1 Coarse Aggregate

Since aggregates occupy largest volume in the concrete and affect the strength and other properties, therefore in selection of aggregate need special attention. The important parameters of coarse aggregate shape, texture and maximum size affect the performance of concrete to great extent. Generally, aggregate strength is stronger than paste, therefore it is not a major factor for normal strength concrete. But in case of high strength concrete, the strength of aggregate and bond between paste and aggregate are of great concern. Crushed stone produces higher strength than rounded stone. This may be due to formation of stronger mechanical bond between cement paste and aggregate surface. It is observed that for the given

strength, there is optimum size of aggregate that will yield maximum compressive strength. Yaqub (2006) found through their investigation that 9.5 mm to 12.5 mm aggregate produce optimum strength [186].

As per ACI 363R-10 and ACI 211.4R-93 and Aitcin (1998) et al., general guidelines for the selection of materials to be used in high strength concrete are that the higher the targeted compressive strength, the smaller the maximum size of coarse aggregate. Up to 70 MPa compressive strength can be produced with good coarse aggregate of maximum size ranging from 20 to 28 mm. [5, 6, 10, 31, 90, 134].

In present investigation, the maximum size of coarse aggregate 20 mm has been used.

4.3.2 Fine Aggregate

Less mixing water is required for rounded and smooth textured fine aggregate. Aitcin (1998) recommends the use of fine aggregate with higher fineness modulus around 3.0. His reasoning's are (a) high strength concrete mixtures already have large amount of small particles of cement and pozzolana, therefore fine particles of aggregate will not improve the workability of the mix (b) use of coarser fine aggregates require less water to obtain the same workability (c) during the mixing process, the coarser fine aggregates will generate higher shearing stresses that can help in preventing the flocculation of the cement paste [10].

For concrete strength of 70 MPa or greater fineness modulus (F.M.) should be in the range 2.8 and 3.2 and should not vary by more than 0.1 from the F.M. selected for the duration of the project. Sand having F.M. between 2.5 and 2.7 may produce mix with lower strength and sticky mixtures [31].

In the present investigation, the fine aggregate of FM 2.89 has been used.

4.3.3 Cement

Physical and chemical characteristics of cement plays very vital role in development of compressive strength and rheology of concrete. Fineness of cement is very important parameter. Finer cement leads to early development of strength but may leads to rheological deficiency. Studies have shown that cement containing low C_3A should be preferred because it is easy to control rheology. Higher content of C_3A causes rapid loss of flow in fresh concrete and also create problem for cement-super plasticizer compatibility [2].

For the present investigation, OPC- 43 grade cement of Jay Pee Brand with normal consistency of 30% and fineness 290 M^2/kg has been used throughout the study.

4.3.4 Chemical Admixture

According to Mehta and Aitcin (1990) in production of high strength concrete, the use of chemical admixture is essential. Low water cementitious material ratio is possible by the use of high range water reducer or super plasticizer chemical admixture. They improve the workability of concrete requiring less amount of water. Different types of chemical admixture are plasticizer, super plasticizer, retarder and air entraining agent [105]. Plasticizer and super plasticizer lower the water cementitious ratio, retarder slows down the loss of slump i.e. it retains the workability for longer time. Workability and resistance to deterioration can be enhanced by introducing air entraining agent [10, 31, and 90].

In present investigation, chemical admixture Sikament -170 1.6% by weight of cement has been used.

4.3.5 Mineral Admixture

Commonly used mineral admixtures in production of high strength concrete are fly ash, silica fume and blast furnace slag. The use of supplementary cementitious materials such as blast furnace slag, fly ash and natural pozzolana reduce the production cost of concrete and also maintain the slump for long time.

The optimum substitution level of mineral admixture is often determined by the loss in 12 or 24 hour strength, for given climatic conditions or the minimum strength required. Generally silica fume is not necessary for compressive strength less than 70 MPa. Generally high strength concrete mix contains it. The gain in strength by the use of mineral admixture cannot be attained by using additional cement alone. These supplementary cementitious materials are added at dosage rate of 5% to 20% or higher by mass of cementing material [5, 6, 10, 31and 90].

In the present investigation fly ash has been used as mineral admixture at dosage level of approximately 11% by weight of cement.

4.3.6 Mixing Water

If potable water is used during production of concrete then there is no need of testing the water, otherwise water should be tested for suitability in accordance with IS: 456-2000.

In present investigation potable water has been used for concrete mix and water cementitious material ratio adopted is 0.29.

4.3.7 Trial Mix

The trial mixture approach is the best for selecting proportions for the development of high strength concrete. Low water to cementitious material ratio and high cement content is essential for the production of high strength concrete. For the given size of coarse aggregate, the water requirement increases as the fine aggregate content is increased. Since the cementitious material content is high, therefore the content of fine aggregate should be kept low.

For the present study, the concrete of grade M60 has been developed using fly ash. The target strength of the mix was 68.25 MPa. The mix has been proportioned on the basis of trial mix. The batching of ingredients of aggregate and cement was done by weight mix ratio [31, 134]. The FM of coarse aggregate and fine aggregate was 6.7 and 2.89 respectively. The trial mixes are shown in the Table 4.5.

Table: 4.5: Results of Trial Mixes

Sl. No.	Mix ratio	Water cementitious ratio	Super plasticizer (percent)	Percent of fly ash	Slump (mm)	7 days average compressive strength of five cubes (MPa)	7-days target strength (MPa)
1	1:1.2 : 2.3	0.295	2	7	30	32.00	44.36
		0.301	2	7	35	29.08	
2.	1:1.1 : 1.9	0.29	2	11	80	48.82	44.36
		0.30	2	11	130	42.57	
		0.31	2	11	180	38.81	
		0.29	1.6	11	35	48.24	
		0.30	1.6	11	90	43.84	
		0.31	1.6	11	150	40.20	

4.4 MIX PROPORTION

Finally, trial mix having mix proportion 1:1·1:1·9 was adopted with water cementitious ratio 0·29. Fly ash was used 11% and 1.6% high range water reducer was used by weight of cement.

4.5 MIXING

A small amount of water mixed with super plasticizer was fed first followed by all solid materials simultaneously into the mixer i.e. the fine aggregate first then part of coarse aggregate, cement and water and then finally the remaining coarse aggregate was fed into the machine so as to break up any modules of mortar. Mixing was done for 1 to 2 minutes. Photograph - 4.1 shows the mixing process of HSHPC mix.

Photograph 4.1 Mixing Process of HSHPC Mix

4.6 TESTINGS OF WORKABILITY AND STRENGTH PARAMETERS OF HSHPC MIX

4.6.1 Workability

As per ACI 211.4R-93 the workability is the property of fresh concrete that determines the ease with which it can be mixed, placed, consolidated and finished without segregation [5]. The addition of fly ash enhances the workability and reduces the water demand due to its

lubricating effect. There are various methods for measuring workability like as Slump Test, Flow Test, Vee-Bee Consistometer Test, Compacting Factor Test and Kelly Ball Test. Slump Test is commonly used to measure the consistency of concrete. In present investigation Slump Test has been used to measure the workability. The variability in slump measurement is attributed mainly due to variation in mix proportions. As per ACI 211.4R-93, State of the Art Report (1998), Shetty (2008), this is a very good test for quality control because it easily detects the change in composition of concrete due to change in slump. IS: 456-2000 also recommends slump value to determine the workability. The slump tests were carried out in accordance with IS: 1199-1959. Slump values are shown in Tables 4.5 to 4.7 [2, 5, 76, and 147].

4.6.2 Strength Tests for Concrete

The concrete mix containing 11% fly ash and 1.6% super plasticizer were tested for compressive strength, flexural strength and modulus of elasticity.

The test specimens were prepared in standard size i.e. 150 mm x 150 mm x 150 mm cube for compressive strength in cast iron mould. The specimens for flexural strength test of standard size 100 mm x 100 mm x 500 mm were prepared in cast iron mould. The cylindrical specimen of standard size 150 mm diameter and 300 mm height were prepared in cast iron mould for modulus of elasticity test as per Indian Standard Code of Practices. The specimens were vibrated on a vibration table at a speed range of 12000 ± 400 rpm and amplitude of 0.055 mm for about a minute. The cast specimens were kept under standard moist conditions of at least 90% relative humidity and at a temperature of $(27\pm2)^0$ C for the first 24 hours and then taken out from the mould and cured in water for 28 days. After 28 days curing, the specimens were taken out of water and kept for half an hour in air for dry. Then samples were tested according to IS: 516-1959 [76, 77].

Photograph 4.2 shows the testing of specimen for compressive strength and Photograph 4.3 shows the broken specimen during the testing for compressive strength. Photograph 4.4 shows the testing of specimen for flexural strength and Photograph 4.5 shows the broken specimen during the testing for flexural strength. Photograph 4.6 shows the testing

of specimen for modulus of elasticity and Photograph 4.7 shows the broken specimen during the testing for modulus of elasticity.

Photograph 4.2 Testing of Specimen for Compressive Strength

Photograph 4.3 The Broken Specimen of Compressive Strength Test

Photograph 4.4 Testing of Specimen for Flexural Strength

Photograph 4.5 Broken Specimen of Flexural Strength Test

Photograph 4.6 Testing of Specimen for Modulus of Elasticity Test

Photograph 4.7 Broken Specimen of Modulus of Elasticity Test

4.6.2.1 Test results

The objective of compressive, flexural and modulus of elasticity tests are to assess the suitability of HSHPC for laying the concrete pavement. The strength characteristics of HSHPC containing approximately 11% fly ash and 1.6% super plasticizer are shown in Tables 4.6 & 4.7. According to IRC-15-2002, the slump of paving concrete mix compacted by vibration should be in the range of 30 ± 15 mm and that in manual construction using needle vibrators for compaction, the slump shall not be more than 40 mm [58].

Table 4.6: Results of High Strength High Performance Concrete Design Mix

Sl. No.	Design mix ratio	Compressive strength (MPa)		Flexural strength (MPa)		Modulus of elasticity (GPa)	Slump (mm)
		7 days	28 days	7 days	28 days		
1.		48.81	72.0	4.06	6.9	40.1	30
	C:FA:CA	44.25	69.0	5.50	6.1	42.2	35
		45.60	70.5	4.90	6.3	42.2	30
		46.04	71.0	-	6.3	43.8	-
	1:1.1:1.9	46.02	69.5	-	-	40.0	-
	Average	46.14	70.4	4.82	6.4	41.7	31.67

Table 4.7: Results of High Strength High Performance Concrete Mix Prepared during the Laying of Different Pavements Sections

Sl. No.	Design mix ratio	Compressive strength (MPa)		Flexural strength (MPa)		Modulus of elasticity (GPa)	Slump (mm)
		7 days	28 days	7 days	28 days		
1.	Results for HSHPC mix casted during laying of 160 mm thick pavement						
	C:FA:CA	41.40	67.26	4.30	6.1	40.49	28
		42.20	61.04	4.60	6.6	40.81	30
	1:1.1:1.9	43.81	62.62	5.56	6.5	43.80	32
	Average	42.47	63.5	4.82	6.4	41.7	30
2.	Results for HSHPC mix casted during laying of 200 mm thick pavement						
	C:FA:CA	-	62.80	-	6.5	-	33

		-	68.00	-	7.0	-	30
	1:1.1:1.9	-	63.33	-	7.3	-	29
	Average		64.71		6.93		30.67
3.	Results for HSHPC mix casted during laying of 240 mm thick pavement						
	C:FA:CA	-	67.26	-	6.7	-	30
		-	61.95	-	7.1	-	32
	1:1.1:1.9	-	64.17	-	7.3	-	31
	Average		64.46		7.03		31

As evident from above Table 4.7, it is clear that 7 days and 28 days compressive strength obtained are 42.47 MPa and 63.50 MPa respectively. 7 days and 28 days flexural strength are 4.82 MPa and 6.4 MPa respectively. 28 days modulus of elasticity is 41.7 GPa and average measured slump is 30 mm for HSHPC mix casted during laying of 160 mm thick pavement. These values have been used in the analysis. Poisson's ratio 0.2 of HSHPC has been taken for the entire analysis.

Considering all samples the mean and standard deviations had been calculated. The mean value of compressive strength was 66.46 MPa and standard deviation was 3.72. For flexural strength the mean value was 6.67 MPa and standard deviation was 0.42. The mean value of modulus of elasticity was 41.68 GPa and standard deviation was 1.56. The mean value of slump was 30.83 mm and standard deviation was 1.9.

4.7 TESTINGS OF SUBGRADE AND SUBGRADE SOIL

IRC: 58-2011 recommends plate load test for the determination of strength of foundation in terms of modulus of subgrade reaction (K). Modulus of subgrade reaction is defined as pressure per unit deflection of the foundation.

4.7.1 Testing of Soil Subgrade

Roorkee soil has been used throughout the experiment. Soil and subgrade were tested for type of soil, optimum moisture content, dry density, plate load test and CBR as per IRC Standard Code of practices. The Roorkee soil was classified as A-3 as per U.S.P.R.A soil classification which is sandy soil. Modified proctor or modified AASHO compaction or IS

heavy compaction test was used to find out OMC. OMC has been found approximately 11% and dry unit weight 1.92 g/cm^3. Testing had been done as per IS: 2720. Four days Soaked CBR test was done on remolded soil at OMC using 1S heavy compaction or modified proctor test. The CBR had been found 6% for Roorkee soil [73, 74].The results are shown in Table 4.8.

4.7.2 Plate Load Test

The plate load test was done as per IS: 9214-1979. The plate load test was done on subgrade using 750 mm diameter mild steel plate. Initially a seating load of 6.2 kN was first applied for one minute and then released to ensure seating of the plate on the subgrade. The reading of all dial gauges was done at zero at this stage. The load was then applied in increments for an average settlement of 0.25 mm. The K value was determined for the limiting design deflection of 1.25 mm adopted for concrete pavements. Results are shown in Tables 4.9 to 4.11.The CBR and plate load test are shown in Photographs 4.8 & 4.9 [70].

Table 4.8: Properties of Soil Subgrade

Sl. No.	Test at different location in pit	Type of soil	K value for subgrade (kg/cm^3)	CBR (percent)	OMC (percent)	Dry unit weight (g/cm^3)
1	1st	Sandy soil A-3 as	4.20			
2	2nd	per U.S.P.R.A.	4.96			
3	3rd	soil classification	4.72	6	11	1.92
4.	Average		4.63	6	11	1.92

Photograph 4.8 CBR Test for Soil Subgrade

Photograph 4.9 Plate Load Test for Soil Subgrade

Table 4.9 Plate Load Test on Subgrade Soil at Location-1

Plate size = 750 mm Seating Load = 6.2 kN (620 kg)

Least count of dial gauge = 0.01 mm, Proving ring, 4 div = 10 kN,

Moisture content = 3.63%

Sl. No.	Proving dial guage reading in no. of div.	Load (kN)	Stress (MPa)	Dial gauge readings			Average dial gauge reading in no. of div.	Average dial gauge reading (mm)
				DG_1 in no. of div.	DG_2 in no. of div.	DG_3 In no. of div.		
1.	2	5	0.0113	25	15	22	20.67	0.21
2	3	7.5	0.017	50	27	48	41.67	0.42
3	5	12.5	0.0283	75	42	60	59.0	0.59
4	7	17.5	0.0396	100	55	80	78.33	0.78
5	9	22.5	0.0510	125	70	105	100.0	1.00
6	10	25.0	0.0566	150	85	125	120.0	1.20
7	12	30.0	0.0679	175	105	150	143.33	1.43
8	13	32.5	0.0736	200	115	170	161.67	1.62
9	15	37.5	0.0850	225	130	195	183.33	1.83
10	16	40.0	0.0905	250	140	210	200.00	2.00

DG=Dial Gauge

Table 4.10: Plate Load Test on Subgrade Soil at Location-2

Plate size = 750 mm Seating Load = 6.2 kN (620 kg)

Least count of dial gauge = 0.01 mm, Proving ring, 4 div = 10 kN,

Moisture content = 6.03%

Sl. No.	Proving dial guage reading in no. div.	Load (kN)	Stress (MPa)	Deal gauge reading			Average dial gauge reading in no. of div.	Average dial gauge reading (mm)
				DG_1 in no. of div.	DG_2 in no. of div.	DG_3 in no. of div.		
1.	5.5	13.75	0.0311	25	35	40	33.33	0.33
2	7	17.50	0.0396	50	70	70	63.33	0.63
3	8	20.00	0.0453	75	104	100	93.00	0.93
4	9	22.50	0.0510	100	135	130	121.67	1.22
5	10	25.00	0.0566	125	150	150	141.67	1.42
6	11	27.50	0.0622	150	205	190	181.67	1.82
7	11.5	28.75	0.0651	175	230	220	208.33	2.08

DG=Dial Gauge

Table 4.11: Plate Load Test on Subgrade Soil at Location-3

Plate size = 750 mm, Seating Load = 6.2 kN (620 kg)

Least count of dial gauge = 0.01 mm, Proving ring, 4 div = 10 kN,

Moisture content = 5.43%

Sl. No.	Proving dial guage reading in no. div.	Load (kN)	Stress (MPa)	Dial gauge reading			Average dial gauge reading in no. of Div.	Average dial gauge reading (mm)
				DG_1 in no. of div.	DG_2 in no. of div.	DG_3 in no. of div.		
1.	3	7.5	0.017	25	50	50	41.67	0.42
2	6.5	16.25	0.037	50	95	95	80.00	0.80
3	9	22.50	0.051	75	140	130	115.00	1.15
4	12	30.00	0.068	100	185	170	151.67	1.52
5	14.5	36.25	0.082	125	228	210	187.67	1.88
6	17.0	42.50	0.096	150	270	240	220.00	2.2
7	20.0	50.00	0.113	175	315	280	256.67	2.57

DG=Dial Gauge

4.7.3 Poisson's Ratio of Soil

The poisson's ratio is defined as ratio of lateral strain to axial strain. Theoretically its value is 0.25 for isotropic elastic materials. For sandy soil, its value range from 0.15 to 0.25 and for sand between 0.30 and 0.35. Poisson's ratio of Roorkee soil is 0.305 and modulus of elasticity is 20.96 MPa. These values were used for calculations of stresses, strains and deflections of pavement.

4.8 PREPARATION OF SUBGRADE

The subgrade was prepared according to IRC: 15-2011 [58]. This is shown in Photograph 4.10. The top 150 mm layer of subgrade soil was sieved and organic matter and other deleterious substances were removed. The soil was compacted at optimum moisture

content and dry density. The surface was then leveled and the irregularities, if any, were rectified and the surface rolled till a firm, leveled surface was achieved. The subgrade was compacted with a plate vibrator for pavement size 1800 mm x 1800 mm. All the pavements slab were compacted with plate vibrator. Since all the pavement slabs were cast in the transportation engineering laboratory and pavement testing hall, the moisture content and temperature in shade remained practically the same or did not show any significant change.

Photograph 4.10 Preparation of Soil Subgrade for Laying of HSHPC Pavements

4.9 LAYING OF PAVEMENTS FOR TESTINGS

By using high strength high performance concrete mix developed in the lab of grade M60 having fly ash 11% and super plasticizer 1.6%, three concrete pavements of size 1800 mm x 1800 mm had been cast with varying thicknesses viz. 160 mm, 200 mm and 240 mm. All the pavements with different thicknesses were cast directly over the compacted subgrade. From strength considerations, concrete pavements may be directly laid over subgrade. From economical considerations also an increase in the subgrade reaction due to provision of a base course may be negligible. In the present study, therefore, all the pavement sections were directly laid over a compacted subgrade.

The clean and dry aggregate were weighed and stored in gunny bag nearby the location of pavement laying site according to design mix. The uniform mixing of the concrete

ingredient was done in rotating drum mixer. After 2 minutes, the uniform mix was poured on floor and then being taken to the pavement laying site by pan. The form work with steel girder and brick was prepared for laying of HSHPC pavements. Laying of HSHPC mix is shown in Photograph 4.11. After laying, the concrete was compacted with a plate vibrator. The placing of concrete was done in two layer. The finishing of the surface was done with trowel and float. Finished surface of HSHPC pavements are shown in Photograph 4.12. After laying of concrete pavement, the initial curing was done for 24 hours under standard moisture condition and with wet gunny bags. Then water was filled for 14 days on the surface of pavement by making the raised longitudinal and transverse dykes with sand. The curing of HSHPC pavement is shown in Photograph 4.13. All the three HSHPC pavements cast for investigations are shown in Photograph 4.14. The surface was made ready for testing after 28 days.

Photograph 4.11 Laying of HSHPC Mix for Pavements

Photograph 4.12 Finished Surface of HSHPC Pavements

Photograph 4.13 Curing of HSHPC Pavement

Photograph 4.14 Three HSHPC Pavements Cast for Investigations

4.10 LOADING ARRANGEMENT

The loading arrangement for applying a static load to the pavement consisted of a 250 kN capacity reaction frame fabricated with steel portal frame and steel girders. The reaction loading frame was mobile for carrying out the plate load test at any position along or across the test pit 2000 mm x 8000 mm in size. The testing was done in test hall of transportation engineering group. An arrangement for providing mobility to the loading device was developed by fabricating a mechanical device consisting of chain and pulley block arrangement with wire ropes was developed. With the help of this device, loading arrangement can be moved forward and backward. The pulley blocks were fixed to vertical column support consisting of steel channel section firmly embedded in cement concrete. The loading of the mobile loading device was done by drums, gunny bags filled with soil and tested pavement blocks. With the help of mechanical device, It was possible to move the 250 kN loading device to any desired position conveniently for carrying out the plate load test on the subgrade or pavement slabs at any loading position up to a static load of 250 kN.

4.11 INSTRUMENTATION

4.11.1 Strains Measurement

To determine the stresses in pavement, the surface strains have been measured by Huggenberger mechanical deformeter. Preparation is being shown in photograph 4.15 for pasting studs on surface to measure strains. For measuring the strains on surface, the studs have been fixed with araldite on cleaned pavement surface. The arrangements of studs have been shown in photograph 4.16 and Figs 4.1 to 4.3. In photograph 4.19 surface strains is being measured during the testing.

4.11.2 Deflections Measurement

To measure the deflections of pavement surface due to loading, eight mechanical dial gauges with least count 0.01 mm were used. The dial gauges were fixed to the datum frame with the help of magnetic bases. The arrangement showing position of dial gauges on the pavement slab under different loading positions i.e. central, edge and corner loading is shown in Photographs 4.17 to 4.20 and in Figures 4.1 to 4.3 respectively. For measurement of deflections of pavement slab under the loading plate, the dial gauges were fixed with their spindles.

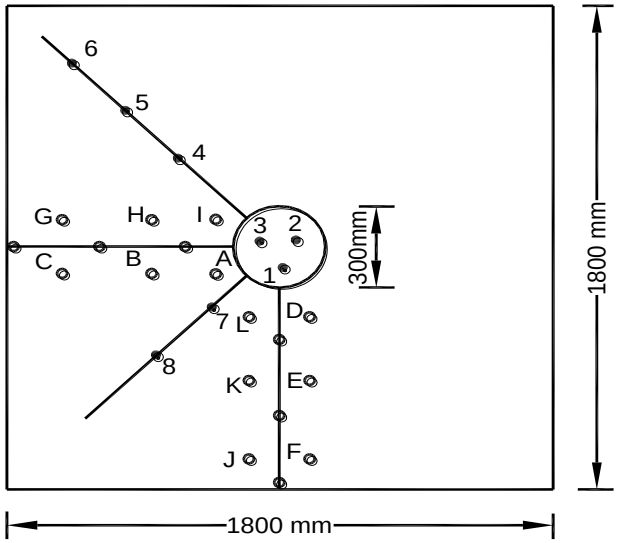

1,2,3 . . . . . 8 Positions of Dial Gauges
A, B, C . . . . . L Position of Strain Gauges

Fig. 4.1: Position of Dial Gauges, Studs and Strain Gauges under Central Loading

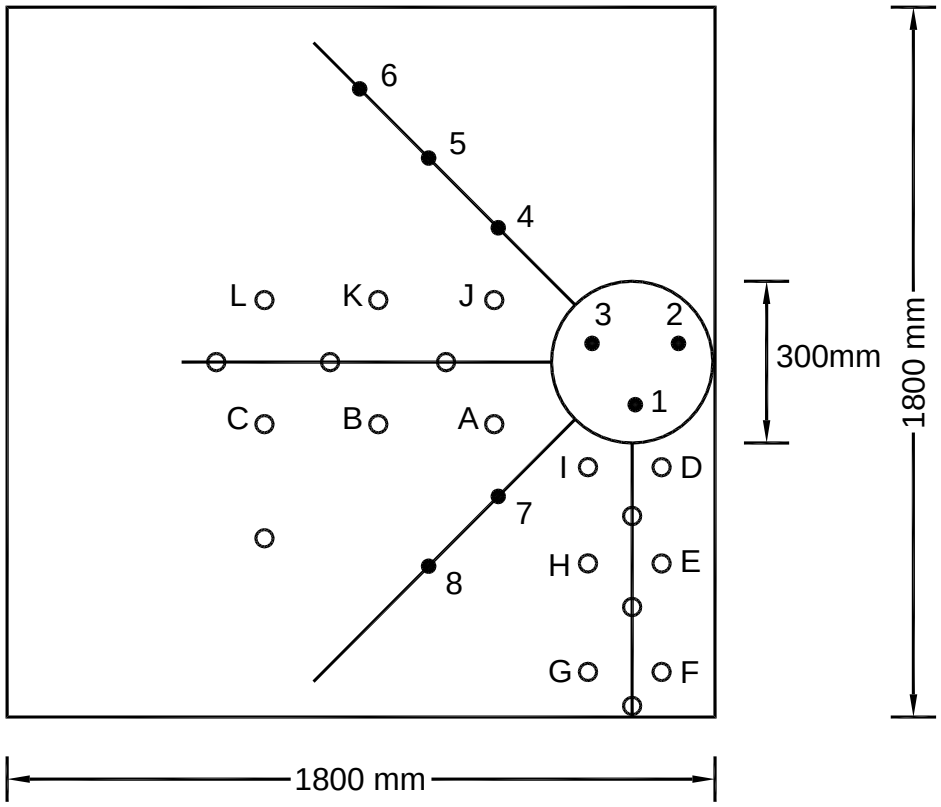

1, 2, 3 . . . . . 8 Positions of Dial Gauges

A, B, C . . . . . L Position of Strain Gauges

Fig. 4.2: Position of Dial Gauges, Studs and Strain Gauges under Edge Loading

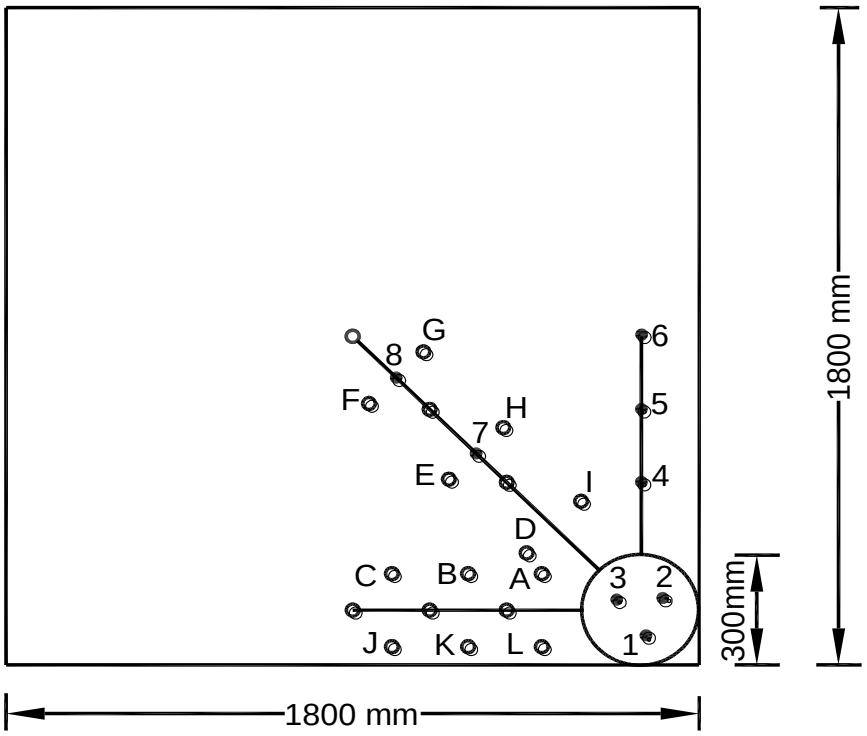

1, 2, 3 . . . . . 8 Positions of Dial Gauges
A, B, C . . . . . L Position of Strain Gauges

Fig. 4.3: Position of Dial Gauges, Studs and Strain Gauges under Corner Loading

4.12 TESTING OF CONCRETE PAVEMENTS

All HSHPC pavement slabs were tested for corner, edge and central loading positions. Before carrying out tests for different positions, the pavement surface was cleaned, white washed and preparation was made for pasting studs. This is shown in Photograph 4.15. Studs were pasted with araldite. Studs on surface of HSHPC pavement are shown in Photograph 4.16. The dial gauges and studs were numbered for each position of testing. The surface was leveled by spreading fine sand and 300 mm diameter plate was seated over it. Initially a seating load 5 kN was applied for 2 minutes to ensure proper seating. A proving ring and hydraulic jack of capacity 50 tonnes was used. The initial strains and deflections were recorded. The load was applied in increment and retained for 40 to 60 seconds. The readings of deflections and strains were recorded for incremental load. The load was applied upto the capacity of loading frame (23 tonnes).

Photograph 4.15 Preparation for Pasting the Studs

Photograph 4.16 Studs on Surface of HSHPC Pavements

Photograph 4.17 Testing of HSHPC Pavement for Central Position Showing Loading Arrangement and Dial Gauges

Photograph 4.18 Testing of HSHPC Pavement for Edge Position Showing Loading Arrangement and Dial Gauges

Photograph 4.19 Surface Strains Reading is being Taken during the Testing of HSHPC Pavement for Edge Position

Photograph 4.20 Testing Of HSHPC Pavement for Corner Position Showing Loading Arrangement and Dial Gauges

Photograph 4.21 Testing of HSHPC Pavement for Corner Position Showing Lifting from Opposite Corner

4.13 STATIC PLATE LOAD TEST ON HSHPC PAVEMENTS

Three HSHPC pavements of thicknesses 160 mm, 200 mm and 240 mm have been cast directly on compacted subgrade using M60 grade high strength high performance concrete mix in pavement testing hall. Dimensions of all pavements are 1800 mm x 1800 mm. Each HSHPC pavement had been tested for different positions i.e. central, edge and corner.

4.13.1 Testing of 160 mm Thick HSHPC Pavement

First, the pavement was tested for corner position. The arrangement for corner testing is shown in Photograph 4.20 and Figure 4.3. The load was applied in increment of 10 kN. As the load reached 80 kN, the opposite corner started lifting. This is shown in Photograph 4.21. For each incremental loading, the deflections and strains were measured. As the load reached 130 kN, it had been observed that opposite corner had lifted by 65 mm which was too high. At this point the maximum deflection was 11.45 mm and maximum strain was 320.3 $x10^{-6}$. Therefore, further loading was stopped. Up to this loading, any types of cracks even hair line crack was not observed and upto this load pavement did not fail.

Secondly, the test was conducted for edge position. Arrangement is shown in Photograph 4.18 and Figure 4.2. The load was applied in increment of 10 kN. The deflections and strains were measured for each incremental loading. At 210 kN load, the maximum measured deflection was 10.07 mm and maximum strain was 418 $x10^{-6}$. As the load reached 220 kN, the pavement suddenly broke into two approximately equal parts. This is shown in Photograph 4.22. Before failure, there were no signs of any types of cracks. The crack pattern was straight line and which divided pavement into two approximately equal parts passing through under the testing plate centrally. There was no any sign of prior failure. Failure took place suddenly. The crack width in loaded condition was 1.86 mm. This is shown in Figure 4.4.

Due to failure at edge position the pavement could not tested for central position. Deflections and strains corresponding to different loadings are shown in Tables 4.12 and 4.13.

Photograph 4.22: Failure of 160 mm Thick HSHPC Pavement at Edge during Testing

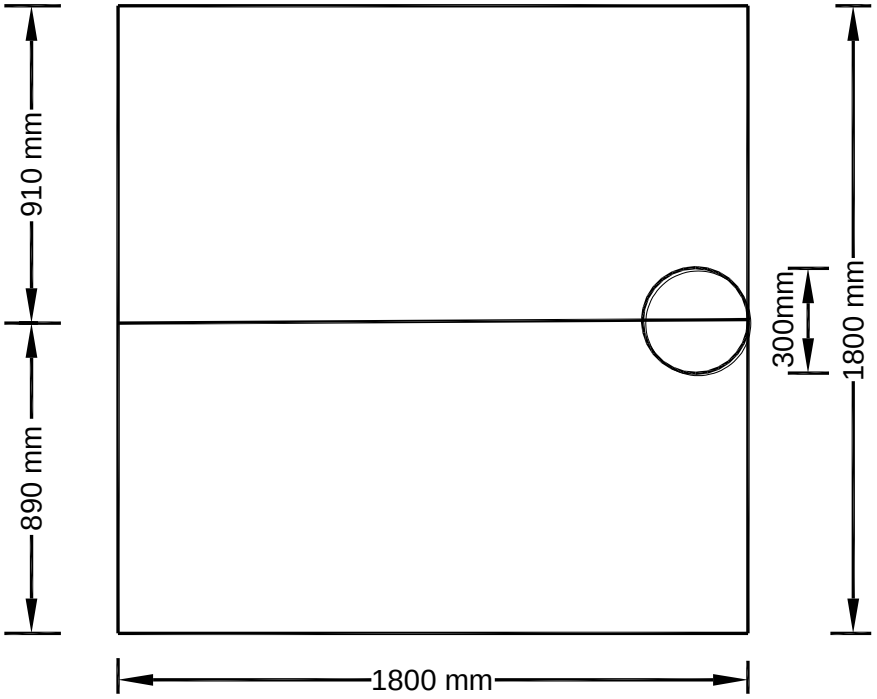

Fig. 4.4: Position of Failure Line when 160 mm Thick HSHPC Pavement Failed at Edge Position

Table 4.12: Deflections at Different Load for 160 mm Thick Pavement for Corner and Edge Positions

Sl. No.	Loads (kN)	Deflections at corner (mm)	Deflections at edge (mm)
1	10	1.55	1.12
2	20	2.23	1.83
3	30	3.00	2.47
4	40	3.85	2.97
5	50	4.33	3.47
6	60	4.97	3.87
7	70	5.45	4.29
8	80	6.78	4.70
9	90	7.40	5.07
10	100	8.25	5.53
11	110	9.22	6.00

12	120	9.88	6.50
13	130	11.45	6.90
14	140	-	7.35
15	150	-	7.65
16	160	-	7.75
17	170	-	8.10
18	180	-	8.40
19	190	-	8.77
20	200	-	9.23
21	210	-	10.07

Table 4.13: Strains at Different Loads for 160 mm Thick Pavement at Corner and Edge Positions

Sl. No.	Loads (kN)	Strains at corner x 10^{-6}		Strains at edge x 10^{-6}	
		LD	TD	LD	TD
1	10	26.52	6.12	24.06	4.10
2	20	57.51	12.10	45.12	7.14
3	30	84.91	17.00	74.18	12.23
4	40	115.12	22.62	95.34	17.0
5	50	142.60	28.00	120.30	21.70
6	60	170.81	32.12	150.24	25.20
7	70	201.12	36.56	178.60	29.30
8	80	227.69	40.81	200.60	32.40
9	90	259.12	44.12	231.00	37.00
10	100	287.40	48.00	255.14	40.3
11	110	295.81	53.62	260.20	44.00
12	120	307.61	60.12	265.00	48.00
13	130	320.30	65.00	290.40	51.00
14	140	-	-	307.30	54.00

15	150	-	-	331.14	57.30
16	160	-	-	336.40	61.12
17	170	-	-	340.30	66.20
18	180	-	-	355.24	72.50
19	190	-	-	380.40	76.80
20	200	-	-	398.09	82.30
21	210	-	-	418.00	90.5

LD = Longitudinal direction, TD = Transverse direction

4.13.2 Testing of 200 mm Thick HSHPC Pavement

First, the pavement was tested for corner position. Arrangement for corner testing is shown in Photograph 4.20 and Fig. 4.3. The load was applied in increment of 10 kN and corresponding deflections and strains were noted. As the load continuously increased, it had been observed that the opposite corner started lifting. Lifting of opposite corner started at 90 kN load and it reached 55 mm at 210 kN, which is sufficiently high. This is shown in Photograph 4.21. At this time the maximum deflection was observed 18.53 mm and maximum strain was observed 375.2 $x10^{-6}$ respectively. Therefore further loading was stopped beyond 210 kN. Upto this load even hair line crack was not observed and also pavement did not fail.

Secondly, the pavement was tested for edge position. Arrangement is shown in Photograph 4.18 and Fig. 4.2. At this position also, load has been applied in increment of 10 kN and corresponding to each load deflections and strains were measured. Load was applied upto 230 kN. The maximum deflection and strain was observed as 10.73 mm and 312.8 $x10^{-6}$ respectively at 230 kN. At this load i.e. 230 kN, there was no hair line crack was observed and pavement did not fail upto this load.

Thirdly, the pavement was tested for central position. The arrangement for testing is shown in Photograph 4.17 and Fig. 4.1. Load was applied in the same manner as in edge and corner position testing. The deflections and stains were measured for each incremental loading. The load had been increased up to 230 kN. At this load it had been noticed that there were no cracks in the pavement and pavement did not fail up to this load. The maximum

deflection was recorded as 4.78 mm and strain was recorded as 275.3 x10^{-6}. Deflections and strains corresponding to the loads are shown in Tables 4.14 and Table 4.15.

Table 4.14: Deflections at Different Loads at Corner, Edge and Central Positions for 200 mm Thick Pavement.

Sl. No.	Loads (kN)	Deflections at corner (mm)	Deflections at edge (mm)	Deflections at central (mm)
1	10	0.91	0.70	0.32
2	20	1.49	1.00	0.67
3	30	2.21	1.55	1.22
4	40	2.49	1.94	1.44
5	50	3.22	2.27	1.90
6	60	3.90	2.76	2.17
7	70	4.75	3.08	2.28
8	80	5.37	3.51	2.38
9	90	6.03	4.01	2.55
10	100	6.63	4.43	2.92
11	110	7.65	4.78	3.17
12	120	8.65	5.68	3.33
13	130	9.65	6.00	3.52
14	140	10.40	6.70	3.72
15	150	11.33	7.03	3.73
16	160	12.50	7.27	3.88
17	170	13.47	7.65	4.08
18	180	14.53	8.23	4.17
19	190	15.97	8.70	4.32
20	200	17.13	9.17	4.43
21	210	18.53	9.60	4.55
22	220	-	10.12	4.67
23	230	-	10.73	4.78

Table 4.15: Strains at Different Loads at Corner, Edge and Central Positions for 200 mm Thick Pavement.

Sl. No.	Loads (kN)	Strains at corner x 10^{-6}		Strains at edge x 10^{-6}		Strains at centre x 10^{-6}	
		LD	TD	LD	TD	LD	TD
1	10	20.30	3.00	18.25	2.00	13.10	0
2	20	38.16	7.14	30.72	4.50	25.12	0
3	30	57.18	10.68	52.50	7.12	36.81	0
4	40	77.79	15.10	70.62	10.50	49.12	2.00
5	50	98.50	18.50	85.74	13.20	62.45	3.50
6	60	117.71	22.21	95.67	15.12	73.12	5.71
7	70	138.72	28.10	113.25	17.54	83.82	7.91
8	80	156.68	30.61	134.53	18.12	96.12	10.21
9	90	176.32	35.12	149.00	20.00	106.24	13.61
10	100	195.25	40.20	165.56	21.40	117.30	15.60
11	110	214.21	42.10	175.66	22.50	128.50	17.81
12	120	233.81	44.56	190.26	24.60	137.91	19.21
13	130	254.21	46.10	202.36	28.30	148.21	21.50
14	140	272.81	47.91	218.25	30.50	157.95	23.11
15	150	292.50	50.4	235.93	32.50	167.40	25.40
16	160	307.12	55.16	247.31	35.00	184.91	28.81
17	170	318.81	60.26	258.26	38.40	200.85	30.11
18	180	333.61	65.34	274.65	41.46	219.61	33.61
19	190	347.11	70.12	290.82	44.25	237.80	34.91
20	200	360.60	76.50	307.45	47.30	255.60	38.50
21	210	375.20	80.30	309.52	52.50	262.31	41.11
22	220	-	-	311.24	56.35	268.82	43.81
23	230	-	-	312.80	60.20	275.30	45.70

LD = Longitudinal direction, TD = Transverse direction

4.13.3 Testing of 240 mm Thick HSHPC Pavement

Firstly, the pavement was tested for corner loading. The arrangement is shown in Photograph 4.20 and Fig. 4.3. The load was applied up to 200 kN in increment of 10 kN. Corresponding to the each load the deflections and strains were noted. As the load was increased, it had been noticed that opposite corner started lifting as shown in Photograph 4.21. The lifting of opposite corner was noticed at 100 kN load. At 200 kN load, the lifting was observed 45 mm. it is too high. Therefore, further loading was stopped at 200 kN. No crack was observed in pavement and also pavement did not fail. At 200 kN load the maximum deflection and strain was 12.35 mm and 240.3 x 10^{-6}respectively.

Secondly, the pavement was tested for edge position. Arrangement is shown in Photograph 4.18 and Fig. 4.2. The load was applied in the same manner as in previous testing. The load was applied up to 230 kN. The deflections and strains were noted corresponding to each loading. At 230 kN load the maximum deflection was 8.22 mm and maximum strain was 207.36 x 10^{-6}. Upto this loading, any types of cracks had not been observed. Still the pavement was in capable of carrying more loads.

Thirdly, the pavement was tested for central position. Arrangement for testing is shown in Photograph 4.17 and Fig. 4.1. Load was being continuously applied to the pavement up to 230 kN. For different loadings, the deflections and strains were noted. Upto this load, any types of crack in pavement surface had not been noticed and also the pavement did not fail. The maximum deflection and strain was noticed as 2.67 mm and 182.5 x 10^{-6} respectively. Pavement was still in condition of carrying more loads. Deflections and strains corresponding to the loads are shown in Tables 4.16 and 1.17 respectively.

Table 4.16: Deflections at Different Loads for 240 mm Thick Pavement for Corner, Edge and Central Positions

Sl. No.	Loads (kN)	Deflections at corner (mm)	Deflections at edge(mm)	Deflections at corner (mm)
1	10	0.60	0.53	0.13
2	20	1.13	0.92	0.27
3	30	1.56	1.32	0.45
4	40	1.94	1.72	0.57
5	50	2.85	2.03	0.70
6	60	3.14	2.35	0.82
7	70	3.46	2.63	0.97
8	80	4.18	3.02	1.05
9	90	4.50	3.63	1.17
10	100	4.81	4.07	1.28
11	110	5.37	4.27	1.42
12	120	5.81	4.57	1.52
13	130	6.45	4.93	1.65
14	140	6.99	5.65	1.77
15	150	7.51	5.90	1.87
16	160	8.43	6.13	2.08
17	170	9.10	6.43	2.17
18	180	10.16	6.70	2.27
19	190	11.07	6.97	2.38
20	200	12.35	7.23	2.48
21	210	-	7.60	2.53
22	220	-	7.90	2.58
23	230	-	8.22	2.67

Table 4.17: Strains at Different Loads for 240 mm Thick Pavement for Corner, Edge and Central Positions

Sl. No.	Loads (kN)	Strains at corner x 10^{-6}		Strains at edge x 10^{-6}		Strains at centre x 10^{-6}	
		LD	TD	LD	TD	LD	TD
1	10	13.50	2.56	10.5	0	10.15	0
2	20	25.64	4.31	25.5	0	19.50	0
3	30	40.64	6.15	30.68	3.50	26.50	2.00
4	40	56.84	8.24	42.56	4.60	38.12	2.00
5	50	70.25	10.50	55.10	5.14	45.30	3.20
6	60	84.50	12.56	62.31	7.50	53.50	4.56
7	70	100.70	14.14	70.62	8.50	61.12	5.80
8	80	114.23	17.50	82.56	9.50	69.50	6.90
9	90	124.14	19.23	92.34	11.00	75.12	8.91
10	100	135.40	22.50	101.85	13.40	85.25	10.20
11	110	147.50	23.00	104.35	14.65	91.27	11.56
12	120	158.25	25.02	112.36	16.50	97.85	13.12
13	130	170.50	26.13	121.34	17.56	104.31	14.56
14	140	181.25	27.12	126.89	18.45	111.57	15.61
15	150	193.30	28.30	138.99	20.50	120.90	16.40
16	160	201.50	30.50	142.35	22.34	129.50	16.40
17	170	211.65	32.12	152.35	24.10	137.61	18.50
18	180	222.70	35.13	160.39	26.63	143.12	19.00
19	190	232.65	37.12	167.34	28.40	152.17	19.00
20	200	240.30	40.50	176.98	29.30	162.70	20.50
21	210	-	-	190.25	32.00	167.56	22.61
22	220	-	-	200.69	36.50	176.12	24.61
23	230	-	-	207.36	38.30	182.50	28.30

LD = Longitudinal direction, TD = Transverse direction

4.14 SUMMARY

In this chapter, the experiments have been done to test the soil subgrade, modulus of subgrade reaction, CBR, to develop the HSHPC mix and to assess the suitability of HSHPC mix. For which cubes of size 150 mm , cylinders 150 mm diameter and 300 mm height and beams of size 100 mm x 100 mm x 500 mm were cast to find out compressive strength, modulus of elasticity and flexural strength. HSHPC pavements were cast on compacted subgrade of semi full scale size 1800 mm x 1800 mm with different thicknesses i.e. 160 mm, 200 mm and 240 mm. The HSHPC pavements were tested for edge, corner and central positions for stresses and deflections. The experimental observations were noted and shown in Tables 4.12 to 4.17. Analysis and discussions of the results have been made in Chapter – 5.

CHAPTER - 5

ANALYSIS AND DISCUSSION OF RESULTS

5.1 GENERAL

The laboratory study on HSHPC shows that it has significant flexural strength which is key parameter for designing the rigid pavement. Therefore, it is expected that the load carrying capacity would be high. Various investigators have also established through their experiments that concrete containing fly ash have high durability, resistance to chloride penetration, resistance to abrasion, resistance to freeze-thaw etc. Being high durability the pavement could be designed for more design life. In present investigation, the objective was to study the possibility of laying HSHPC pavement with varying thicknesses using conventionally mixed materials using chemical admixture and fly ash. For which, the various experiments had been conducted. Also the load carrying capacity of pavement of different thicknesses had been assessed in the lab.

To understand the behavior of HSHPC pavements, the crack formation, the crack patterns, the crack widths and the crack propagation had also been studied. The loads had been applied to the pavements at various positions i.e. central, edge and corner up to failure at a interval of 10 kN and strains and deflections had been measured. It was assumed that temperature remain constant since all experiments had been conducted in the pavement testing hall. Therefore, temperature has not been taken into account. Only load has been taken into account.

In this chapter, the properties of HSHPC mix and analysis of stresses, strains and deflections of pavements of different thicknesses have been presented under different loading positions. Analysis of stresses, strains and deflections by finite element analysis for edge position for different thicknesses have also been presented. The results of stresses, strains and deflections of experimental and theoretical analysis have been compared for different positions i.e. central, edge and corner at varying loads. Therefore, the analysis consists of computing the following:

1. Calculations of stresses by Westergaard, Mayerhof, IRC-58 methods for central, edge and corner positions for different thicknesses of pavement.
2. Analysis of deflections, strains and stresses for edge position by finite element method for various thicknesses of pavement.
3. Comparison of stresses calculated by theoretical methods with the observed and finite element method.
4. Comparison of analytical and observed results of strains and deflections.
5. Economic analysis of the pavements.

5.2 CHARACTERISTICS OF MATERIALS

5.2.1 Properties of Soil Subgrade

Roorkee soil had been used throughout the experiment. It is A-3, sandy soil, as per U.S.P.R.A. soil classification system. Its 4 days soaked CBR value was found to be 6%. The optimum moisture content and dry unit weight of Roorkee soil was found to be 11% and 1.92 g/cm^3 respectively. The modulus of subgrade reaction on which the concrete pavement was directly laid in the pavement lab was found to be 4.63 kg/cm^3. The properties of soil are given in Table 5.1.These values were used in analysis of pavement. Young's modulus and poisson's ratio of soil used was 20.93 MPa and 0.305 respectively.

Table 5.1: Properties of Soil Subgrade

Sl. No.	Type of soil	K value of subgrade (kg/cm^3)	CBR (%)	OMC (%)	Dry unit weight (g/cm^3)
1	Sandy soil, A-3 as per U.P.S.R.A. soil classification	4.63	6	11	1.92

5.2.2 Properties of HSHPC Design Mix

The mix design has been explained in Chapter-4. The trial mix approach was adopted for finalization of mix. Finally, the mix ratio was found to be 1:1.1:1.9. Fly ash and super plasticizer was used 11% and 1.6% by weight of cement respectively in development of M60 grade concrete mix. Its compressive strength was found to be 46.14 MPa at 7 days and 70.4

MPa at 28 days, flexural strength was found to be 4.82 MPa at 7 days and 6.4 MPa at 28 days and modulus of elasticity was found to be 41.7 GPa. Poisson's ratio of HSHPC mix used in the analysis was 0.2. The slump of the mix was found to be 31.67 mm as shown in Table 5.2. IRC-15 states that slump of concrete mix for pavements compacted by vibration should be in range of 30 ± 15 mm and that in manual construction using needle vibrators for compaction, the slump should not be more than 40 mm.

Table 5.2: Properties of High Strength High Performance Concrete Design Mix

Sl. No.	Average compressive strength (MPa)		Flexural strength (MPa)		Modulus of elasticity (GPa)	Slump (mm)
	7 days	28 days	7 days	28 days	28 days	
1	46.14	70.40	4.82	6.40	41.70	31.67

5.3 ANALYSIS OF STRESSES, STRAINS AND DEFLECTIONS BY FINITE ELEMENT METHOD

For different thicknesses of pavements the finite element analysis had been carried out at edge position to find out deflections, strains and stresses. For the FEM analysis, depth of the soil in vertical direction and length of the soil in horizontal direction had been taken as 2.0 m and 6.0 m respectively. The contact between soil and concrete had been assumed elastic during the analysis and elastic analysis had been carried out. The analysis had been carried out by considering 3-D eight noded linear brick elements as shown in Figures 5.1 to 5.9. The results are shown in Tables 5.3 to 5.5.

Table 5.3: Stresses, Strains and Deflections for 160 mm Thick Pavement by Finite Element Analysis at Edge Position

Sl. No.	Loads (kN)	Deflections (mm)	Stresses (MPa)	Strains in radial direction x 10^{-6}
1	0	0.00	0.00	0.00
2	10	0.41	0.77	18.21
3	20	0.82	1.54	36.43
4	30	1.23	2.32	54.64

5	40	1.63	3.09	72.86
6	50	2.04	3.86	91.07
7	60	2.45	4.63	109.29
8	70	2.86	5.40	127.50
9	80	3.27	6.18	145.71
10	90	3.68	6.95	163.93
11	100	4.09	7.72	182.14
12	110	4.49	8.49	200.36
13	120	4.90	9.26	218.57
14	130	5.31	10.03	236.79
15	140	5.72	10.81	255.00
16	150	6.13	11.58	273.21
17	160	6.54	12.35	291.43
18	170	6.95	13.12	309.64
19	180	7.35	13.89	327.86
20	190	7.76	14.67	346.07
21	200	8.17	15.44	364.29
22	210	8.58	16.21	382.50

*Stresses are under critical conditions

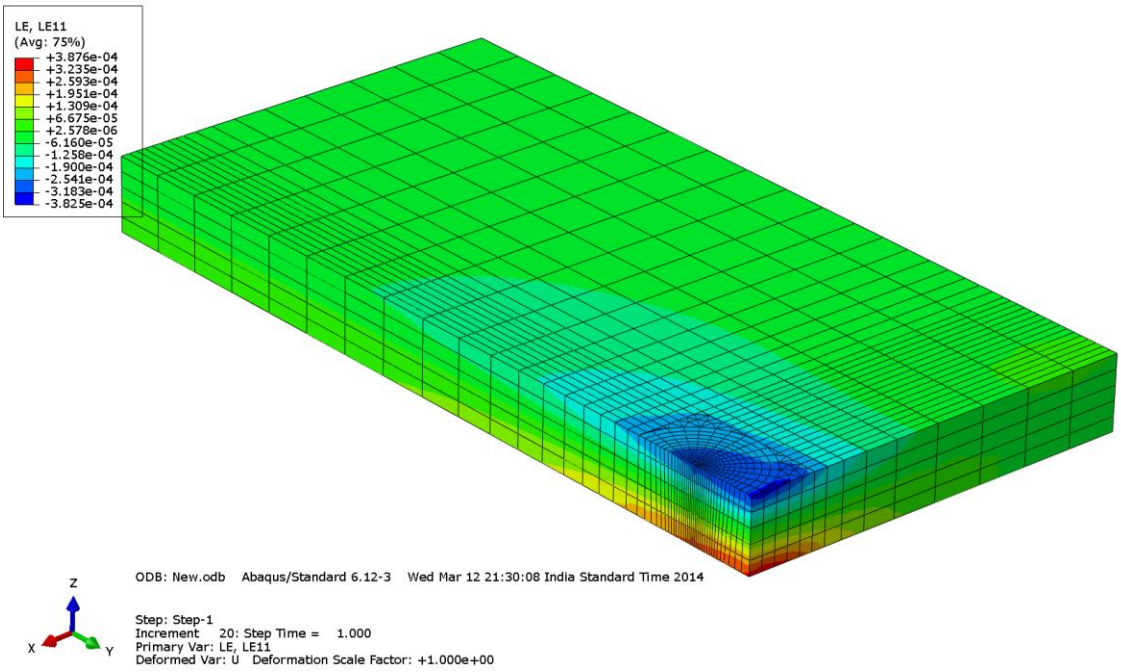

Fig. 5.1: Strains by Finite Element Analysis for 160 mm Thick Pavement at Edge Position

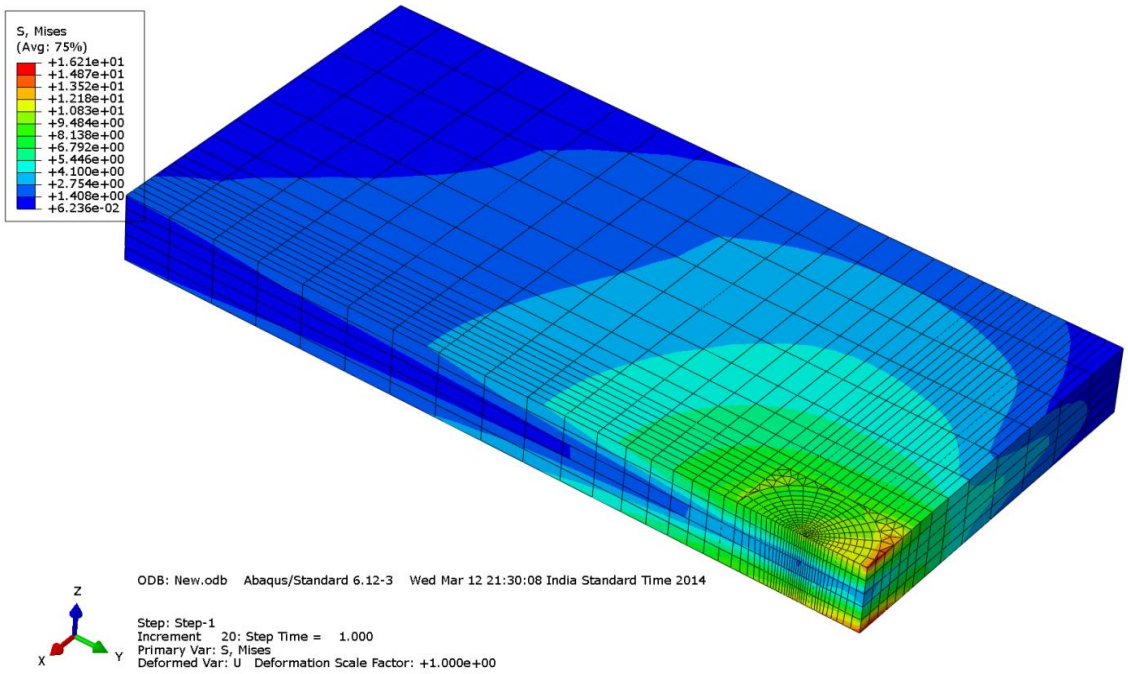

Fig. 5.2: Stresses by Finite Element Analysis for 160 mm Thick Pavement at Edge Position

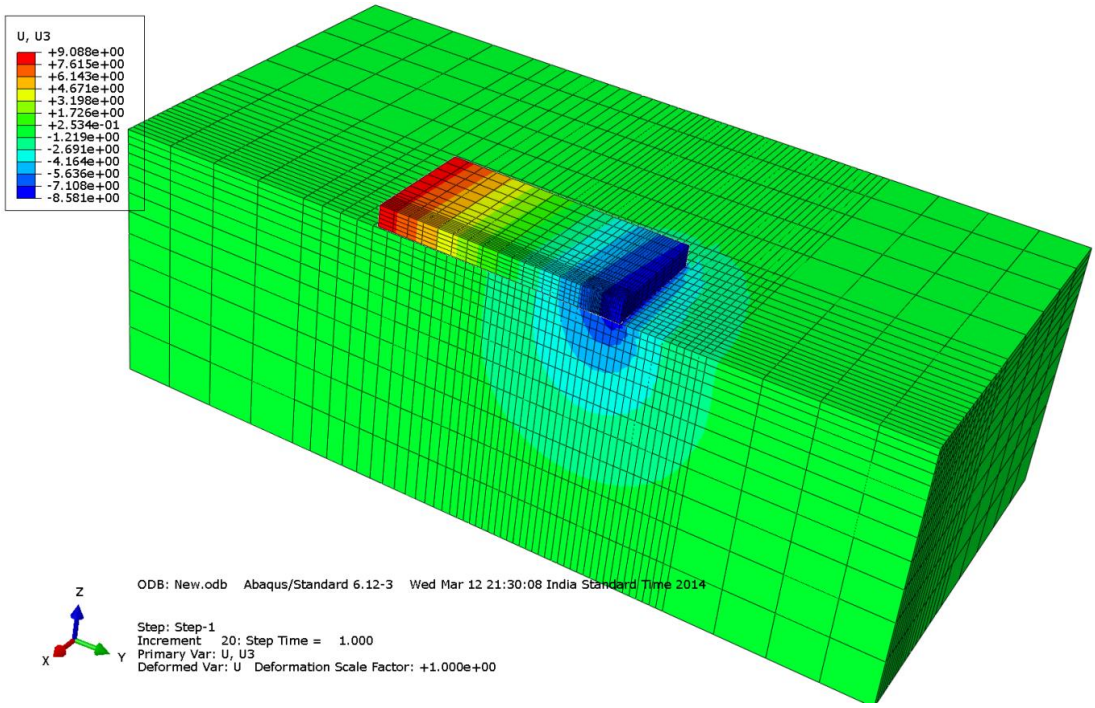

Fig. 5.3: Deflections by Finite Element Analysis for 160 mm Thick Pavement at Edge Position

Table 5.4: Stresses, Strains and Deflections for 200 mm Thick Pavement by Finite Element Analysis at Edge Position

Sl. No.	Loads (kN)	Deflections (mm)	Stresses (MPa)	Strains in radial direction x 10^{-6}
1	0	0.00	0.00	0.00
2	10	0.40	0.50	11.87
3	20	0.80	1.01	23.75
4	30	1.20	1.51	35.62
5	40	1.60	2.02	47.50
6	50	2.00	2.52	59.37
7	60	2.40	3.02	71.24
8	70	2.80	3.53	83.12
9	80	3.20	4.03	94.99
10	90	3.60	4.54	106.87
11	100	4.00	5.04	118.74
12	110	4.40	5.54	130.61
13	120	4.81	6.05	142.49
14	130	5.21	6.55	154.36
15	140	5.61	7.05	166.23
16	150	6.01	7.56	178.11
17	160	6.41	8.06	189.98
18	170	6.81	8.57	201.86
19	180	7.21	9.07	213.73
20	190	7.61	9.57	225.60
21	200	8.01	10.08	237.48
22	210	8.41	10.58	249.35
23	220	8.81	11.09	261.23
24	230	9.21	11.59	273.10

*Stresses are under critical conditions

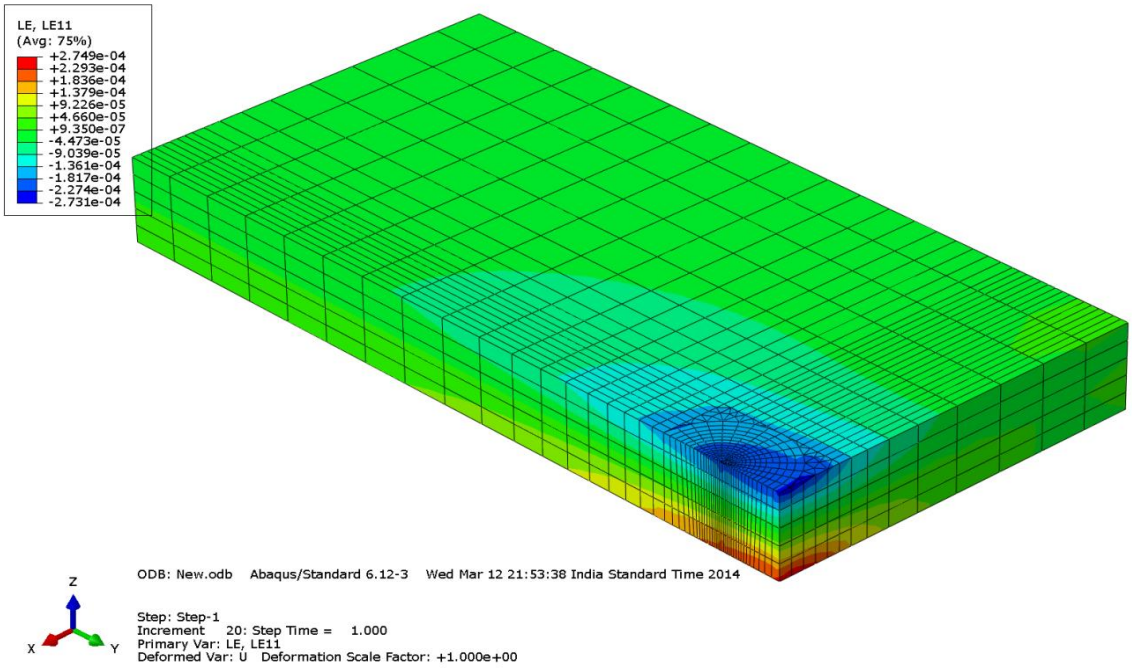

Fig. 5.4: Strains by Finite Element Analysis for 200 mm Thick Pavement at Edge Position

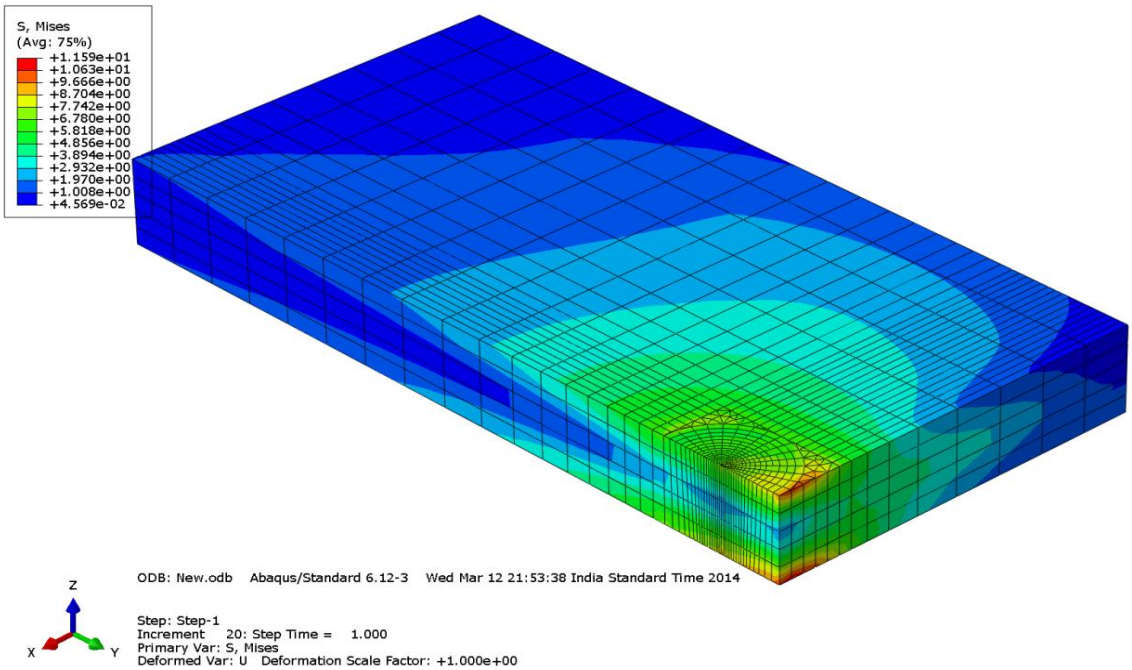

Fig. 5.5: Stresses by Finite Element Analysis for 200 mm Thick Pavement at Edge Position

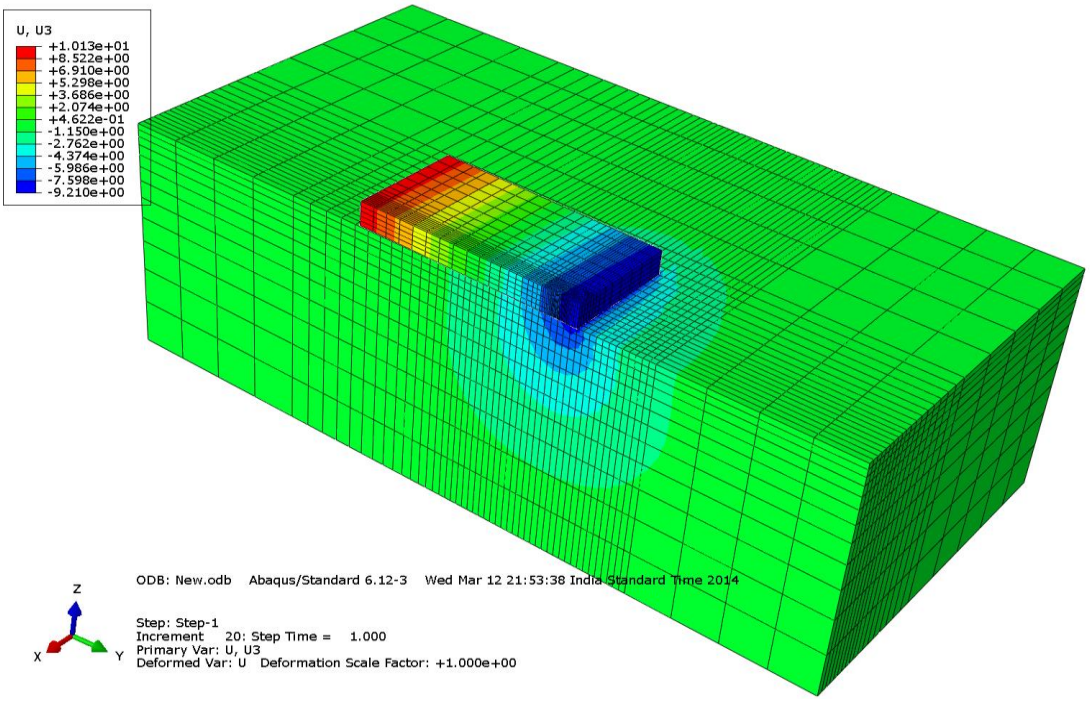

Fig. 5.6: Deflections by Finite Element Analysis for 200 mm Thick Pavement at Edge Position

Table 5.5: Stresses, Strains and Deflections for 240 mm Thick Pavement by Finite Element Analysis at Edge Position

Sl. No.	Loads (kN)	Deflections (mm)	Stresses (MPa)	Strains in radial direction x 10^{-6}
1	0	0.00	0.00	0.00
2	10	0.40	0.35	8.37
3	20	0.80	0.71	16.75
4	30	1.19	1.06	25.12
5	40	1.59	1.41	33.50
6	50	1.99	1.76	41.87
7	60	2.39	2.12	50.24
8	70	2.79	2.47	58.62
9	80	3.18	2.82	66.99
10	90	3.58	3.18	75.37
11	100	3.98	3.53	83.74
12	110	4.38	3.88	92.11
13	120	4.78	4.23	100.49
14	130	5.18	4.59	108.86
15	140	5.57	4.94	117.23
16	150	5.97	5.29	125.61
17	160	6.37	5.64	133.98
18	170	6.77	6.00	142.36
19	180	7.17	6.35	150.73
20	190	7.56	6.70	159.10
21	200	7.96	7.06	167.48
22	210	8.36	7.41	175.85
23	220	8.76	7.76	184.23
24	230	9.16	8.11	192.60

*Stresses are under critical conditions

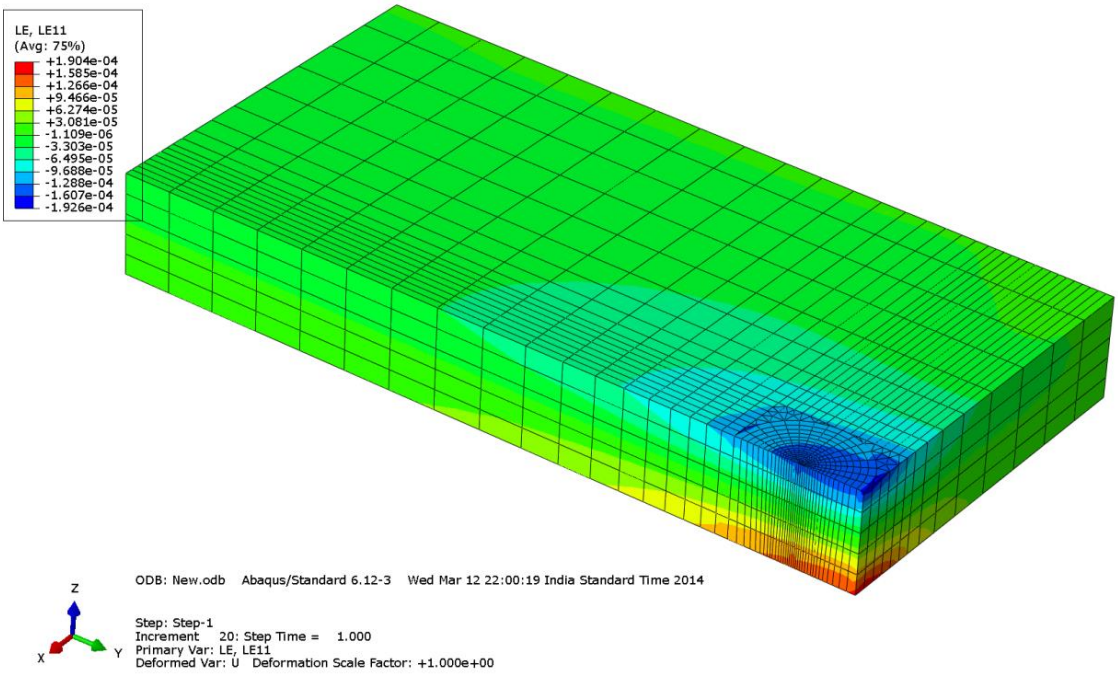

Fig. 5.7: Strains by Finite Element Analysis for 240 mm Thick Pavement at Edge Position

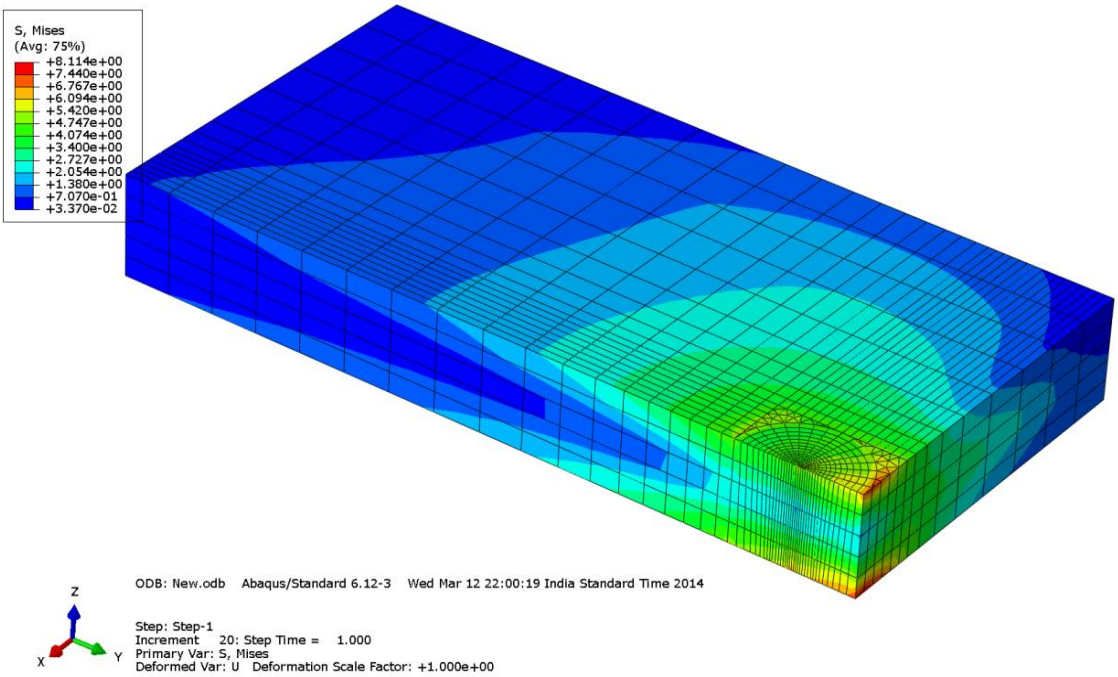

Fig. 5.8: Stresses by Finite Element Analysis for 240 mm Thick Pavement at Edge Position

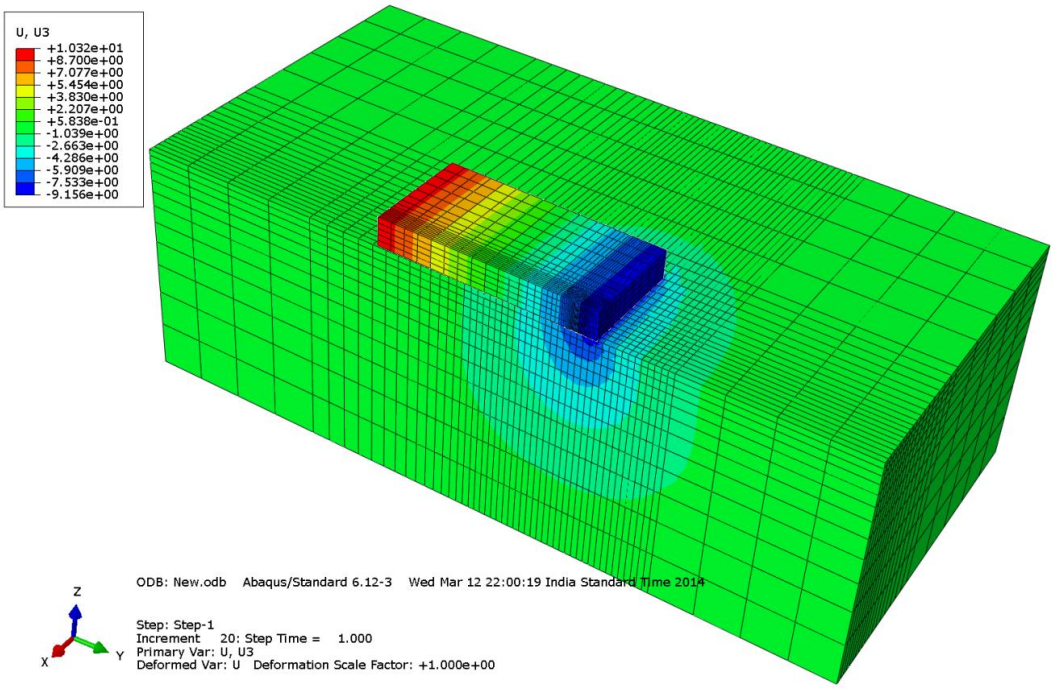

Fig. 5.9: Deflections by Finite Element Analysis for 240 mm Thick Pavement at Edge Position

5.4 DEFLECTINOS IN HSHPC PAVEMENTS

The pavements were laid over subgrade having modulus of subgrade reaction 0.0463 N/mm^3 (4.63 kg/cm^3). For 160 mm thick pavement, the maximum deflections were 11.45 mm at corner position and 10.07 mm at edge position at loads 130 kN and 210 kN respectively. The variation of deflections with loads for different positions is shown in Figure 5.10. The deflections for edge position are lower than corner position for the same load being higher flexural rigidity at edge than the corner position. The results are shown in Table 5.6.

For 200 mm thick pavement, the maximum deflections observed were 18.53 mm at corner for 210 kN load and 10.73 mm at edge and 4.78 mm at central position for load 230 kN. Figure 5.11 shows the variation of deflections with loads for different positions. From Figure 5.11, it could be observed that deflection is lowest for central position and highest for corner position for the same load being highest flexural rigidity at central and lowest at corner position. The results are shown in Table 5.7.

For 240 mm thick pavement, the maximum deflections noticed were 12.35 mm at corner position for 200 kN, 8.22 mm at edge position and 2.67 mm at central position for load 230 kN. The results are shown in Table 5.8. The variations of deflections with loads are shown in Figure 5.12 for different positions. For the same load, the deflection is lowest for central position and highest for corner position.

Comparisons of deflections for the same positions at same load with different thicknesses of pavements have been made i.e. central, edge and corner positions. The comparisons of deflections with load are shown in Figures 5.13 to 5.15. From Figures, it could be inferred that for each position, the deflections decrease with increasing thickness of the pavement due to increase in flexural rigidity. The results are shown in Tables 5.9 to 5.11.

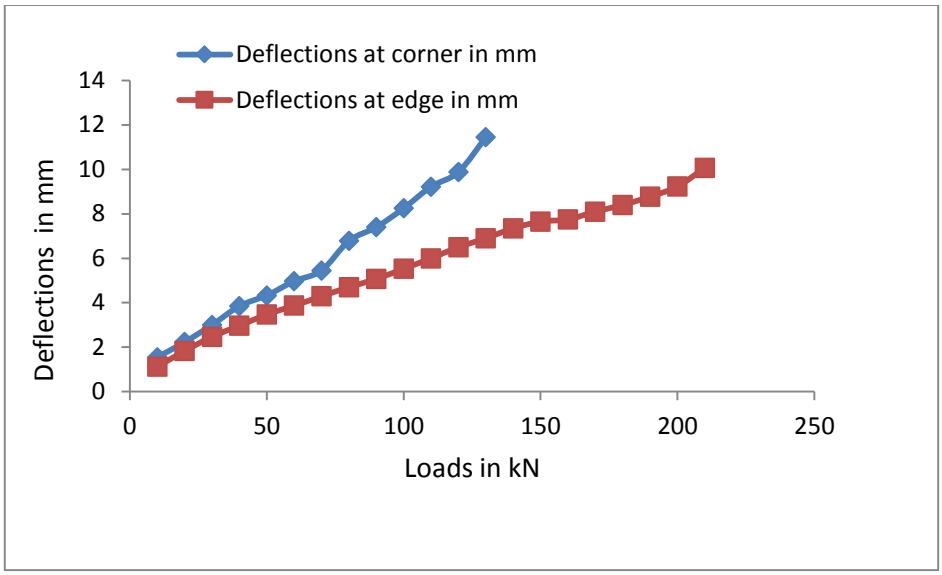

Fig. 5.10 Variation of Deflections with Varying Loads for Different Positions for 160 mm Thick Pavement

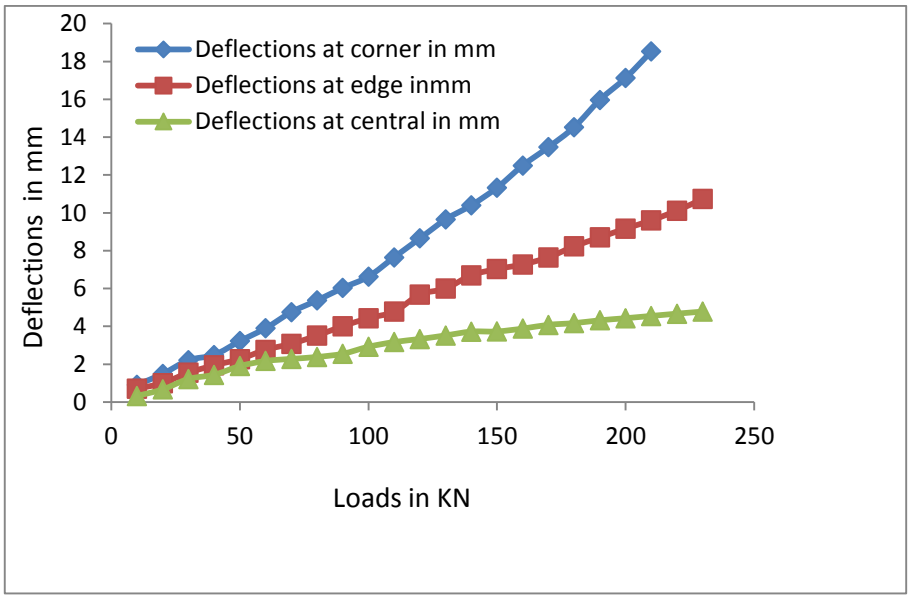

Fig. 5.11 Variation of Deflections with Varying Loads for Different Positions for 200 mm Thick Pavement

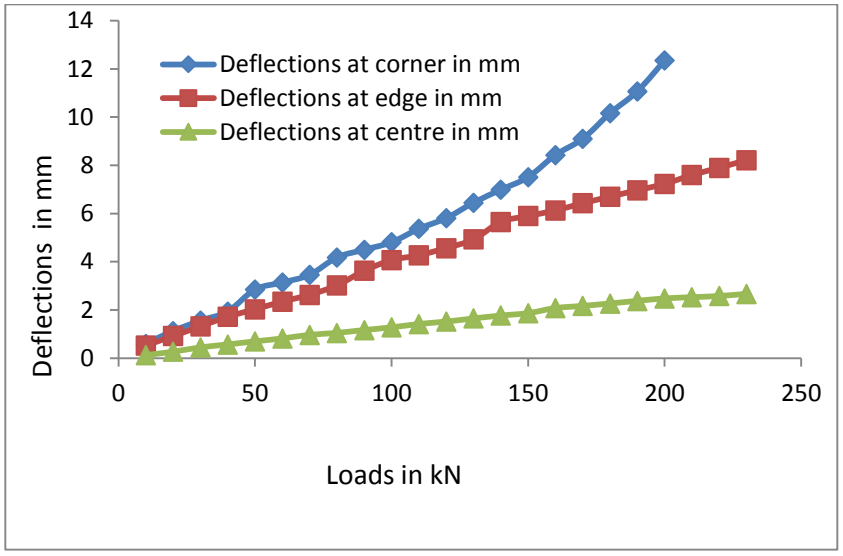

Fig. 5.12 Variation of Deflections with Varying Loads for Different Positions for 240 mm Thick Pavement

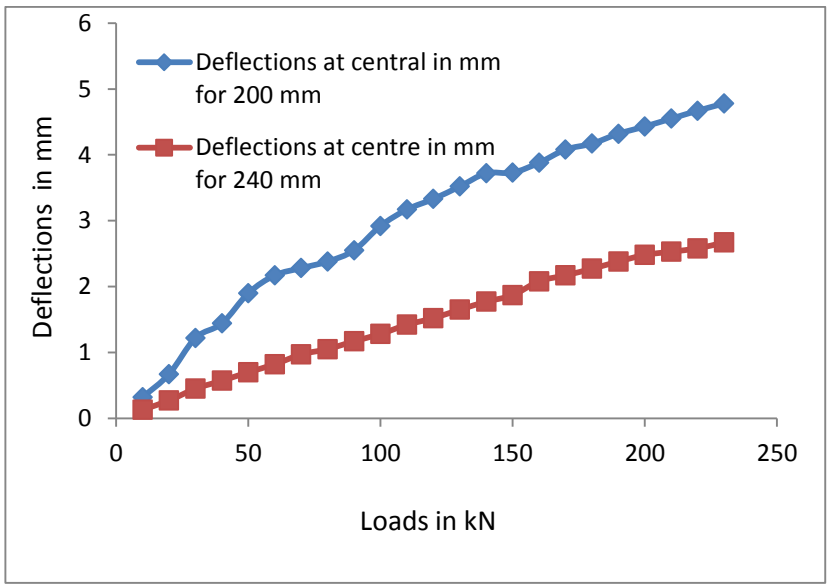

Fig. 5.13 Variation of Deflections with Varying Loads for Different Thicknesses of Pavement at Central Position

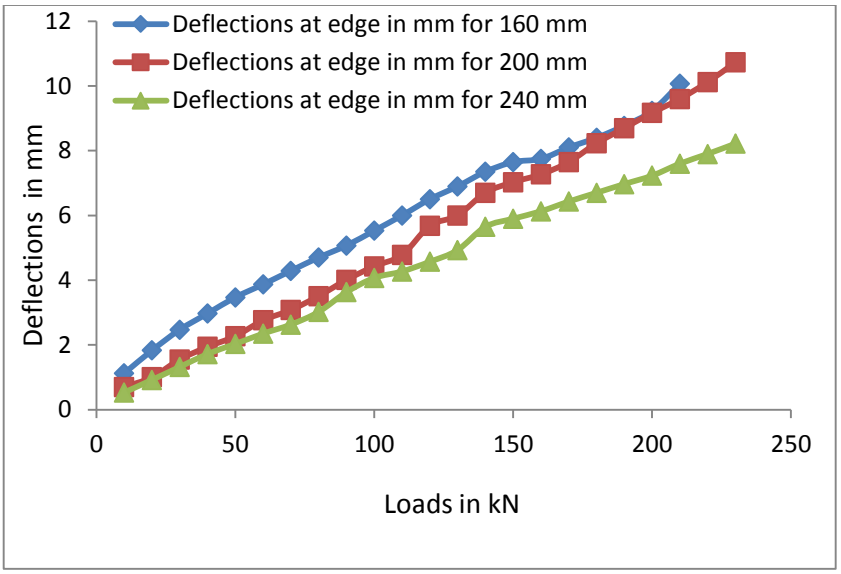

Fig. 5.14 Variation of Deflections with Varying Loads for Different Thicknesses of Pavement at Edge Position

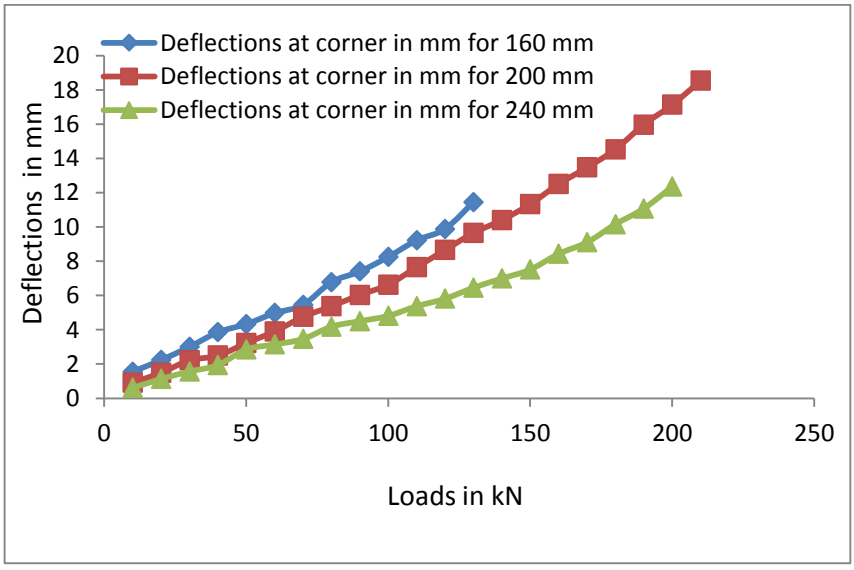

Fig. 5.15 Variation of Deflections with Varying Loads for Different Thicknesses of Pavement at Corner Position

Table 5.6: Observed Deflections at Different Loading at Corner and Edge Positions for 160 mm Thick Pavement

Sl. No.	Loads (kN)	Deflections at corner (mm)	Deflections at edge (mm)
1	50	4.33	3.47
2	100	8.25	5.53
3	130	11.45	6.90
4	150	-	7.65
5	200	-	9.23
6	210	-	10.07

Table 5.7: Observed Deflections at Different Loading at Corner, Edge and Central Positions for 200 mm Thick Pavement

Sl. No.	Loads (kN)	Deflections at corner (mm)	Deflections at edge (mm)	Deflections at centre (mm)
1	50	3.22	2.27	1.90
2	100	6.63	4.43	2.92
3.	150	11.33	7.03	3.73
4.	200	17.13	9.17	4.43
5.	210	18.53	9.60	4.55
6.	230	-	10.73	4.78

Table 5.8: Observed Deflections at Different Loading at Corner, Edge and Central Positions for 240 mm Thick Pavement

Sl. No.	Loads (kN)	Deflections at corner (mm)	Deflections at edge (mm)	Deflections at centre (mm)
1	50	2.85	2.03	0.70
2	100	4.81	4.07	1.28
3.	150	7.51	5.90	1.87
4.	200	12.35	7.23	2.48
5.	230	-	8.22	2.67

Table 5.9: Comparison of Deflections in mm at Different Loading for Edge Position for Different Thicknesses of Pavements

Sl. No.	Loads (kN)	Pavement thicknesses (mm)		
		160	200	240
1	50	3.47	2.27	2.03
2	100	5.53	4.43	4.07
3.	150	7.65	7.03	5.90
4.	200	9.23	9.17	7.23
5.	210	10.07	9.60	7.60
6.	230	-	10.73	8.22

Table 5.10: Comparison of Deflections in mm at Different Loading for Corner Position for Different Thicknesses of Pavements

Sl. No.	Loads (kN)	Pavement thicknesses (mm)		
		160	200	240
1	50	4.33	3.22	2.85
2	100	8.25	6.63	4.81
3.	130	11.45	9.65	6.45
4.	150	-	11.33	7.51
5.	200	-	17.13	12.35
6.	210	-	18.53	-

Table 5.11: Comparison of Deflections in mm at Different Loading for Central Position for Different Thicknesses of Pavements

Sl. No.	Loads (kN)	Pavement thicknesses (mm)		
		160	200	240
1	50	-	1.90	0.70
2	100	-	2.92	1.28
3.	150	-	3.73	1.87
4.	200	-	4.43	2.48
5.	230	-	4.78	2.67

5.4.1 Comparison of Deflections Obtained through FEM Analysis and Experimental Values for Edge Position

Deflections for edge position for different thicknesses have been analyzed using FEM and the results are being shown in Tables 5.3 to 5.5. Comparison of results obtained through FEM and experimental values are being shown in Table 5.12. The ratio of observed to FEM values range from 1.13 to 1.70 for 160 mm thick pavement, 1.11 to 1.17 for 200 mm thick pavement and 0.90 to 1.02 for 240 mm thick pavement. These ratios represent that value calculated through FEM analysis is in good agreement with the observed values. The analytical as well as observed deflections keep reducing with increasing thickness of pavement. This is because the flexural rigidity increases with increase in thickness. Observed and FEM values of deflections are plotted in Figures 5.16 to 5.18. At 210 kN load, the maximum deflection was 10.07 mm for edge position for 160 mm thick pavement. A wheel load of 230 kN produced the deflections 10.73 mm and 8.22 mm for 200 mm and 240 mm thick pavement respectively.

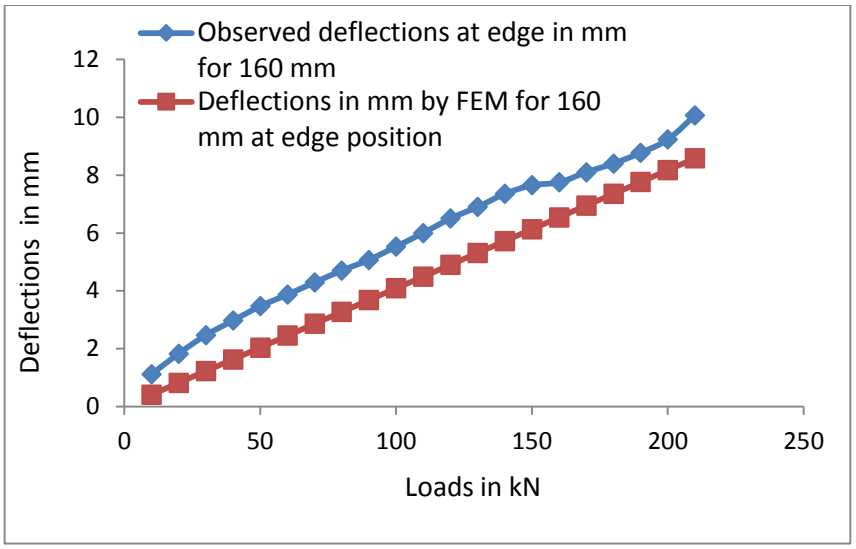

Fig. 5.16 Comparison of Observed Deflections with Analytical Deflections by FEM at Edge Position for 160 mm Thick Pavement

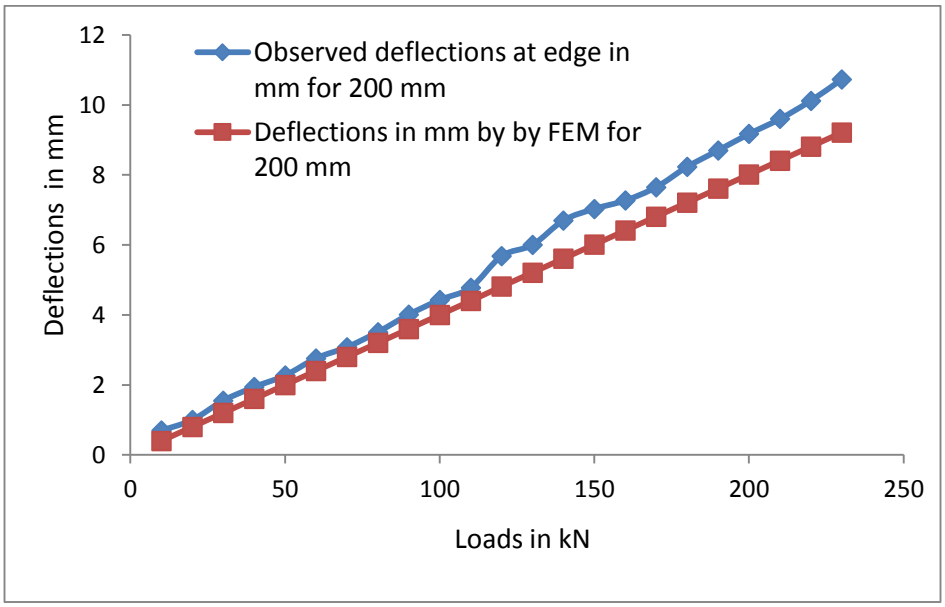

Fig. 5.17 Comparison of Observed Deflections with Analytical Deflections by FEM at Edge Position for 200 mm Thick Pavement

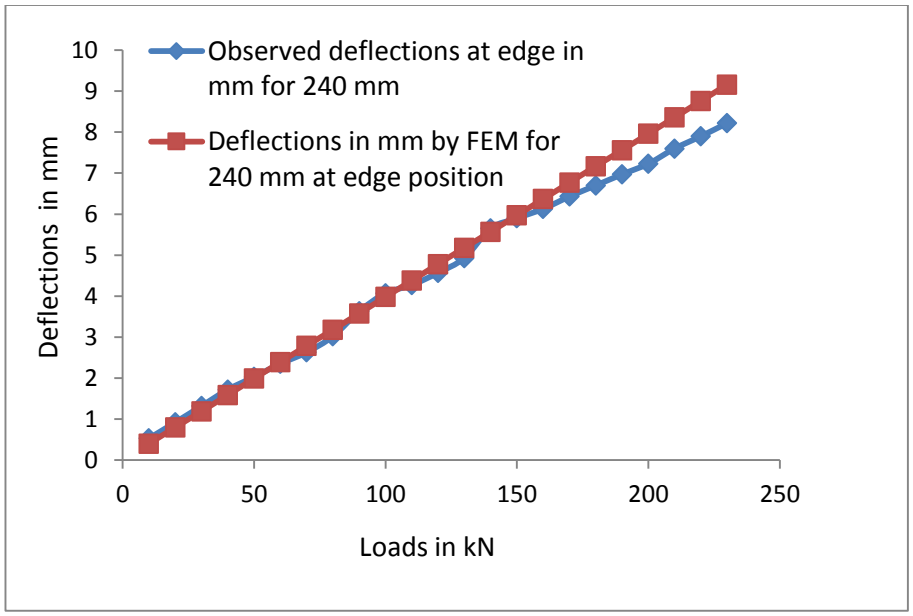

Fig. 5.18 Comparison of Observed Deflections with Analytical Deflections by FEM at Edge Position for 240 mm Thick Pavement

Table 5.12: Comparison of Deflections at Edge Position between Observed and through FEM Analysis at Different Loadings

Sl. No.	Pavement thicknesses (mm)	Loads (kN)	Observed deflections (mm)	Deflections through FEM (mm)	Ratio (observed / FEM)	% variation
1	160	50	3.47	2.04	1.70	41.21
		100	5.53	4.09	1.35	26.03
		150	7.65	6.13	1.25	19.86
		200	9.23	8.17	1.13	11.48
		210	10.07	8.58	1.17	14.80
2	200	50	2.27	2.00	1.14	11.90
		100	4.43	4.00	1.11	9.70
		150	7.03	6.01	1.17	14.50
		200	9.17	8.01	1.14	12.60
		230	10.73	9.21	1.17	14.16
3	240	50	2.03	1.99	1.02	1.97
		100	4.07	3.98	1.02	2.21
		150	5.90	5.97	0.99	-1.18
		200	7.23	7.96	0.91	-10.10
		230	8.22	9.16	0.90	-11.44

5.5 STRAINS IN HSHPC PAVEMENTS

The strains in pavements were measured in longitudinal direction i.e. radial direction and transverse direction. The strains in transverse direction are generally very low than the radial direction.

For 160 mm thick pavement, strains were measured at corner and edge position for the varying load. Strains were measured 320.3 x 10^{-6} at 130 kN load for corner position and 418.0 x 10^{-6} for edge position at 210 kN load. For the same load the strain at corner position was higher than the edge position. This is due to higher flexural rigidity at edge position than the corner position. The variations of strains with loads are shown in Figure 5.19 and results are shown in Table 5.13.

For 200 mm thick pavement, at different positions i.e. central, edge and corner, the strains were measured for different loading. Strains were measured 375.2 x 10^{-6}at 210 kN load for corner positions, 312.8 x 10^{-6} at 230 kN load for edge position and 275.3 x 10^{-6} at 230 kN for central position. It has been observed that, for the same loading, the strain is highest for corner position and lowest for central position. The variations of strains with loads are shown in Figure 5.20 and results are shown in Table 5.14.

For 240 mm thick pavement, strains were measured for the varying loads at different positions i.e. central, edge and corner. The strains measured were 240.3 x 10^{-6} at 200 kN load for corner position, 207.36 x 10^{-6} at 230 kN for edge position and 182.5 x 10^{-6} at 230 kN for central position. It has been observed that for the same loading, the strain is highest for corner position and lowest for central position. The variations of strains with loads are shown in Figure 5.21 and results are shown in Table 5.15.

Strains are lowest at central position and highest at corner position being highest flexural rigidity in the central position and lowest in corner position.

For the same position, the strains were compared for different thicknesses of pavements. Figures 5.22 to 5.24 show the variation of strains for the same positions with the different thicknesses of the pavement. It has been noticed that for each position, the strain decreases with increasing thickness of the pavement due to increase in flexural rigidity. The results are shown in Tables 5.16 to 5.18.

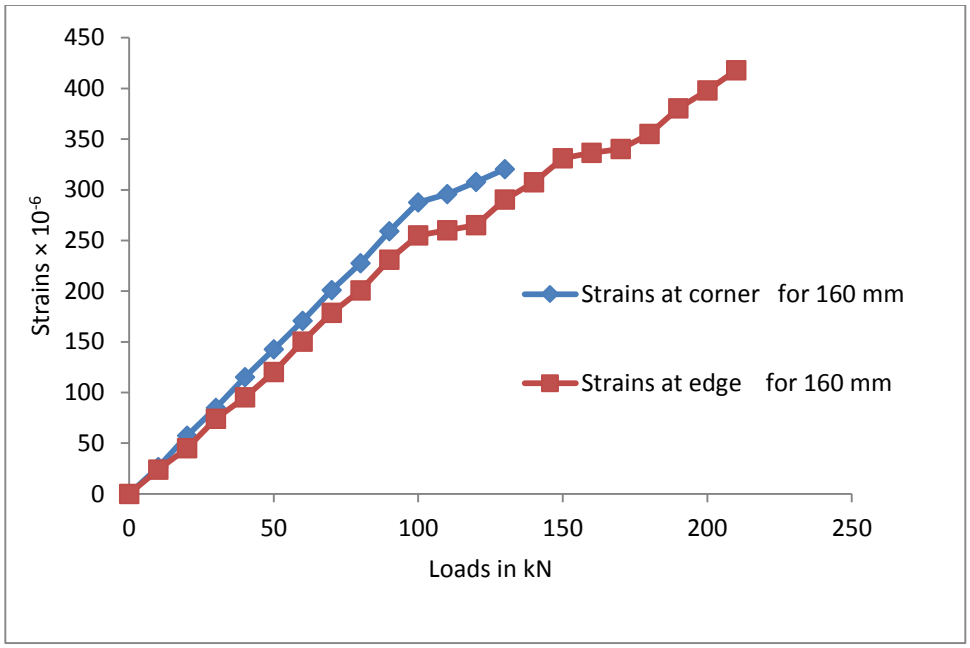

Fig. 5.19 Variation of Strains with Varying Loads for Different Positions for 160 mm Thick Pavement

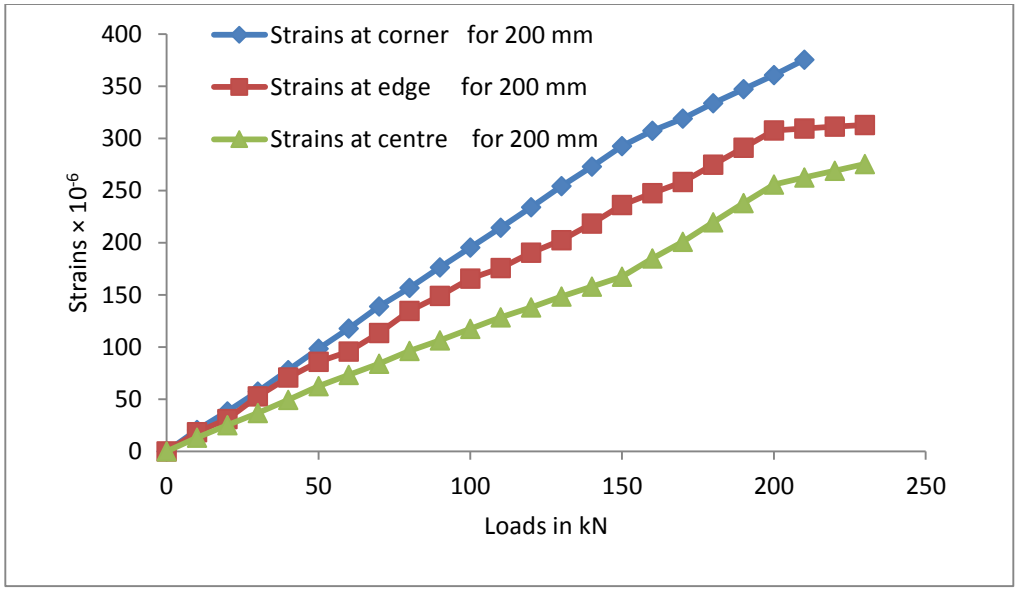

Fig. 5.20 Variation of Strains with Varying Loads for Different Positions for 200 mm Thick Pavement

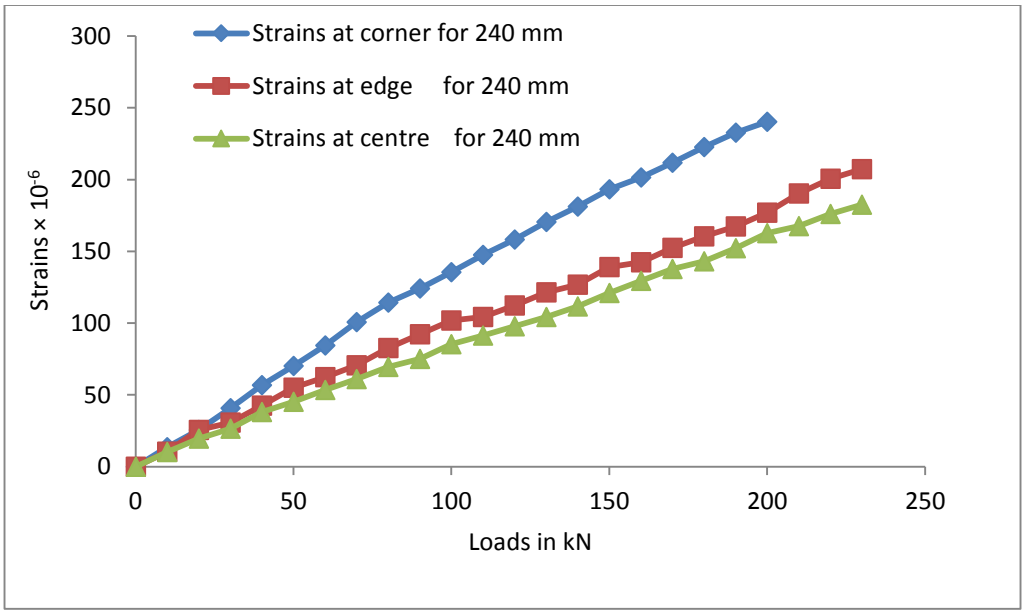

Fig. 5.21 Variation of Strains with Varying Loads for Different Positions for 240 mm Thick Pavement

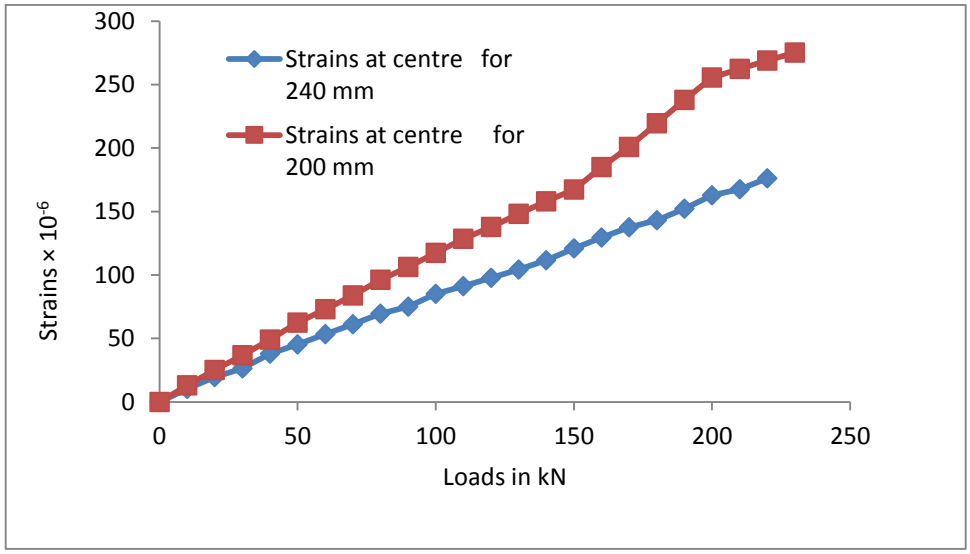

Fig. 5.22 Variation of Strains with Varying Loads for Different Thicknesses of Pavement at Central Position

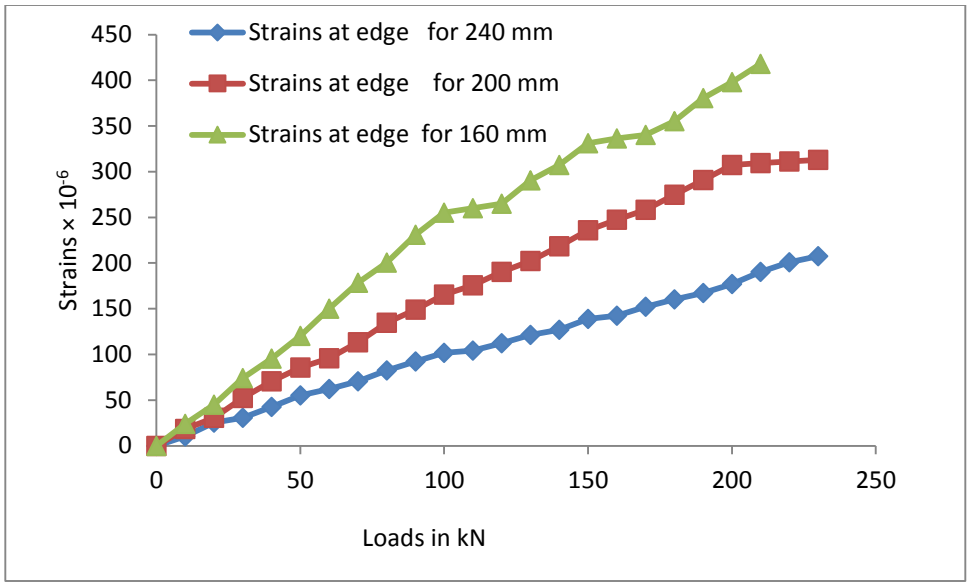

Fig. 5.23 Variation of Strains with Varying Loads for Different Thicknesses of Pavement at Edge Position

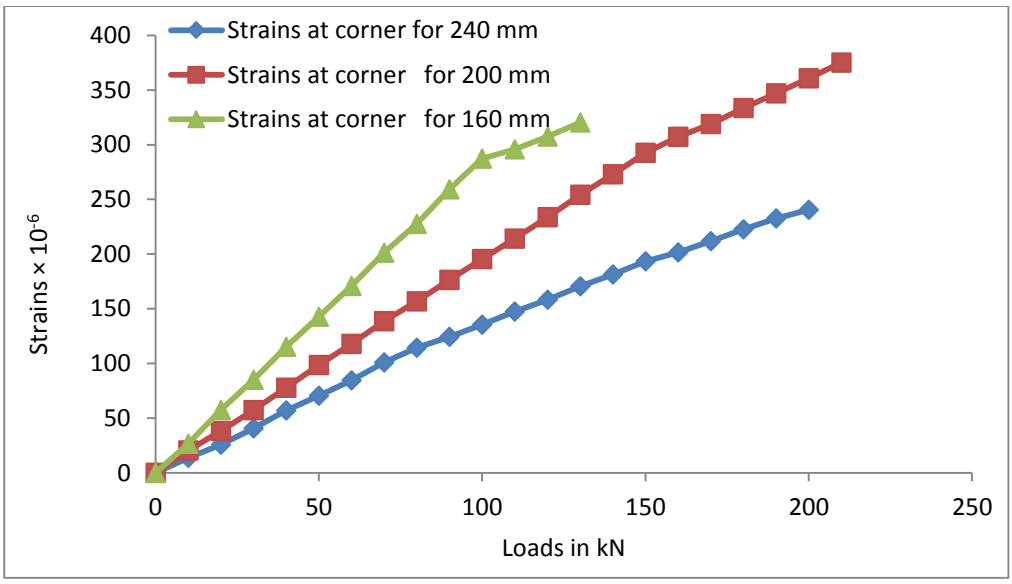

Fig. 5.24 Variation of Strains with Varying Loads for Different Thicknesses of Pavement at Corner Position

Table 5.13: Longitudinal Strains at Different Loading for Corner and Edge Position for 160 mm Thick Pavement

Sl. No.	Loads (kN)	Strains at corner x 10^{-6}	Strains at edge x 10^{-6}
1	50	142.60	120.30
2	100	287.40	255.14
3	130	320.30	290.40
4	150	-	331.14
5	200	-	398.09
6	210	-	418.00

Table 5.14: Longitudinal Strains at Different Loading for Corner, Edge and Central Positions for 200 mm Thick Pavement

Sl. No.	Loads in (kN)	Strains at corner x 10^{-6}	Strains at edge x 10^{-6}	Strains at centre x 10^{-6}
1	50	98.50	85.74	62.45
2	100	195.25	165.56	117.30
3	150	292.50	235.93	167.40
4	200	360.60	307.45	255.60
5	210	375.20	309.52	262.31
6	230	-	312.80	275.30

Table 5.15: Longitudinal Strains at Different Loading for Corner, Edge and Central Positions for 240 mm Thick Pavement

Sl. No.	Loads (kN)	Strains at corner x 10^{-6}	Strains at edge x 10^{-6}	Strains at centre x 10^{-6}
1	50	70.25	55.10	45.30
2	100	135.40	101.85	85.25
3	150	193.30	138.99	120.90
4	200	240.30	176.98	162.70
5	230	-	207.36	182.50

Table 5.16: Comparison of Longitudinal Strains at Edge Position for Different Thicknesses of Pavements

Sl. No.	Loads (kN)	Strains (X 10^{-6}) for different pavement thicknesses (mm)		
		160	200	240
1	50	120.30	85.74	55.10
2	100	255.14	165.56	101.85
3	150	331.14	235.93	138.99
4	200	398.09	307.45	176.98
5	210	418.00	309.52	190.25
6	230	-	312.80	207.36

Table 5.17: Comparison of Longitudinal Strains at Corner Position for Different Thicknesses of Pavements

Sl. No.	Loads (kN)	Strains (X 10^{-6}) for different pavement thicknesses (mm)		
		160	200	240
1	50	142.60	98.50	70.25
2	100	287.40	195.25	135.40
3	130	320.30	254.21	170.50
4	150	-	292.50	193.30
5	200	-	360.60	240.30
6	210	-	375.20	-

Table 5.18: Comparison of Longitudinal Strains at Centre Position for Different Thicknesses of Pavement

Sl. No.	Loads (kN)	Strains (X 10^{-6}) for different pavement thicknesses (mm)		
		160	200	240
1	50	-	62.45	45.30
2	100	-	117.30	85.25
3	150	-	167.40	120.90
4	200	-	255.60	162.70
5	230	-	275.30	182.50

5.5.1 Comparison of Strains Obtained Through FEM Analysis and Experimental Values for Edge Position

Strains obtained through FEM analysis at edge position for different thickness are shown in Tables 5.3 to 5.5. Comparison of results obtained through FEM analysis and observed values are presented in Table 5.19.

Analysis of results shows that FEM and experimental values are in good agreement. The ratio of observed and FEM values range from 1.09 to 1.40 for 160 mm thick pavement, 1.15 to 1.44 for 200 mm thick pavement and 1.06 to 1.32 for 240 mm thick pavement. The limiting strain measured at 210 kN for 160 mm thick pavement before failure was 418.0 x 10^{-6}. As the load reached 220 kN, the pavement suddenly broken into two approximately equal part. The limiting strains could not be measured for 200 mm and 240 mm thick pavement due to maximum capacity of loading frame being limited to 250 kN. From the observations, it is quite clear that pavement of thicknesses 200 mm and 240 mm still could carry more loads. Figures 5.25 to 5.27 show the comparison of strains obtained through FEM analysis and experimental observed values.

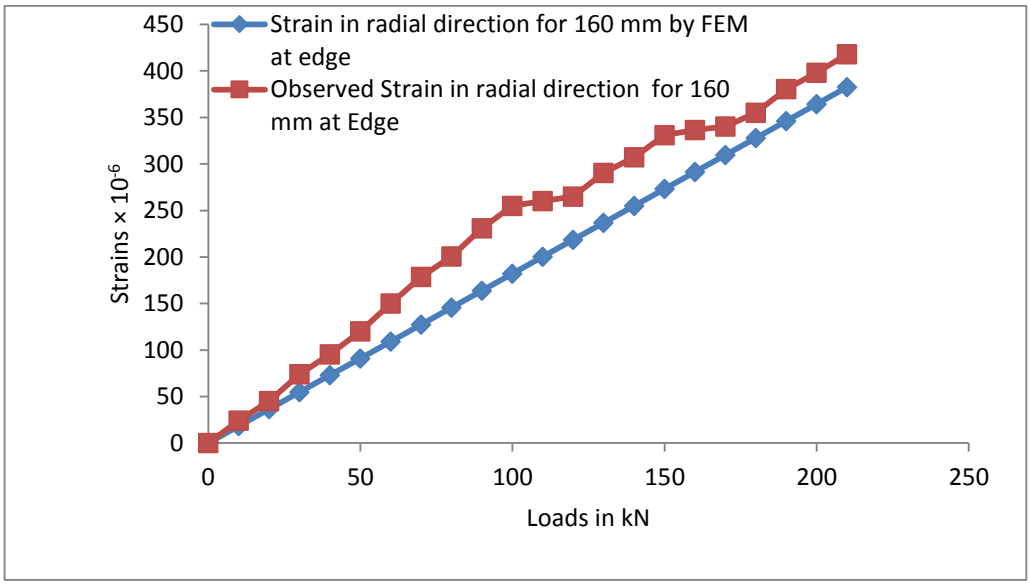

Fig. 5.25 Comparison of Observed Strains with Analytical Strains by FEM at Edge Position for 160 mm Thick Pavement

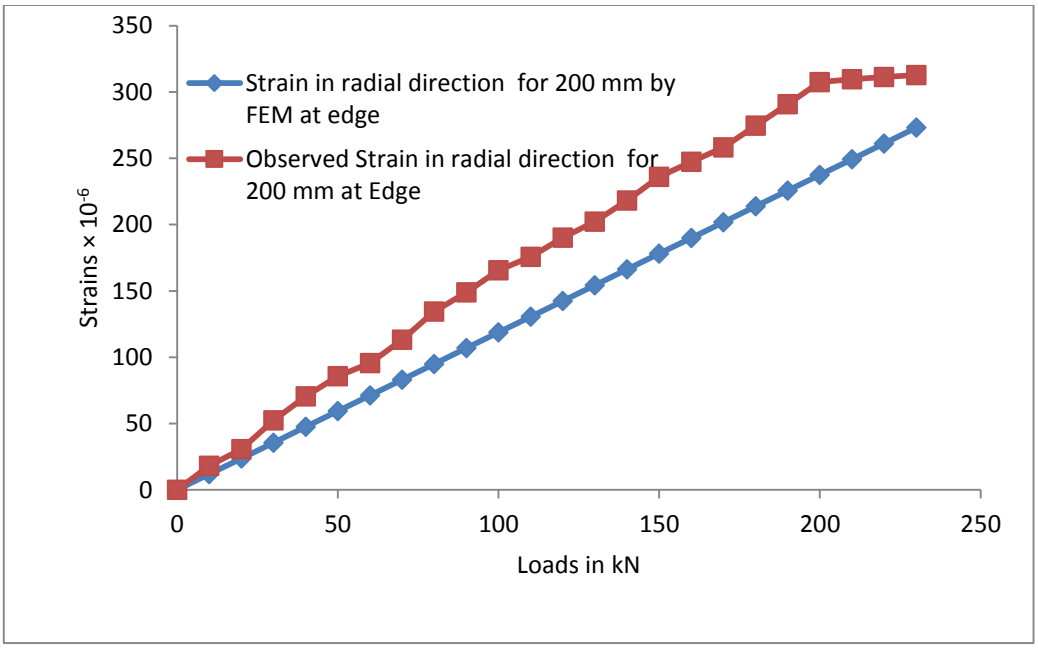

Fig. 5.26 Comparison of Observed Strains with Analytical Strains by FEM at Edge Position for 200 mm Thick Pavement

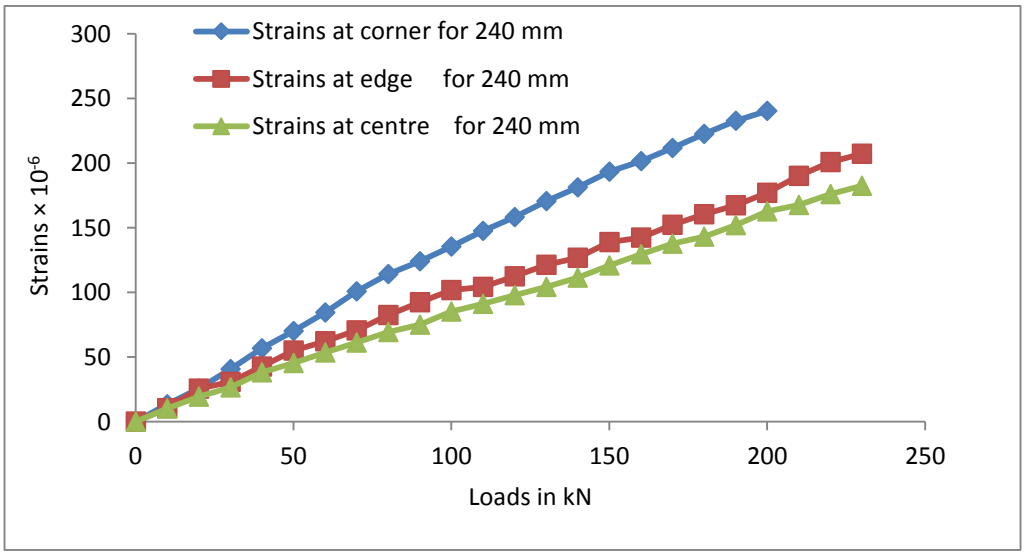

Fig. 5.27 Comparison of Observed Strains with Analytical Strains by FEM at Edge Position for 240 mm Thick Pavement

Table 5.19: Comparison of Strains at Edge Position Between Observed and Obtained Through FEM Analysis

Sl. No.	Pavement thickness (mm)	Loads (kN)	Observed strains x 10^{-6}	Strains through FEM x 10^{-6}	Ratio (observed / FEM)	% variation
1	160	50	120.30	91.07	1.32	24.3
		100	255.14	182.14	1.40	26.6
		150	331.14	273.21	1.21	17.5
		200	398.09	364.29	1.09	8.5
		210	418.00	382.50	109	8.5
2	200	50	85.74	59.37	1.44	30.76
		100	165.56	118.74	1.39	28.28
		150	235.93	178.11	1.32	24.5
		200	307.45	237.48	1.29	22.76
		230	312.80	273.10	1.15	12.7
3	240	50	55.10	41.87	1.32	24.0
		100	101.85	83.74	1.22	17.78
		150	138.99	125.61	1.11	9.63
		200	176.98	167.48	1.06	5.37
		230	207.36	192.60	1.08	7.11

5.6 WHEEL LOAD STRESSES IN HSHPC PAVEMENTS

Wheel load stresses at different loads have been calculated by using Westergaard, Mayerhof, Ghosh and by Indian Road Congress (IRC) methods for different thicknesses of pavements. Wheel load stresses at varying loads for different positions for various thicknesses of pavements and variations of theoretical stresses with respect to observed values are shown in Tables 5.20 to 5.22.

Table 5.20: Wheel Load Stresses at Varying Loads through Different Theories for Slab Thickness 160 mm

Dimension of the slab = 1800 mm x 1800 mm, Thickness of the slab, 'h' = 160 mm

Radius of loaded area, 'a' = 150 mm, Equivalent radius of resisting section, 'b' = 140.2 mm

Modulus of subgrade reaction, 'K' = 0.0463 N/mm^3 (4.63 kg/cm3) Modulus of elasticity of concrete 'E' = 4.17 x 10^4 N/mm^2

Poisson's ratio of concrete, 'μ' = 0.2 Flexural strength of concrete, 'σ_b' = 6.4 N/mm^2

Radius of relative stiffness, '*l*' = 750 mm

Sl. No.	Loads (P) (kN)	By Westergard Analysis (MPa)				By Mayerhof's analysis				By IRC-58 Method of analysis (MPa)				Experimentally observed values (MPa)	
		S_e		S_c		S_e		S_c		S_e		S_c		S_e	S_c
		Calculated	% variation	Calculated	% variation	Calculated	% variation	Calculated	% variation	Calculated	% variation	Calculated	% variation		
1	50	3.65	27.3	3.11	47.73	1.42	71.7	2.34	60.67	4.19	16.5	4.57	23.19	5.02	5.95
2	100	7.31	31.3	6.23	48.04	2.84	73.3	4.69	60.68	8.37	21.3	9.14	23.77	10.64	11.99
3	130	9.50	21.6	8.09	39.45	3.70	69.4	6.09	54.42	10.88	10.16	1.88	11.07	12.11	13.36
4	150	10.96	20.6	-	-	4.27	69.1	-	-	12.55	9,12	-	-	13.81	-
5	200	14.62	11.93	-	-	5.69	65.7	-	-	16.74	-0.84	-	-	16.60	-
6.	210	15.35	11.93	-	-	5.97	65.7	-	-	17.58	-0.86	-	-	17.43	-

*Thermal stress at edge region = 0.13 N/mm^2 as calculated by as per Bradbury concept [62]

Table 5.21: Wheel Load Stresses at Varying Loads through Different Theories for Slab Thickness 200 mm

Dimension of slab = 1800 mm x 1800 mm, Thickness of slab, 'h' = 200 mm

Radius of loaded area, 'a' = 150 mm, Equivalent radius of resisting section, 'b' = 140.7 mm

Modulus of subgrade reaction, 'K' = 0.0463 N/mm^3 (4.63 kg/cm^3) Modulus of elasticity of concrete 'E' = 4.17 x 10^4 N/mm^{2-}

Poisson's ratio of concrete, 'μ' = 0.2 Flexural strength of concrete, 'σ_b' = 6.4 N/mm^2

Radius of relative stiffness, '*l*' = 889.3 mm

Sl. No	Loads, (P) (kN)	By Westergaard analysis (MPa)						By Mayerhoff analysis (MPa)						By IRC-58 Method of analysis (MPa)				Experimentally observed values (MPa)		
		S_i		S_e		S_c		S_i		S_e		S_c		S_e		S_c		S_i	S_e	S_c
		Calculated	% variation	Calculated	% variation	Calculated	% variation	Calculated	% variation	Calculated	% variation	Calculated	% variation	Calculated	% variation	Calculated	% variation			
1	50	1.69	36.47	2.55	28.8	2.16	47.44	0.56	78.95	0.93	74.02	1.56	62.04	2.89	19.27	3.08	25.06	2.66	3.58	4.11
2	100	3.37	31.08	5.09	26.23	4.33	46.81	1.13	76.89	1.86	73.04	3.12	61.67	5.78	16.23	6.16	24.32	4.89	6.90	8.14
3	150	5.06	27.5	7.63	22.55	6.49	46.80	1.69	75.79	2.80	71.54	4.68	61.63	8.67	11.89	9.24	24.26	6.98	9.84	12.20
4	200	6.75	36.68	10.19	20.51	8.65	42.49	2.25	78.89	3.73	70.90	6.23	58.58	11.56	9.8	12.31	18.15	10.66	12.82	15.04
5	210	7.08	35.28	10.69	17.20	9.09	41.92	2.37	78.34	3.91	69.71	6.55	58.15	12.14	5.96	12.93	17.38	10.94	12.91	15.65
6	230	7.76	32.40	11.71	10.20	-	-	2.59	77.44	4.29	67.10	-	-	13.29	-1.92	-	-	11.48	13.04	-

*Thermal stress at edge region = 0.11 N/mm^2 as calculated by as per Bradbury concept [62]

Table 5.22: Wheel Load Stresses at Varying Loads through Different Theories for Slab Thickness 240 mm

Dimension of slab = 1800 mm x 1800 mm, Thickness of slab, 'h' = 240 mm

Radius of loaded area, 'a' = 150 mm, Equivalent radius of resisting section, 'b' = 143.9 mm

Modulus of subgrade reaction, 'K' = 0.0463 N/mm^3 (4.63 kg/cm^3) Modulus of elasticity of concrete 'E' = 4.17 x 10^4 N/mm^2

Poisson's ratio of concrete, 'μ' = 0.2 Flexural strength of concrete, 'σ_b' = 6.4 N/mm^2

Radius of relative stiffness, 'l' = 1019.6 mm

Sl. No	Loads (P) (kN)	By Westergaard analysis (MPa)						By Mayerhoff analysis (MPa)						By IRC-58 method of analysis (MPa)				Experimentally observed values (MPa)		
		S_i		S_e		S_c		S_i		S_e		S_c		S_e		S_c		S_i	S_e	S_c
		Calculated	% variation	Calculated	% variation	Calculated	% variation	Calculated	% variation	Calculated	% variation	Calculated	% variation	Calculated	% variation	Calculated	% variation			
1	50	1.23	34.92	1.87	18.7	1.59	45.73	0.39	79.37	0.66	71.3	1.11	62.12	2.11	8.26	2.21	24.57	1.89	2.30	2.93
2	100	2.45	31.18	3.73	12.24	3.18	43.72	0.79	77.81	1.32	68.94	2.22	60.70	4.23	0.47	4.42	21.76	3.56	4.25	5.65
3	150	3.68	26.98	5.60	3.45	4.77	40.82	1.18	76.59	1.97	66.03	3.33	58.68	6.34	-9.31	6.63	17.74	5.04	5.80	8.06
4.	200	4.90	27.84	7.47	-1.22	6.36	36.53	1.58	76.73	2.63	64.36	4.44	55.69	8.45	-14.5	8.83	11.88	6.79	7.38	10.02
5	230	5.64	25.89	8.59	0.69	-	-	1.81	76.22	3.03	64.97	-	-	9.72	-12.36	-	-	7.61	8.65	-

*Thermal stress at edge region = 0.096 N/mm^2 as calculated by as per Bradbury concept [62]

5.6.1 Comparison of Wheel Load Stresses for Edge Position

A comparison of wheel load stresses calculated by analytical method i.e. FEM, theoretical methods i.e. Westergaard, Mayerhof, IRC-58 method with the observed values of stresses are shown in Table 5.23 and the results are plotted in Figures 5.28 to 5.33.

The ratios of observed to theoretical stresses are 1.37 by Westergaard method, 3.53 by Mayerhof method, 1.2 by IRC method and 1.3 by FEM analysis at 50 kN load for 160 mm thick pavement. For 200 mm thick pavement these ratios are 1.4 by Westergaard, 3.83 by Mayerhof, 1.24 by IRC and 1.42 by FEM analysis at 50 kN load. For 240 mm thick pavement, these ratios are 1.23 by Westergaard, 3.5 by Mayerhoff, 1.09 by IRC and 1.31 by FEM analysis at 50 kN load. Results of FEM analysis and Westergaard are in very good agreement with the observed values. Results obtained by Westergaard and FEM analysis are approximately equal. Results obtained by IRC method are more close to the observed values than Finite Element and Westergaard analysis, but there is no much difference in values.

Results obtained by Westergaard, IRC and FEM analysis are in good agreement with the observed values. For 200 kN load, the ratio of observed to Westergaard analysis are 1.14, 1.26 and 0.99 for 160 mm, 200 mm and 240 mm thick pavements respectively. The corresponding results obtained by Mayerhof's are 2.92, 3.44 and 2.8 for 160 mm, 200 mm and 240 mm thick pavements respectively. The results computed by FEM are 1.08, 1.27 and 1.05 much closer to observed values for 160 mm, 200 mm and 240 mm thick pavement respectively. By IRC method at 200 kN load the ratios are 0.99 for 160 mm, 1.11 for 200 mm and 0.87 for 240 mm thick pavements.

For 160 mm thick pavement at edge as the load was being applied beyond the 210 kN, the pavement suddenly broke into two approximately equal parts. At 210 kN load, the ratios are 1.14 by Westergaard, 2.92 by Mayerhof's, 0.99 by IRC and 1.08 by FEM analysis. These results reflect that stresses computed by Westergaard, IRC and FEM analysis are very much close to the observed results. These also demonstrate that

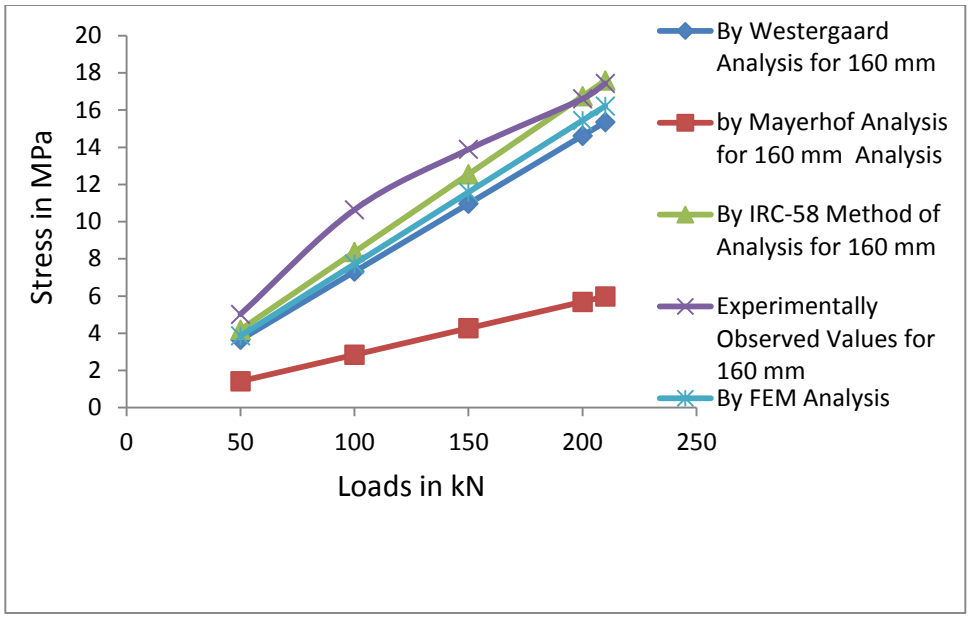

Fig. 5.28 Comparison of Observed Stresses with Theoretical and Analytical (FEM) Stresses at Edge Position for 160 mm Thick Pavement

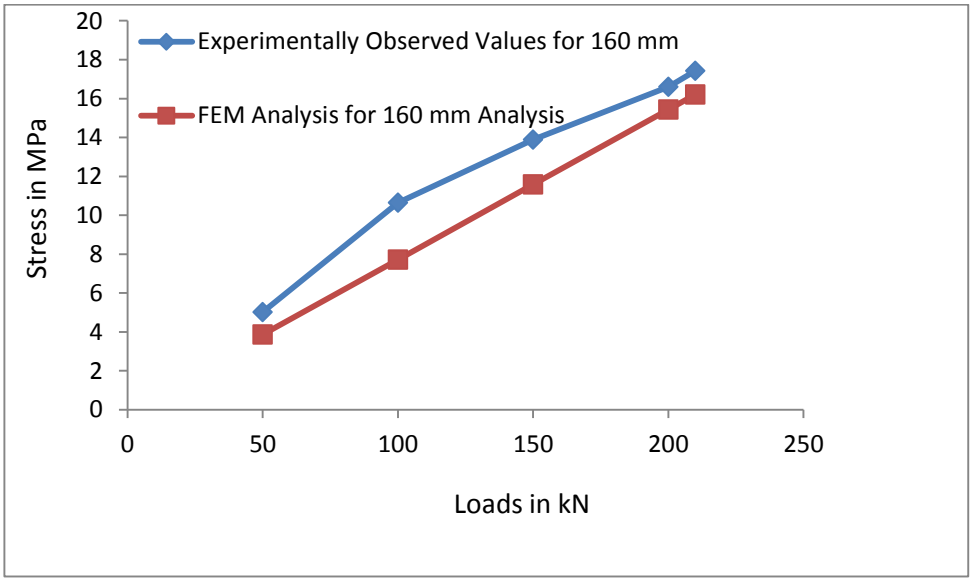

Fig. 5.29 Comparison of Observed Stresses with Analytical Stresses by FEM at Edge Position for 160 mm Thick Pavement

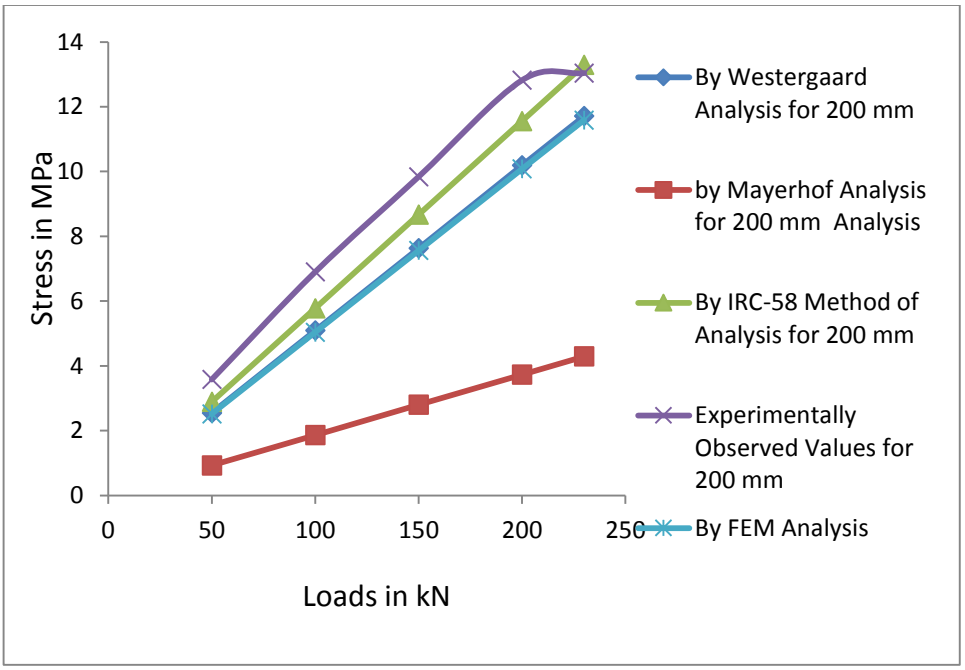

Fig. 5.30 Comparison of Observed Stresses with Theoretical and Analytical (FEM) Stresses at Edge Position for 200 mm Thick Pavement

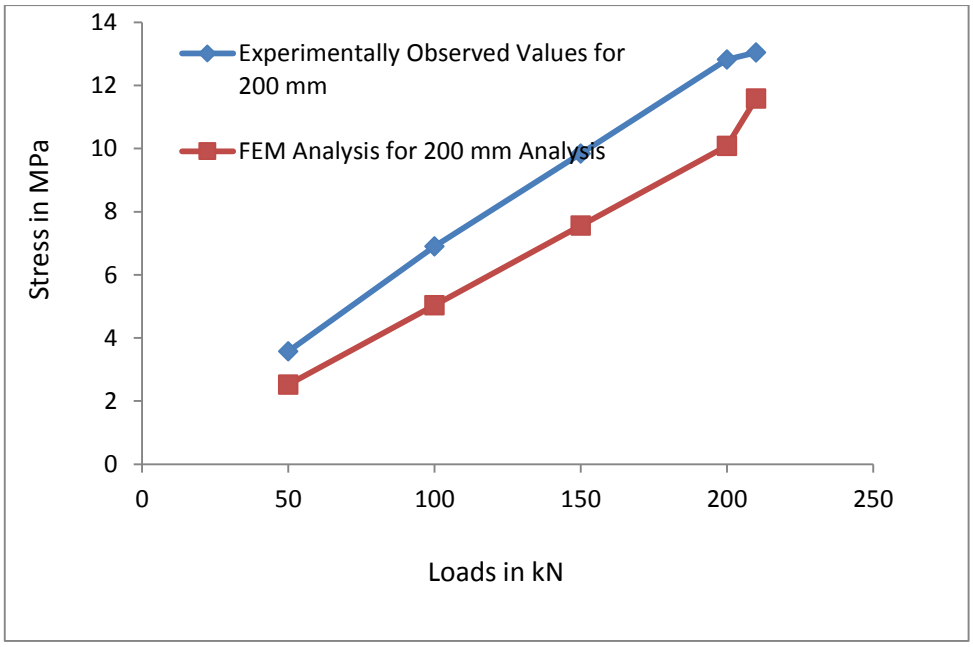

Fig. 5.31 Comparison of Observed Stresses with Analytical Stresses by FEM at Edge Position for 200 mm Thick Pavement

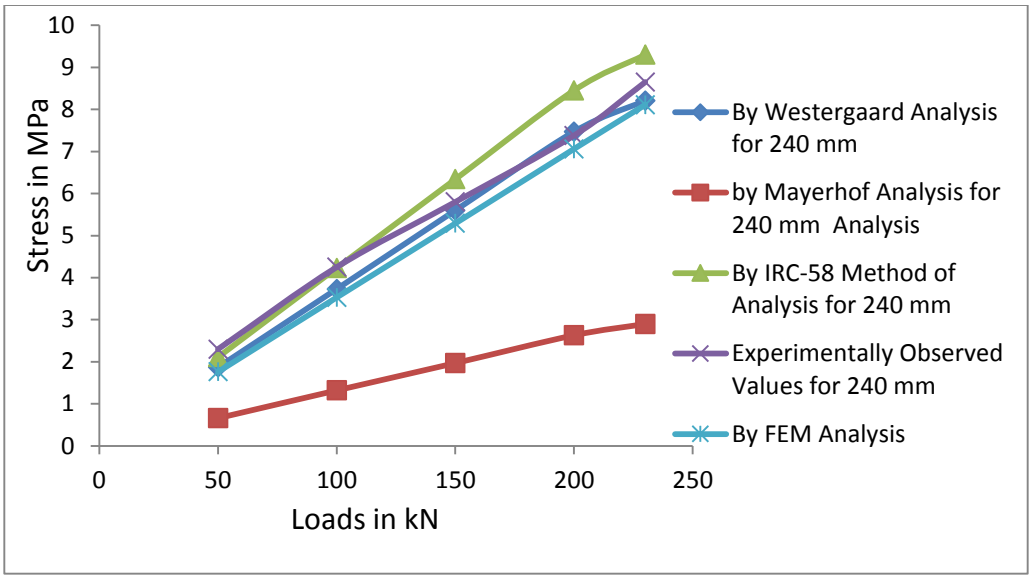

Fig. 5.32 Comparison of Observed Stresses with Theoretical and Analytical (FEM) Stresses at Edge Position for 240 mm Thick Pavement

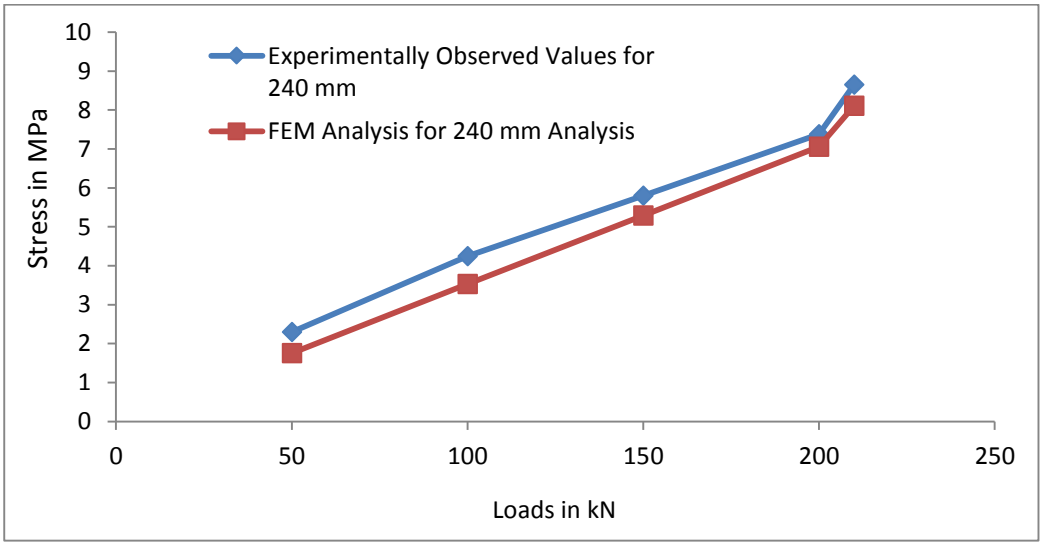

Fig. 5.33 Comparison of Observed Stresses with Analytical Stresses (FEM) at Edge Position for 240 mm Thick Pavement

200 mm and 240 mm thick HSHPC pavement was also subjected to maximum load of 230 kN. Both the pavement did not fail. Also, there was no sign of prior failure. At this load i.e. 230 kN the ratios are 1.11 by Westergaard, 3.04 by Mayerhof, 0.98 by IRC and 1.13 by FEM for 200 mm thick pavement. Results computed by Westergaard, IRC and FEM analysis are approximately equal to the observed values.

For 240 mm thick pavement the computed ratios are 1.01 by Westergaard, 2.85 by Mayerhof, 0.89 by IRC and 1.07 by FEM analysis. The results computed by Westergaard, IRC and FEM analysis are in good agreement with observed values.

It is of significance to note that at higher load i.e. 200 kN and above the observed stresses are lower than by the IRC method. Ratios range from 0.87 to 0.99, for each pavement i.e. 160 mm, 200 mm and 240 mm; while through FEM analysis, the results are in good agreement with the observed values and ratios varies from 1.05 to 1.27. The excellent structural behavior of HSHPC pavement at higher load may be attributed due to the absence of structural cracks and due to crack arrest properties of HSHPC mixes. Results for different thicknesses also demonstrate that HSHPC pavement can bear stresses significantly higher than the flexural strength of concrete mix.

Due to high flexural stress bearing capacity, the pavement may be expected to carry much higher number of load repetitions and appreciable longer life. The observed stresses were found to be 2.8 to 3.83 times the Mayerhof values. Therefore, an appropriate factor of safety should be incorporated while analyzing the HSHPC pavement by Mayerhof theory. A factor of safety between 2 to 3 may be recommended for HSHPC pavement. The results obtained from FEM analysis are in good agreement with the observed values.

Table: 5.23: Comparison of Wheel loads stresses at Edge Position for Different Thicknesses of Pavements

Sl. No.	Thicknesses of pavements in mm	Loads (P) (kN)	Stress by Westergaard analysis in (MPa)	Ratio	% variation	Stress by Mayerhof analysis (MPa)	Ratio	% variation	Stress by IRC-58 method of analysis (MPa)	Ratio	% variation	Stress by FEM analysis (MPa)	Ratio	% variation	Experimentally observed stress values (MPa)
1	160	50	3.65	1.37	27.3	1.42	3.53	71.7	4.19	1.20	16.5	3.86	1.30	23,08	5.02
		100	7.31	1.46	31.3	2.84	3.74	73.3	8.37	1.27	21.3	7.72	1.38	27.54	10.64
		150	10.96	1.26	20.6	4.27	3.24	69.1	12.55	1.10	9.12	11.58	1.19	15.97	13.81
		200	14.62	1.14	11.93	5.69	2.92	65.7	16.74	0.99	-0.84	15.44	1.08	7.40	16.60
		210	15.35	1.14	11.93	5.97	2.92	65.7	17.58	0.99	-9.86	16.21	1.08	7.40	17.43
2	200	50	2.55	1.40	28.8	0.93	3.83	74.02	2.89	1.24	19.27	2.52	1.42	29.58	3.58
		100	5.09	1.36	26.23	1.86	3.70	73.04	5.78	1.19	16.23	5.04	1.37	27.01	6.90
		150	7.63	1.29	22.55	2.80	3.52	71.54	8.67	1.13	11.89	7.56	1.3	23.08	9.84
		200	10.19	1.26	20.51	3.73	3.44	70.90	11.56	1.11	9.8	10.08	1.27	21.26	12.82
		230	11.71	1.11	10.20	4.29	3.04	67.10	13.29	0.98	-1.92	11.59	1.13	11.50	13.04
3	240	50	1.87	1.23	18.7	0.66	3.50	71.3	2.11	1.09	8.26	1.76	1.31	23.66	2.30
		100	3.73	1.14	12.24	1.32	3.23	68.94	4.23	1.00	0.47	3.53	1.20	16.67	4.25
		150	5.60	1.04	3.45	1.97	2.94	66.03	6.34	0.91	-9.31	5.29	1.10	9.10	5.80
		200	7.47	0.99	-1.22	2.63	2.80	64.36	8.45	0.87	-14.5	7.06	1.05	4.76	7.38
		230	8.59	1.01	0.69	3.03	2.85	64.97	9.72	0.89	-12.36	8.11	1.07	6.54	8.65

5.6.2 Comparison of Wheel Load Stresses for Interior Position

Comparison of wheel load stresses calculated by theoretical methods with the experimentally observed values is shown in Table 5.24 and results are plotted in Figures 5.34 and 5.35.

A study of results show that at 50 kN load, the observed stress is 1.54 times the stress computed by Westergaard and 4.62 times the stress computed by Mayerhof analysis for 200 mm thick pavement. For 240 mm thick pavement, the observed stress is 1.54 times the Westergaard stress and 4.79 times the stress computed by Mayerhof analysis. It is evident that the experimental values of stresses are close to Westergaard stresses. A factory of safety 4 should be applied when Mayerhof analysis is adopted.

At higher load i.e. at 200 kN load, the observed stress is 1.58 times the stress computed by Westergaard and 4.73 times the stress computed by Mayerhof analysis for 200 mm thick pavement. For 240 mm thick pavement, the observed stress is 1.38 times the stress computed by Westergaard and 4.3 times the stress computed by Mayerhof analysis. When maximum load i.e. 230 kN was applied, the observed stresses were 1.48 times the stress computed by Westergaard and 4.43 times the stress computed by Mayerhof for 200 mm thick pavement. For 240 mm thick pavement, the observed stresses were 1.35 times the stress calculated by Westergaard and 4.20 times the stress calculated by Mayerhof analysis. But pavements did not fail up to the maximum load i.e. at 2.30 kN.

From the above discussion, it is quite clear that observed stresses are in good agreement to the stresses computed by Westergaard. A factor of safety of 4 should be applied, when the analysis is to be done by Mayerhof method. The significant outcome is that Westergaard analysis is applicable for HSHPC pavement.

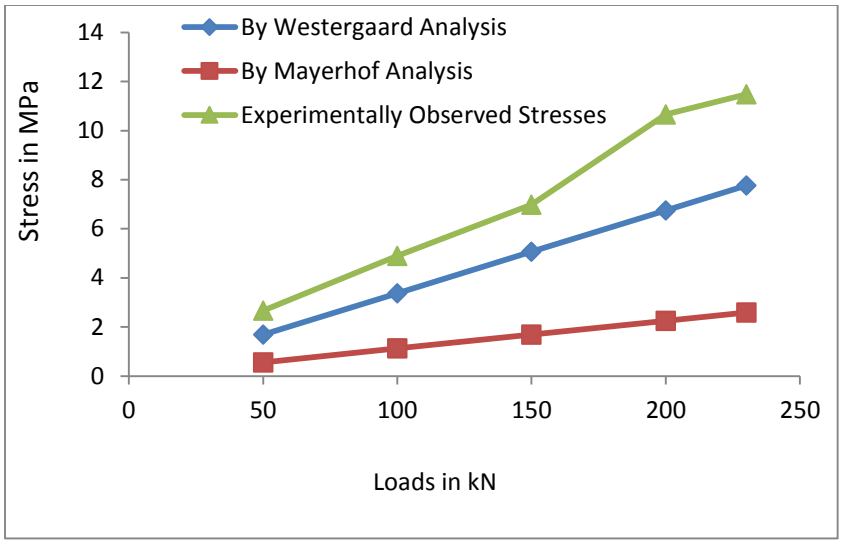

Fig. 5.34 Variation of Stresses with Varying Loads by Different Theories at Central Position for 200 mm Thick Pavement

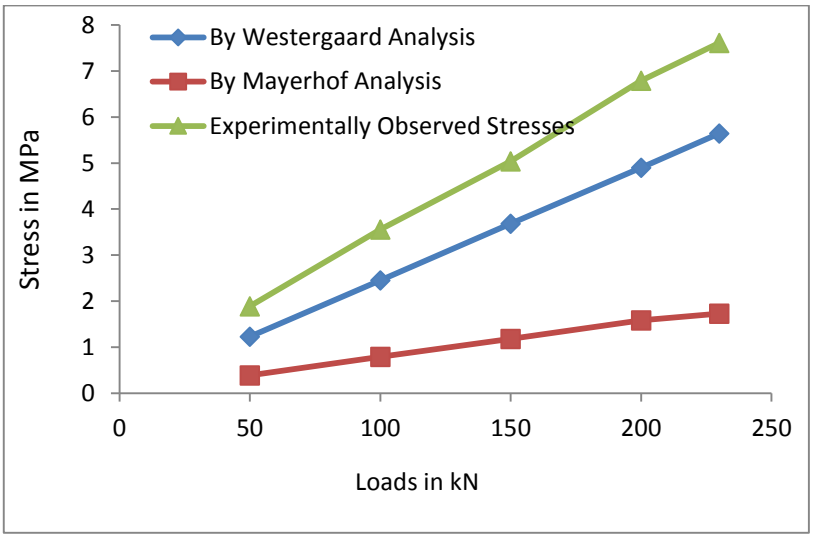

Fig. 5.35 Variation of Stresses with Varying Loads by Different Theories at Central Position for 240 mm Thick Pavement

Table 5.24: Comparison of Wheel load Stresses at Interior Position for Different Thicknesses of Pavements

Sl. No.	Thicknesses of pavements (mm)	Loads (P) (kN)	Stress by Westergaard analysis (MPa)	Ratio	% variation	Stress by Mayerhof analysis (MPa)	Ratio	% variation	Experimentally observed stresses (MPa)
1	160*	-	-	-		-	-		-
2	200	50	1.69	1.54	36.47	0.56	4.62	78.95	2.66
		100	3.37	1.45	31.08	1.13	4.34	76.89	4.89
		150	5.06	1.38	27.5	1.69	4.13	75.79	6.98
		200	6.75	1.58	36.68	2.25	4.73	78.89	10.66
		230	7.76	1.48	32.40	2.59	4.43	77.44	11.48
3	240	50	1.23	1.54	34.92	0.39	4.79	79.37	1.89
		100	2.45	1.45	31.18	0.79	4.51	77.81	3.56
		150	3.68	1.37	26.98	1.18	4.26	76.59	5.04
		200	4.90	1.38	27.84	1.58	4.30	76.73	6.79
		230	5.64	1.35	25.89	1.81	4.20	76.22	7.61

*Slab having thickness 160 mm could not be tested at central position.

5.6.3 Comparison of Wheel Load Stresses for Corner Position

A comparison of corner load stresses observed experimentally and computed by different methods is given in Table 5.25 and variations of results are shown in Figures 5.36 to 5.38.

Results of stress analysis show that the ratios, observed stress to theoretical stress, are 1.91 by Westergaard, 2.54 by Mayerhof and 1.3 by IRC methods for 160 mm thick pavement at 50 kN load. For 200 mm thick pavement, these ratios are 1.9, 2.63 and 1.33 by Westergaard, Mayerhof and IRC methods respectively. These ratios are 1.84, 2.64 and 1.33 by Westergaard, Mayershof and IRC methods respectively for 240 mm thick pavement.

At 100 kN load, these ratios are 1.92, 2.56 and 1.31 for 160 mm thick pavement, for 200 mm thick pavement, these ratios are 1.88, 2.61 and 1.32 and for 240 mm thick pavement these ratios are 1.78, 2.54 and 1.28 by Westergaard, Mayerhof and IRC methods respectively.

At 200 kN maximum load the ratios are 1.74, 2.41 and 1.22 for 200 mm thick pavement and for 240 mm thick pavement, these ratios are 1.58, 2.26 and 1.13 by Westergaard, Mayerhof and IRC methods respectively. All the pavements i.e. 160, 200 and 240 mm did not fail at maximum loading.

Analysis of results shows that stresses obtained by IRC method are closest to the observed stresses. All the time, the observed stresses are more than two times the stresses computed by Mayerhof analysis. This shows that a factor of safety of 2 needs to be applied while analysis is being carried out by Mayerhof method. Westergaard analysis gives much conservative results.

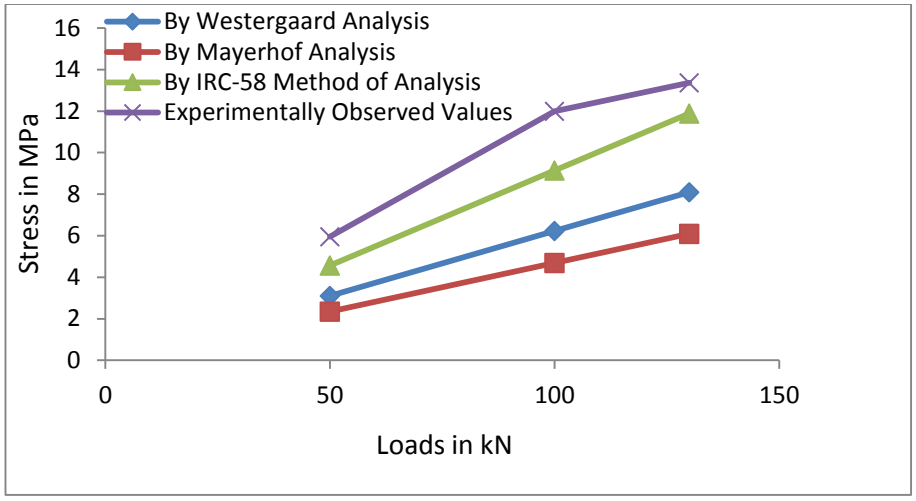

Fig. 5.36 Variation of Stresses with Varying Loads by Different Theories at Corner Position for 160 mm Thick Pavement

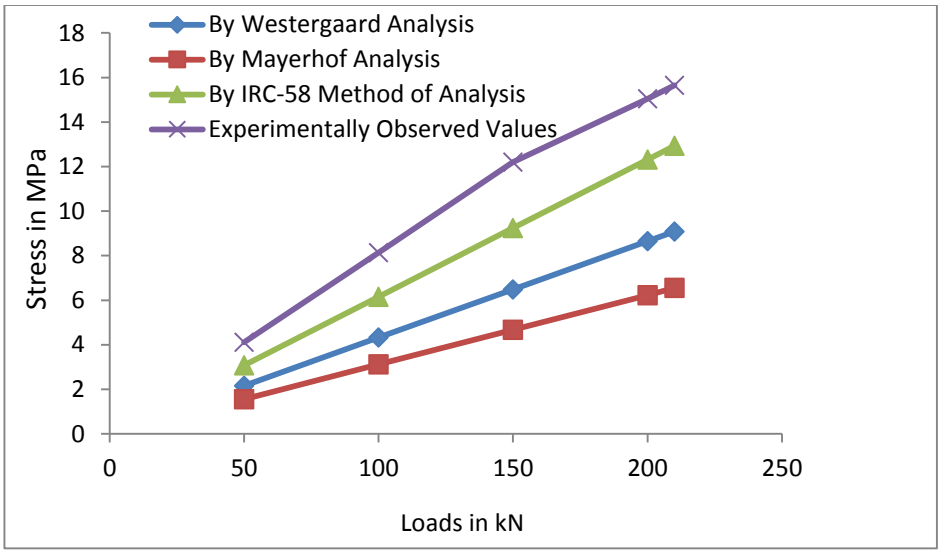

Fig. 5.37 Variation of Stresses with Varying Loads by Different Theories at Corner Position for 200 mm Thick Pavement

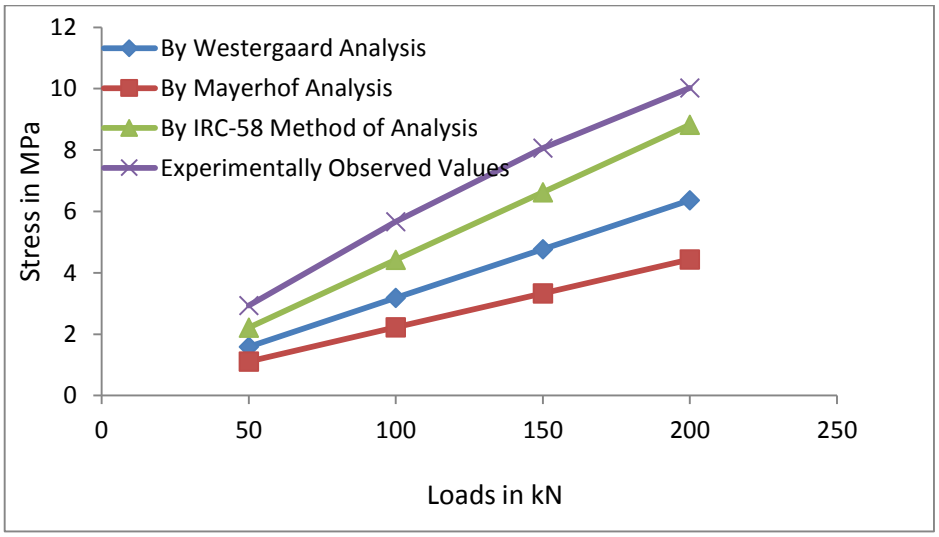

Fig. 5.38 Variation of Stresses with Varying Loads by Different Theories at Corner Position for 240 mm Thick Pavement

Table 5.25: Comparison of Wheel Load Stresses at Corner Position for Different Thicknesses of Pavements

Sl. No.	Thicknesses of pavements, (mm)	Loads (P) (kN)	Stress by Westergaard analysis (MPa)	Ratio	% variation	Stress by Mayerhof analysis (MPa)	Ratio	% variation	Stress by IRC method of analysis (MPa)	Ratio	% variation	Experimentally observed stresses (MPa)
1	160	50	3.11	1.91	47.73	2.34	2.54	62.67	4.57	1.30	23.19	5.95
		100	6.23	1.92	48.04	4.69	2.56	60.88	9.14	1.31	23.77	11.99
		130	8.09	1.65	39.45	6.09	2.19	54.42	11.88	1.12	11.07	13.36
2	200	50	2.16	1.90	47.44	1.56	2.63	62.04	3.08	1.33	25.06	4.11
		100	4.33	1.88	46.81	3.12	2.61	61.67	6.16	1.32	24.32	8.14
		150	6.49	1.87	46.80	4.68	2.60	61.63	9.24	1.32	24.26	12.20
		200	8.65	1.74	42.49	6.23	2.41	58.58	12.31	1.22	18.15	15.04
		210	9.09	1.72	41.92	6.55	2.39	58.15	12.93	1.21	17.38	15.65
3	240	50	1.59	1.84	45.73	1.11	2.64	62.12	2.21	1.33	24.57	2.93
		100	3.18	1.78	43.72	2.22	2.54	60.70	4.42	1.28	21.76	5.65
		150	4.77	1.69	40.82	3.33	2.42	58.68	6.63	1.22	17.74	8.06
		200	6.36	1.58	36.53	4.44	2.26	55.69	8.83	1.13	11.88	10.02

5.7 LOAD CARRYING CAPACITY OF HSHPC PAVEMENTS

Static plate load test results are shown in Table 4.12 for 160 mm thick pavement. For corner position, it had been observed that as the load was continuously increased, the pavement started lifting from opposite corner. As the load reached 130 kN, the lifting of opposite corner was observed 65 mm. Due to excessive lifting of opposite corner further application of load was stopped. There was no sign of failure at corner position at 130 kN load. At edge position up to 210 kN load, there was no sign of failure. As the load reached 220 kN, the pavement failed suddenly. There was no prior sign of failure.

For 200 mm thick pavement, static plate load test results are shown in Table 4.14 for each position i.e. central, edge and corner. At corner position, as the load was increased continuously, the pavement started lifting from opposite corner. This phenomenon was observed at 90 kN load and lifting was 55 mm at 210 kN load. Due to excessive lifting further application of load was stopped. At central and edge position load was applied up to the maximum capacity i.e. 230 kN. But there was no sign of failure for any positions i.e. central, edge and corner. Pavement was still in position to carry more loads. There was no sign of failure at load 210 kN for corner and 230 kN for edge and central position.

For 240 mm thick pavement, static plate load test results are shown in Table 4.16 for each position i.e. central, edge and corner. Load had been applied at different positions of pavement. At corner position, it had been observed that as the load was continuously increased, the opposite corner started lifting. This phenomenon was noticed at load 100 kN. Lifting was 45 mm at 200 kN load. Due to considerable lifting, further application of load was not permitted. Upto maximum capacity of reaction frame, the load was applied at central and edge position i.e. 230 kN. No sign of failure had been observed for any positions of pavement. The pavement still could carry more load at all positions. No sign of failure were observed for edge, corner and central positions.

The lifting of opposite corner of the pavement is shown in Photograph 4.21.

5.8 MAXIMUM LOAD CARRYING CAPACITY AT FLEXURAL STRENGTH

Comparison of maximum yield and ultimate load for central, edge and corner position, by Westergaard, IRC-58, Mayerhof and Ghosh are presented in Table 5.26.

The 160 mm thick pavement failed at 220 kN load for edge position. The pavement did not fail at 130 kN load for corner position. The yield loads evaluated by Westergaard method come out to be 130.24 kN, 87.52 kN and 102.79 kN for centre edge and corner position respectively. By IRC-58 method the yield load come out as 76.47 kN and 69.99 kN for edge and corner position respectively for 160 mm. The ultimate load computed by Mayerhof method are 367.66 kN, 225.02 kN and 136.53 kN for centre, edge and corner positions respectively. The yield load by Westergaard method is 39.78% and 34.76% by IRC of the experimental value and ultimate load by Mayerhof method is approximately 100% of the experimental value for edge position. The ultimate load calculated by Mayerhof is closest to the experimental value. The ultimate load analysed by Ghosh method is 354.98 kN for central position. The ultimate loads calculated by Mayerhof and Ghosh are nearly equal for central position.

The 200 mm thick pavement did not fail at any position i.e. central, edge and corner up to the maximum loading capacity of reaction frame. The maximum load of 230 kN was applied at centre and edge position and 210 kN load was applied at corner position. The yield loads evaluated by Westergaard method are 189.63 kN, 125.68 kN and 147.98 kN for centre, edge and corner positions respectively. By IRC-58 method the yield load come out as 110.75 kN and 103.95 kN for edge and corner position respectively for 200 mm. These yield loads are sufficiently less than the experimentally applied loads respectively. The ultimate loads calculated by Mayerhof method are 568.11 kN, 343.31 kN and 205.29 kN for centre, edge and corner positions respectively. These computed ultimate loads are much higher than the experimentally applied loads respectively. The ultimate load calculated by Ghosh theory for central position is 551.67 kN, which is nearly equal to the ultimate load calculated by Mayerhof method for central position.

Also, the 240 mm thick pavement did not fail at any position upto the maximum experimentally applied load 230 kN at centre and edge position and 200 kN load was applied at corner position. The yield loads calculated by Westergaard method are 260.95 kN, 171.38 kN and 201.44 kN for centre, edge and corner positions respectively. The yield load at centre position is higher than the experimentally applied load and yield load at corner is nearly equal to the experimentally applied load. By IRC-58 method the yield load come out as 151.37 kN and 144.89 kN for edge and corner positions respectively for 240 mm. The ultimate loads calculated by Mayerhof method are 811.89 kN, 486.49 kN and 288.15 kN for centre, edge and corner positions respectively. The ultimate load calculated by Ghosh theory for central position is 791.48 kN, which is in close agreement with Mayerhof. The ultimate loads calculated by Mayerhof and Ghosh method are much higher than the experimentally applied load.

From the above discussion, it is quite clear that the maximum load carrying capacities of HSHPC pavements are exceptionally high. The maximum load carrying capacities continuously increase with increase in thickness for each position. This may be attributed due to increase in flexural rigidity of the pavement and absence of structural cracks. High load carrying capacities also reflect that HSHPC has high resistance to crack development and crack propagation.

Table 5.26: Comparison of Maximum Yield Load and Ultimate Load Carried by Pavements**

Sl. No.	Pavement thicknesses in mm	Positions	Maximum yield load by Westergaard 'kN'	% of experime-ntally Applied Load	Ultimate load by Mayerhof in kN	% of experimentally applied Load	Ultimate Load By Ghosh Method in kN	% of experimentally applied load	Maximum yield load by IRC 'kN'	% of experimentally applied load	Experimentally applied load in kN
1	160	Centre	130.24	-	367.66	-	354.98	-	-	-	-
		Edge	87.52	39.78	225.02	100	-	-	76.47	34.76	220
		Corner	102.79	-	136.53	-	-	-	69.99	-	130
2.	200	Centre	189.63	-	568.11	-	551.67	-	-	-	230
		Edge	125.68	-	343.31	-	-	-	110.75	-	230
		Corner	147.98	-	205.29	-	-	-	103.95	-	210
3.	240	Centre	260.95	-	811.89	-	791.48	-	-	-	230
		Edge	171.38	-	486.49	-	-	-	151.37	-	230
		Corner	201.44	-	288.15	-	-	-	144.89	-	200

*Pavement did not crack and failed up to 230 kN load.

**At Flexural Strength 6.4 Mpa and Modulus of Subgrade Reaction (K) 0.0463 N/mm^3 or 4.63 kg/cm^3

5.9 OPTIMIZATION OF THE DESIGN THICKNESS OF HIGH STRENGTH HIGH PERFORMANCE CONCRETE PAVEMENTS

From the analysis for 200 mm thick pavement, it is quite clear that yield load carrying capacity by Westergaard and IRC method is 125.68 kN and 110.75 kN respectively for edge position at flexural strength, which is quite lower than the experimentally applied load. By Westergaard analysis, for central and corner position, the yield load carrying capacities are 189.63 kN and 147.98 kN respectively at flexural strength. By IRC method the yield load at corner position is 103.95 kN. Corresponding to flexural strength, the ultimate load carrying capacities at different positions are 568.11 kN for central, 343.31 kN for edge and 205.29 kN for corner by Mayerhoof method. At 230 kN load, stresses calculated by different methods are by Westergaard 11.71 MPa, by IRC 13.29 MPa, by FEM 11.59 MPa and by Mayerhof 4.29 MPa for edge position. These stresses are more than the flexural strength of the mix and closer to the observed values. From this it is clear that pavement can bear stresses beyond the flexural strength and could carry more load. At 230 kN load, the observed deflection and strain are 10.73 mm and 312.8 x 10^{-6}. These values are quite lower.

From the above discussions, it is quite clear that the load carrying capacity of 200 mm thick pavement is sufficiently high and pavement did not fail at experimentally applied maximum load i.e. 230 kN. Therefore, 200 mm thick pavement is suitable in all conditions of traffic.

5.10 CRACK PATTERNS AND CRACK WIDTH

The HSHPC pavements of size 1800 mm x 1800 mm with different thicknesses had been tested for edge, corner and central positions. Only 160 mm thick pavement failed under edge loading position. Rest of the pavements did not show any kind of failure at any positions i.e. central, corner and edge positions. For 160 mm thick pavement at edge position, the pattern of the crack was straight line passing through under the testing plate. The crack width was 1.86 mm under the loaded condition. There was sudden failure from bottom to top. Prior failure, there was no visible crack from sides and on surface. The pavement failed at 220 kN load at edge position. This is shown in Photograph 4.22 and Figure 4.4.

5.11 DISCUSSION OF FLEXIBLE PAVEMENTS DESIGN

From the analysis done in Chapter-3 for design of flexible pavements, it is evident that the existing IRC-37 method can be successfully used in the design of flexible pavements for heavy vehicles. Which are based on CBR value of sub-grade and cumulative numbers of standard axles to be carried during design period of 15 years. For 150 msa traffic, the maximum numbers of heavy vehicles are 4500 for two lane single carriageway flexible pavement. As the number of heavy vehicles exceeds, the limit of 150 msa is achieved earlier. For 6000 heavy vehicles per day and 6% CBR, as the design period is increased, the cumulative number of standard axles (msa) increase and also the design thickness of flexible pavements. For 5 year design period, the traffic is 43 msa and total pavement thickness is 668 mm, for 10 year design period, the traffic is 105 msa and the total pavement thickness is 701 mm and for 13 year design period, the traffic is 150 msa and total pavement thickness is 720 mm. These are shown in Table 3.4. It is evident that 150 msa is achieved in 13 years. Therefore, the existing IRC-37 method can be used for design of flexible pavement for heavy vehicles with reduced design period to corresponding to 150 msa

5.12 A COST ANALYSIS

India's economy growth plan over 6 percent per annum will largely depend on an efficient roads infrastructure. Efficient road networks provide faster movement of people and goods with safety and economically. To achieve efficient road infrastructure networks, the Government of India has launched massive National Highways Development Programme and Pradhan Mantri Gram Sarak Yojana (PMGSY).

Pavements cost about 50% of the project cost, therefore, a careful alternative study is necessary in selection of type of pavement i.e. flexible pavements or rigid pavements. A rational decision will lead to lots of money saving.

The selection criteria of the type of pavement should be based on the cost incurring on whole design life of the pavement not on initial cost of construction. This is called life cycle cost analysis. Life cycle cost analysis includes initial construction cost, maintenance / rehabilitation cost, vehicle operating and fuel saving cost over the design life of the pavement.

In U.S.A., a study has demonstrated that there is fuel saving of 20% on concrete roads as compared to bituminous roads having same roughness index. A similar study was done by CRRI, New Delhi on Delhi-Agra National Highway (NH-2) and found that there is a fuel saving of 14% on concrete roads as compared to bituminous roads for commercial vehicles.

In present analysis, it has been assumed that vehicle operating cost and fuel saving cost is same for flexible and as well as rigid pavements. While it is established fact that vehicle operating cost is low for rigid pavements and fuel saving cost is high for concrete pavements than the bituminous roads.

5.12.1 Cost of Flexible Pavements during Design Life

5.12.1.1 Initial construction cost

Two lane Highway with single carriageway, flexible pavements has been designed for 200 heavy vehicles per day having CBR value 6% and design period 15 years. The vehicle damage factor has been considered as 3.5. For 6% CBR and 5 msa traffic, the pavement compositions are GSB = 210 mm, WMM = 250 mm, DBM = 50 mm and BC = 25 mm as per IRC-37-2012. The initial construction cost per km for flexible pavements are given in Table 5.27 for 200 heavy vehicles.

Table 5.27: Details of Initial Construction Cost per km. for Flexible Pavement for 200 Heavy Vehicles

Sl. No.	Pavement composition (mm)	Quantity (m^3 / km)	Rate (Rs. per m^3)	Cost per km (lakhs)
1	GSB = 210	1470	1518.10	22.32
2	WMM = 250	1750	1768.30	30.95
3	DBM = 50	350	10417.90	36.46
4	BC/SDBC = 25	175	11579.70	20.26
			Total	109.99
			Say	110.00 lakh/km

Source: PWD, S.O.R (Schedule of Rates) year 2013

As the number of heavy vehicles increased per day, the thickness of flexible pavements will increase. This will lead to reduction in margin of initial construction cost of rigid and flexible pavement. Considering the case of 4500 heavy vehicles, design life 15 years, vehicle damage factor 4.5 and traffic growth rate 7.5%, the cumulative number of axles to be carried during the design life would be 150 msa.

For CBR 6% and 150 msa, the total flexible pavement thicknesses is 720 mm. the compositions are GSB = 260 mm, WMM = 250 mm, DBM = 140 mm and BC = 50 mm. The initial construction cost per km calculated for 4500 heavy vehicles is shown in Table 5.28.

Table 5.28: Details of Initial Construction Cost per km. for Flexible Pavement for 4500 Heavy Vehicles

Sl. No.	Pavement composition (mm)	Quantity (m^3 / km)	Rate (Rs. per m^3)	Cost per km (lakhs)
1	GSB = 260	1820	1518.10	27.63
2	WMM = 250	1750	1768.30	30.95
3	DBM = 140	980	10417.90	102.10
4	BC = 50	350	11579.70	40.53
			Total	201.21
			Say	202.00 lakh/km

Source: PWD, S.O.R (Schedule of Rates) year 2013

5.12.1.2 Maintenance cost of flexible pavement

Period of analysis has been considered as 30 years being design life of concrete pavement. As per government policy, 12% discount rate has been considered. There may be future rise in cost of materials. To account for it, a inflation rate of 5 percent has been considered.

1) It is assumed that bituminous overlay will be laid on 10^{th}, 20^{th} and 30^{th} year, after the construction of pavement having 50 mm DBM and 25 mm BC

= 7 x 1000 x 0.05 + 7 x 1000 x 0.025

Total quantity= 350 m^3 x DBM + 175 m^3 BC

= 350 x 10417.9 x $(1.05)^{10}$ x 0.88 + 175 x 11579.7 x $(1.05)^{10}$ x 0.88

Cost = 52.26 + 29.05

= 81.31 lacs

2) Surface renewal of 25 mm BC to be done overall in five years as per MORTH guidelines

Quantity = 7 x 1000 x 0.025

= 175 m^3

Cost = 175 x 11579.7 x $(1.05)^5$ x 0.88

= 22.76 lacs

3) Cost of ordinary repairs as per MORTH norms = Rs. 1.9 lakhs (L.S.) (Data taken from NH Division, P.W.D., Uttarakhand)

Maintenance cost in 10 years = 22.07 lakhs

Life cycle construction / maintenance cost for 200 heavy vehicles = 110 + 81.31 + 22.76 + 22.07

= 236.14 lakhs/km

Life cycle construction / maintenance cost for 4500 heavy vehicles = 202 + 81.31 + 22.76 + 22.07

= 328.14 lakhs/km

5.12.2 Cost of Rigid Pavement during Design Life

5.12.2.1 Initial construction cost

The design of rigid pavement depends upon the modulus of subgrade reaction and flexural strength of concrete mix. The design life of concrete pavements is generally 30 years. Our study is based on M60 grade concrete pavement having thicknesses 160, 200 and 240 mm. Therefore, pavement costs have been calculated per km used in the study. For two lane highway, the pavement compositions are given in Table 5.29.

Table 5.29: Details of Initial Construction Cost per km. for Rigid Pavement

Sl. No.	Pavement composition (mm)	Quantity (m^3 / km)	Rate (Rs. per m^3)	Cost per km (lakhs)	Total cost (lakhs)
1	GSB 150	1050	1510.10	15.86	
2	DLC (M10) 150	1050	4357.0	45.75	
3	PQC (M60)				
	160	1120	6711.40	75.17	136.78
	200	1400		93.96	155.57
	240	1680		112.75	174.36

Source: PWD, S.O.R (Schedule of Rates) year 2013

5.12.2.2 Maintenance cost of rigid pavement

The average annually maintenance cost of rigid pavement is approximately Rupees 1.5 lakh/km to cover filling of sealing compound in joints, repairs of concrete spallings etc.

Maintenance Cost = 17.43 lakhs.

The life cycle construction / maintenance cost for HSHPC pavements are given in Table 5.30.

Table 5.30: Life Cycle construction / Maintenance Cost for HSHPC Pavements

Sl. No.	Pavement thickness (mm)	Initial construction cost (lakhs)	Life cycle construction / maintenance cost (lakhs)
1	160	136.78	154.21
2	200	155.57	173.0
3	240	174.36	191.79

The comparative life cycle construction / maintenance cost for HSHPC pavements and flexible pavements are given in Table 5.31 for 200 heavy vehicles.

Table 5.31: Life Cycle Construction / Maintenance Cost for HSHPC Pavements and Flexible Pavements for 200 Heavy Vehicles

Sl. No.	Pavement type	Initial construction cost (lakhs)	Life Cycle construction / maintenance cost (lakhs)	Percent Higher initial construction cost of rigid pavement over flexible pavement	Percent Lower Life cycle construction / maintenance cost of rigid pavement over flexible pavement
1.	Flexible	110	236.14	-	-
2.	Rigid				
	160 mm	136.78	154.21	24.3	34.8
	200 mm	155.57	173.0	41.4	26.7
	240 mm	174.36	191.79	58.5	18.78

The comparative life cycle construction / maintenance cost for HSHPC pavements and flexible pavements are given in Table 5.32 for 4500 heavy vehicles.

Table 5.32: Life Cycle Construction / Maintenance Cost for HSHPC Pavements and Flexible Pavements for 4500 Heavy Vehicles

Sl. No.	Pavement type	Initial construction cost (lakhs)	Life Cycle construction / maintenance cost (lakhs)	Percent lower initial construction cost of rigid pavement over flexible pavement	Percent Lower Life cycle construction / maintenance cost of rigid pavement over flexible pavement
1.	Flexible	202	328.14	-	-
2.	Rigid				
	160 mm	136.78	154.21	32.99	53.00
	200 mm	155.57	173.0	22.99	47.30
	240 mm	174.36	191.79	13.68	41.60

From the above analysis the following conclusions may be drawn:

(i) The initial construction cost of flexible pavement is 110.0 lakhs for 200 heavy vehicles and 202 lakh for 4500 heavy vehicles. The initial construction costs of

rigid pavements are 136.78 lakhs, 155.57 lakhs and 174.36 lakhs for 160, 200 and 240 mm thick pavements respectively. The construction cost of concrete pavements are higher over flexible pavements by 24.3%, 41.4% and 58.5% for 160, 200 and 240 mm thick pavements for 200 heavy vehicles and lower over flexible pavements by 32.99%, 22.99% and 13.68% for 160, 200 and 240 mm thick HSHPC pavements respectively for 4500 heavy vehicles.

(ii) The life cycle construction / maintenance cost per km of flexible pavement is 236.14 lakhs for 200 heavy vehicles and 328.14 lakhs for 4500 heavy vehicles. The life cycle construction / maintenance cost of concrete pavements are 154.21 lakhs, 173.0 lakhs and 191.79 lakhs for 160, 200 and 240 mm pavements respectively. The life cycle construction / maintenance cost of concrete pavement over flexible pavements are less by 34.8%, 26.7% and 18.78% for 160, 200 and 240 mm pavements for 200 heavy vehicles and less by 53%, 47.3% and 41.6% for 4500 heavy vehicles for 160, 200 and 240 mm thick HSHPC pavements respectively.

(iii) As the number of heavy vehicles increase per day, the margin in initial construction cost between HSHPC pavements and flexible pavements reduces. For 4500 heavy vehicles, the initial construction cost of HSHPC pavements are lower over flexible pavements by 32.99%, 22.99% and 13.68% for 160 mm, 200 mm and 240 mm respectively.

From the above results it is quite clear that the life cycle construction / maintenance cost of HSHPC pavements are lower over flexible pavements. Therefore, the choice of HSHPC pavements would be economical which will result in lots of saving of money in the interest of Nation.

5.13 SUMMARY

In this chapter, properties of soil subgrade, properties of HSHPC concrete mix, analysis of stresses, strains and deflections by FEM has been discussed. Calculations of stresses in HSHPC pavements by various existing methods, Westergaard, Mayerhof, Ghosh and IRC-58 have been done. Then comparison of stresses calculated by various theoretical methods with the observed and analytical method (FEM) have been made and found that the

existing theoretical methods and analytical methods can be used successfully in designing of HSHPC pavements. The load carrying capacity at flexural strength is sufficiently high. The yield loads and ultimate loads are also quite high. This demonstrates that the HSHPC pavements can be used as heavy duty pavements. The deflections obtained through analytical method i.e. FEM are in close agreement with the observed values. The stresses, strains and deflections calculated through Finite Element Method are in close agreement with the observed values and the results obtained through existing theoretical methods. This demonstrates that FEM can be successfully use in designing of HSHPC pavements of any thicknesses which is based on characteristic properties of the soil and concrete.

The existing IRC-37 method can be used in designing of flexible pavements for heavy vehicles but the design periods should be reduced to corresponding to 150 msa traffic.

Economic analysis has also been carried out assuming vehicle operating cost for both pavements i.e. flexible pavements and HSHPC pavements same and found that the life cycle / maintenance cost of flexible pavements are higher over the HSHPC pavements. Therefore, HSHPC pavements are right choice over flexible pavements.

On the basis of above discussion, the conclusions have been drawn in Chapter-6.

CHAPTER-6

CONCLUSIONS

6.1 GENERAL

High strength high performance concrete are being commonly used in the field of high rise buildings, long span bridges and fly overs. In pavements, HSHPC are generally used in patch repair works and strengthening of bituminous or concrete pavements by a concrete overly. Due to early gain in strength, the pavement could be opened to the traffic earlier. Full depth HSHPC pavement has not been constructed in India so far.

In the present study an attempt has been made to assess the suitability of HSHPC in full depth pavements. During the investigations, it is observed that HSHPC has high flexural strength, high modulus of elasticity and superior load carrying capacity. Due to high strength, a thinner pavement is capable of carrying the same load than normal strength concrete pavement. Due to improved strength characteristics, resistance to cracks and high durability, the HSHPC is extremely useful for highways, overlays, bridge decks and other structures.

6.2 CONCLUSIONS

The following conclusions have been drawn from the study. The results are valid for the materials characteristics used in the present investigation.

1. The HSHPC mix of grade M60 was developed by using maximum size of coarse aggregate 20 mm having fineness modulus 6.7 and coarse sand having fineness modulus 2.89. The water cement ratio of the mix is 0.29 and the slump is 31.67 mm. The fly ash 11% and super plasticizer 1.6% by weight of cement have been used.
2. Quantity per m^3 of design mix are 508 kg cement, 56 kg fly ash, 1068 kg coarse aggregate in dry condition, 647 kg of coarse sand in dry condition, 8.13 L superplaticizer Sikament (Naphthalene formaldehyde sulphonate) and 163.56 L water.
3. Design mix ratio is 1:1.1:1.9 (cement: coarse sand: coarse aggregate) having modulus of elasticity 41.7 GPa.

4. The average compressive strength at 7 days and 28 days are 46.14 MPa and 70.4 MPa and flexural strength are 4.82 MPa and 6.4 MPa respectively. The flexural strength at 28 days is sufficiently high, which is key parameter in design of rigid pavement.
5. Roorkee soil has been used in the investigations. Roorkee soil is of class A-3 as per U.S.P.R.A. soil classification which is sandy. The average value of modulus of subgrade reaction is 4.63 kg/cm^3. 4 days soaked CBR value of Roorkee soil is 6% at optimum moisture content of 11% and dry unit weight of 1.92 g/cm^3.
6. The experience shows that a low slump HSHPC mix can be compacted and finished using conventional plate vibrator.
7. The investigations show that HSHPC pavements of thicknesses 160 mm, 200 mm and 240 mm carry significantly higher load on compacted subgrade. Only 160 mm thick HSHPC pavement was failed at 220 kN at edge position. At corner position, the 160 mm HSHPC pavement did not fail at 130 kN experimentally applied load.

   The 200 mm and 240 mm thick HSHPC pavement did not fail for any position upto the experimentally applied load of 200 kN.

8. The observed deflections are quite small as compared to commonly adopted deflection. The maximum observed deflection was found to be 18.53 mm at corner position at load 210 kN. From this result, it is evident that HSHPC pavement can take high deflection without failure on a load twice that of normal plying heavy vehicles.
9. The analysis of deflections for edge position by FEM is in good agreement with the observed deflections. The variation in deflection varies from -11.44% to 41.21% with respect to observed values.
10. The observed strains follow the same pattern as in case of deflections of pavement. The maximum observed strain was found to be 418.0 x 10^{-6} at edge of 160 mm thick pavement. The lowest strains in 240 mm thick HSHPC pavement show higher load carrying capacity. The transverse strains are not considered for analysis being very low.
11. The analysis of strains for edge position by FEM method show good agreement with the observed values. The variation of strains vary from 5.37% to 30.76% with respect to observed values.

12. All the three HSHPC pavements laid over prepared subgrade in the pavement testing hall were subjected to the maximum experimental load. The load carrying capacity of HSHPC pavements are high. 200 and 240 mm thick HSHPC pavements were not failed for any positions i.e. central, edge and corner, up to the experimentally applied maximum load. There were no sign of prior failure for any positions at the experimentally applied maximum load. At the load more than 210 kN the 160 mm slab suddenly failed. The crack propagated from bottom to top. The crack was straight line passing through under plate dividing the concrete pavement into approximately two equal parts. The crack width was 1.86 mm under loaded condition.
13. Wheel load stresses calculated by Wastergaard for interior position show good agreement with the observed values of stresses with a factor of safety of 1.35 to 1.58. In case of Mayerhof analysis, the factor of safety was found to be 4.2 to 4.79.
14. For edge position, the wheel load stresses calculated by Westergaard are in good agreement with the observed values with a factor of safety of 0.99 to 1.46.

    In case of Mayerhof, the factor of safety was found to be 2.8 to 3.83. In case of IRC, the factor of safety was found to be 0.87 to 1.27. The factor of safety in case of FEM analysis was found to be 1.05 to 1.43.

15. At corner position, the wheel load stresses calculated by Westergaard show a factor of safety 1.58 to 1.92. In case of Mayerhof analysis a factory of safety was found to be 2.26 to 2.64.

    In the case of IRC, the factor of safety was found to be 1.13 to 1.38.

16. The maximum loads carried by the pavements at flexural strength 6.4 MPa by Westergaard is 87.52 kN for edge position for 160 mm thick HSHPC pavement. At edge the maximum yield load is 39.78% of the failure load by Westergaard method of analysis. The maximum loads carried by 200 mm thick HSHPC pavement, by Westergaard at flexural strength is 125.68 kN for edge position and for 240 mm thick HSHPC pavement is 171.38 kN for edge position. By IRC method, the maximum yield load carried by 160 mm thick HSHPC pavement is 76.47 kN for edge position, by 200 mm thick HSHPC pavement is 110.75 kN for edge position and by 240 mm thick

HSHPC pavement is 151.37 kN for edge position. The maximum yield load increase with increase in thickness due to increase in flexural rigidity. The maximum yield load by IRC method at edge position for 160 mm thick HSHPC pavement is 34.76% of the failure load. The ultimate load at flexural strength by Mayerhof method for 160 mm pavement is 225.02 kN for edge position. At edge, the ultimate load is approximately equal to the collapse load at failure. The ultimate load by Mayerhof at flexural strength for 200 mm thick HSHPC pavement is 343.31 kN for edge position, and the ultimate loads for 240 mm thick HSHPC pavement is 486.49 kN for edge position.

The maximum load carrying capacity at flexural strength of the HSHPC pavements is quite high even when the pavements are laid directly over compacted soil having modulus of subgrade reaction 4.63 kg/cm^3.

17. From the stress analysis and maximum load carrying capacity, it could be concluded that a thinner HSHPC pavement could be laid for carrying the same load. This will result in lots of saving of natural aggregate putting less impact on environment. From the discussion, it is quite clear that 200 mm thick HSHPC pavement can carry high load at each position with low stresses.

18. The pavement cost about 50% cost of the project. Therefore a careful choice should be made between flexible and rigid pavements. The selection of the type of the pavements depends upon the life cycle cost analysis. In this study, assuming vehicle operating and fuel saving cost same for two types of pavements, the life cycle construction / maintenance cost has been calculated. It has been found that all the time for 160 mm, 200 mm and 240 mm thick HSHPC pavements, the life cycle construction / maintenance costs are lower by 34.8%, 26.7% and 18.78% respectively over flexible pavement for 200 heavy vehicles (5 msa traffic). But the initial construction costs of HSHPC pavements are higher over flexible pavements for 200 heavy vehicles (5 msa traffic) by 24.3%, 41.4% and 58.5% for 160 mm, 200 mm and 240 mm thick HSHPC pavements respectively.

For 4500 heavy vehicles (150 msa traffic), the life cycle construction / maintenance cost of 160 mm, 200 mm and 240 mm thick HSHPC pavements is less by 53%, 47.3% and 41.6% respectively. For 4500 heavy vehicles (150 msa traffic), the initial construction cost of 160 mm, 200 mm and 240 mm thick HSHPC pavements are lower over flexible pavements by 32.99%, 22.99% and 13.68% respectively.

From the above discussion, it is quite clear that with the increase in heavy vehicles per day, the margin in initial construction cost between flexible and HSHPC pavement reduces and margin in life cycle construction / maintenance cost increases.

However, during the life cycle cost analysis vehicle operating and fuel saving cost are assumed same for both the pavements but in real the vehicle operation cost is low and fuel saving cost is high for concrete pavements. From the discussion it is quite clear that concrete pavements are far superior to the flexible pavements. Saving of fuel will result in reduction of lots of CO_2. Thus HSHPC pavements are eco-friendly.

19. From the analysis and discussion, it is quite clear that existing methods Westergaard's, Mayerhof's, Ghosh's and IRC-58 for analysis and design of HSHPC pavements can be successfully used for heavy vehicles. In case of Mayerhof's analysis, a suitable factor of safety should be applied. Analytical method i.e. Finite Element Method (FEM) which is based on characteristics properties of soil subgrade, concrete properties and wheel load can be used in designing of HSHPC pavements for any thicknesses.

20. Flexible pavements can be designed for heavy vehicles by using existing IRC-37 method but the design period should be limited to corresponding to 150 msa traffic.

6.3 RECOMMENDATIONS FOR FURTHER RESEARCH

The present investigations on structural behaviour of HSHPC pavements have been done in the laboratory. HSHPC have applications in pavements, overlay and patch repair works area. Further the following studies are recommended:

1) Performance of HSHPC pavements should be studied in actual field conditions to assess the serviceability. Therefore, a long term study is necessary in respect of this.

2) To study the combined effect of wheel loads, temperature stresses and environmental conditions on HSHPC overlay over cracked pavements in the field.

3) Effect of temperature and moisture on the performance of HSHPC pavement during day and night period should be studied.

REFERENCES

1. (1989-1994), "High – Performance Concrete, a State-of-Art Report", Publication Number: FHWA-RD-97-030.
2. (1999), "Measurement of the Rheological Properties of High Performance Concrete : State of the Art Report", Journal of Research of the National Institute of Standards and Technology, Vol. 104, Number 5, September – October.
3. AASHTO, (1993), "Guide for Design of Pavement Structures", American Association of State Highway and Transportation Officials.
4. AASHTO, (2002)-Draft, "Guide for Mechanistic and Empirical Design of New and Rehabilitated Pavement Structures" American Association of State Highway and Transportation Officials.
5. ACI 211.4R-93, (1998), "Guide for Selecting Proportions for High Strength Concrete with Portland cement and Fly Ash", American Concrete Institute.
6. ACI: 363 R-10, (1992), "State-of-the-Art Report on High Strength Concrete" American Concrete Institute, January.
7. Agrawal, P., Siddiqui, R., Agrawal, Y., and Gupta, S.M., (2008), "Self Compacting Concrete – Procedure for Mix Design", Leonardo Electronic Journal of Practices and Technologies, Issue 12, January – June, pp. 15-24.
8. Agrawal, V., Gupta, S.M., and Sachdeva, S.N., (2010), "Concrete Durability through High Volume Fly Ash (HVFC), A Literature Review", International Journal of Engineering Science and Technology, Vol. 2 (9), pp. 4473 – 4477.
9. Agrawal, V., Gupta, S.M., and Sachdeva, S.N., (2012), "Investigations on Fly Ash Concrete for Pavements", International Journal of Civil and Structural Engineering, Vol. 2, No. 3.
10. Aitcin, P.C., (1998), "High performance Concrete", E&FN Span, pp. 10.
11. Aitcin, P.C., (2003), "The Art and Science of Durable High – Performance Concrete", Proceedings of the NelaSpiratos Symposium, Committee for the organization of ANMET/ACI, Conferences, pp. 69-88.

12. Aitcin, Pierre-Claude, and Neville, Adam, (1993), "High-Performance Concrete Demystified", Concrete International, Vol. 15, No. 1, pp. 21 – 26.
13. Alfes, C., (1992), "Modulus of Elasticity and Drying Shrinkage of High Strength Concrete Containing Silica Fume", Proceedings, Fourth International Conference on Fly Ash, Silica Fume, Slag and Natural Pozzolans in Concrete, ACI SP-132, Vol.-II Istanbul, Turkey, May, pp. 1651 – 1671.
14. Amudhavalli, M.K., and Mathew, J., (2012), "Effect of Silica Fume on Strength and Durability Parameters of Concrete", International Journal of Engineering Sciences and Emerging Technologies, August, Vol. 3, Issue 1, pp. 28 – 35.
15. Arediwala, M.A.F., and Jamnu, M.A., (2012), "Relation between Workability and Compressive Strength of Self – Compacting Concrete", International Journal of Advanced Engineering Research and Studies, Vol. 1, Issue-III, April – June, 09 – 11.
16. Arunachalam, K., and Gopalkrishnan, R., (2004), "Experimental Investigation on High Performance Fly Ash Concrete in Normal and Aggressive Environment", 29th Conference on our World in Concrete and Structures, 25 – 26, August, Singapore.
17. Assas, M.M., (2012), "Assessment of the Transport Properties and Strength of Concretes having Different Mix Proportions, Silica Fume and Fly Ash Additions", Jordan Journal of Civil Engineering, Vol. 6, No. 3.
18. Atan, M.M., and Awang, H., (2011) ,"The Compressive and Flexural Strengths of Self – Compacting Concrete Using Raw Rice Husk Ash", Journal of Engineering Science and Technology, Vol. 6, No. 6, 720 – 732.
19. Bagui, S.K., (2012), "Pavement Design of Rural Low Volume Roads using Cement and Lime Treated Base", Jordan Journal of Civil Engineering, Vol. 6, No. 3.
20. Bendapudi, S.C.K., and Saha, P., (2011), "Contribution of Fly Ash to the Properties of Mortar and Concrete", International Journal of Earth Sciences and Engineering, Vol. 4, No. 6 SPL, October, pp. 1017 – 1023.

21. Bhavikatti, S.S., (2010), “Finite Element Analysis”, Book, New Age Internatioal Publisher, Second Edition.
22. Bhikshma, V., Nitturkar, K., and Venkatesham, Y., (2009), “Investigations on Mechanical Properties of High Strength Silica Fume Concrete”, Asian Journal of Civil Engineering (Building and Housing) Vol. 10, No. 3, Pages 335 – 346.
23. Bouzoubaa, M., Zhang, M.H., and Malhotra, V.M., (2011), “Mechanical Properties and Durability of Concrete made with High – Volume Fly Ash Blended Cements Using a Coarse Fly Ash”, Cement and Concrete Research, Vol. 31, No. 3, Oct., pp. 1393 – 1402.
24. Breitenbucher, D.R., (1998), “Developments and Applications of High – Performance Concrete, Materials and Structures / Materials in Constructions”, Vol. 31, April, pp. 209-215.
25. Breitenbucher, I.R., (1998), “Developments and Applications of High – Performance Concrete”, Materials and Structures, Vol. 31, April, pp. 209 – 215.
26. Buenfeld, N.R., and Newman, J.B., (1984), “The Permeability of Concrete in Marine Environment”, Magazine of Concrete Research, Vol. 36, pp. 67.
27. Burmister, D.M., (1943), “Theory of Stresses and Displacements in Layered System and Application to Design of Airport Runways”, Proc. H.R.B, Vol. 23, p. 126-48.
28. Burmister, D.M., (1945), “The General Theory of Stresses and Displacements in Layered Soil System”, I, II, III, Journal of Applied Physics, Vol. 16, No. 2-5.
29. Burmister, D.M., (1958), “Evaluation of Pavement System of WASHO Road Test by Layered System Methods”, H.R.B. Bulletin No. 177, p.p. 26.
30. Carlton, Paul F., Ruth, M.B., Liebenberg, A.C., and Penner, F., (1962), “Discussion on Paper Load Carrying Capacity of Concrete Pavements” Journal of the Soil Mechanics and Foundation Division, ASCE, SM. 6.
31. Chapter-17, (GSY 2010), “High – Performance Concrete Design and Control of Concrete Mixtures”,.

32. Chauhan, M.P.S., Parida, M., Jain, S.S., and Vasan, R.M., (2004), "Quality Control of Concrete Roads in Urban Areas", Seminar on Design, Construction and Maintenance of Cement Concrete Pavements, 8 – 10, October, New Delhi.

33. Choubane, B., and Tia, M., (1992), "Non-Linear Temperature Gradient Effect on Maximum Warping Stresses in Rigid Pavements", Transportation Research Record 1370, Transportation Research Board, Washington D.C., 11-19.

34. Choubane, B., and Tia, M., (1995), "Analysis and Verification of Thermal Gradient Effect on Concrete Pavement", Journal of Transportation Engineering, ASCE, Jan / Feb., 75-81.

35. Dai, Xue - zhen, Xing, Lei, (2011), "Application Analysis of High – Performance Concrete on Heavy Traffic", International Conference on Electric Technology and Civil Engineering (ICETCE), 22 – 24, April, Lushan.

36. Dey, A., Basudhar, P.K., and Chandra, S., (2011), "Distribution of Subgrade Modulus beneath Beams on Reinforced Elastic Foundation", Indian Geotechnical Journal 4 (2).

37. Dhir, R.K., (2013), "Viewing High Performance Cement and Concrete Research through a Wide Angle Lens", Proceedings of the International UKIERI Concrete Congress, NIIT Jalandhar, India, 5-8, March.

38. Dhir, R.K., McCarthy, M.J., and Bai, J., (2012), "Harnessing Fly Ash Potential for Developing High Strength and High Durability Concrete", Indian Concrete Journal, February, Vol. 86, No. 2, 17-25.

39. Elsayed, A.A., (2011), "Influence of silica Fume, Fly Ash, Super Pozz and High Slag Cement on Water Permeability and Strength of Concrete", Jordan Journal of Civil Engineering, Vol. 5, Nov.

40. Final Report, (2007), "FAA Finite Element Design Procedure for Rigid Pavements", August, U.S. Department of Transportation, Federal Aviation Admiistration.

41. Folagbade, and Olufemi, S., (2012), "Effect of Fly Ash and Silica Fume on the Sorptivity of Concrete", International Journal Engineering Science and Technology (IJEST), Vol. 4, No. 99 September, ISSN: 0975 – 5462.

42. Fwa, T.F., and Sinha, K.C., (1991), "Pavement Performance and Life – Cycle Cost Analysis", Journal of Transportation Engineering, 117 (1), pp. 33-46.

43. Fwa, T.F., Tan, K.H., and Li, S., (2000), "Closed – Form and Semi-Closed Form Algorithms for Back – Calculation of Concrete Pavement Parameters", ASTM Special Technical Publication No. 1375, pp. 267-280.

44. Fwa, T.F., Tan, S.A., and Guwe, Y.K., (2001), "Expedient Permeability Measurement for Porous Pavement Surface", International Journal of Pavement Engineering, 2(4), pp. 259-270.

45. George, K.P., Alsherri, A., and Shah, N.S., (1988), "Reliability Analysis of Premium Pavement Design Features", ASCE, Journal of Transportation Engineering, Vol. 114, No. 3, May / June, pp. 278 – 293.

46. George, K.P., and Hussain, S., (1986), "Thickness Design for Flexible Pavement: A Probabilistic Approach", Transportation Research Record, N1095, Transportation Research Board, National Research Council, Washington, D.C., pp. 26-36.

47. Ghorpade, V.G., (2010), "An Experimental Investigation on Glass Fibre Reinforced High Performance Concrete with Silica Fume as Admixture", 35th Conference on Our World in Concrete and Structures, 25 – 27 August, Singapore.

48. Ghosh, R.K., and Dinkaran, M.K., (1970), "Breaking Load for Rigid Pavement", Jr. of Transportation Engg. Proc., ASCE, pp. 87-106.

49. Gjrov, O.E., (1983), "Durability of Concrete Containing Condensed Silica Fume", Proceedings, First International Conference on the Use of Fly Ash, Silica Fume, Slag and other Mineral by products in Concrete, SP-79, Vol. 2, Montebello, ACI, July, pp. 695-708.

50. Goel, S., Singh, S.P., and Singh, P., (2012), "Fatigue Analysis of Plain and Fibre Reinforced Self Consolidating Concrete", ACI Materials Journals, Vol. 109, No. 5, pp. 573 – 582.

51. Goel, S., Singh, S.P., and Singh, P., (2014), "Flexural Fatigue Analysis of Self Compacting Concrete Beams", Construction Materials, Proceedings of Institution of Civil Engineers.

52. Goyal, D.C., (1987), "Some Solutions with Infinite Element", M.E. Thesis, University of Roorkee, Roorkee.
53. Gurusamy, K., (1995), "High Strength Concrete for High – Rise Structures", The Way Forward, CONTECH 95, MENTOR Construction Technology Conference, Oct., Kuala Lumpur, Malaysia.
54. Hall, D.L., (1938), "Thin Plates on Elastic Foundations", Proceedings of International Conference of Applied Mechanics, Cambridge, M.A.
55. Hall, T. Kathleen, (GSY 2009), "State of the Art and Practice in Rigid Pavement Design", TRB.
56. Hogg, A.H.A., (1938), "Equilibrium of Thin Plate Symmetrically Loaded, Resting on an Elastic Sub-grade of Infinite Depth", Philosophical Mag., Sec. 7, Vol. 25.
57. Hooton, R.D., Bentz, E., and Kojundic, T., (2010), "Long-Term Chloride Penetration Resistance of Silica Fume concretes Based on Field Exposure", 2nd International Symposium, Oct. 4 – 6, Service Life Design Infrastructure for Delft, Netherland.
58. IRC: 15 – 1981, "Standard Specifications and Code of Practice for Construction of Concrete Roads" New Delhi.
59. IRC: 37- 2001, "Tentative Guidelines for the Design of Flexible Pavements", New Delhi.
60. IRC: 37-2012, "Tentative Guidelines for the Design of Flexible Pavements", New Delhi.
61. IRC: 44-1972, "Tentative Guidelines for Cement Concrete Mix Design" for Road Pavements, IRC, New Delhi.
62. IRC: 58 – 2002, "Guidelines for the Design of Plain Jointed Rigid Pavements for Highways", Second Revision, New Delhi.
63. IRC: 58-2011, "Guidelines for the Design of Plain Jointed Rigid Pavements for Highways", Third Revision, New Delhi.
64. IRC: 9-1972, "Traffic Census on Non-Urban Roads", New Delhi.
65. IRC: SP: 84 - 2009, "Manual for specifications and Standards for Four Laning of Highways through Public Private Partnership" New Delhi.

66. IRC-59, “Tentative Guidelines for Design of Gap Graded Cement Concrete Mixes for Road Pavements”, New Delhi.
67. IS : 3812 : 1981, “Specification for Fly Ash for use as Pozzolana and Admixture”.
68. IS : 8112 : 1989, “Specification for 43 Grade Ordinary Portland Cement”.
69. IS : 9103 : 1999, “Concrete Admixture – Specificatioln”.
70. IS : 9214 : 1979, “Method for Determination of Modulus of Sub-grade Reaction (K-Value) of Soils in the Field”.
71. IS: 10262 – 1982, “Recommended Guidelines for Concrete Mix Design”, IS, New Delhi.
72. IS: 1199 – 1959, “Methods of Sampling and Analysis of Concrete”, Indian Standard Institute, New Delhi.
73. IS: 2720 : Part 8: 1983, “Methods of Test for Soils”.
74. IS: 2720, (Part 16) (1987, Reaffirmed 2007), “Methods of Test for Soils: Laboratory Determination of CBR”, IS, New Delhi.
75. IS: 383 : 1970, “Specification for Coarse and Fine Aggregates from Natural Sources for Concrete”.
76. IS: 456-2000, “Indian Standard Code of Practice for Plain and Reinforced Concrete”, IS, New Delhi.
77. IS: 516-1959, “Methods for Tests for Strength of Concrete”, IS, New Delhi.
78. IS: SP: 23, “Handbook on Concrete Mixes”, IS, New Delhi.
79. Ismeik, M., (2009), “Effect of Mineral Admixtures on Mechanical Properties of High Strength Concrete Made with Locally Available Materials”, Jordan Journal of Civil Engineering, Vol. 3, No. 1.
80. Jalal, M., Pouladkhan, A.R., Norouzi, H., and Choubdar, G., (2012), “Chloride Penetration, Water Absorption and Electrical Resistivity of High Performance Concrete Containing Nano Silica and Silica Fume”, Journal of American Science, 8 (4).
81. Janbaz, M., and Janbaz, S., (2011), “Foundation Size Effect for Modulus of Subgrade Reaction on Sandy Soil” 6th National Congress on Civil Engineering, April 26 – 27, Semnan University, Semnan, Iran.

82. Joseph, O., and Vipulanandan, C., (2010), "Correlation between California Bearing Ratio (CBR) and Soil Parameter", Proceedings, CIGMAT, Conference and Exhibition.

83. Kachroo, P. N., (1971), "Stresses and Deflections in Layered Pavement System", Ph.D. Thesis, University of Roorkee, Roorkee.

84. Kadiyali, L.R., (2004), "Concrete Roads in India: Quo Vadis", Seminar on Design, Construction and Maintenance of Cement Concrete Pavements, 8 – 10 October, New Delhi.

85. Kadiyali, L.R., (2004), "Pavement Option", Seminar on Design, Construction and Maintenance of Cement Concrete Pavements, October 8 – 10, New Delhi.

86. Kadiyali, L.R., and Prasad, Bageshwar, (2004), "Are India's Concrete Roads over – Designed?", Seminar on Design, Construction and Maintenance of Cement Concrete Pavements, October 8 – 10, New Delhi.

87. Kathuda, H., Hanayneh, B., and Shatarat, N., (2010), "Effect of Micro Silica and Water Proofer on Resistance of Concrete to Phosphoric Acid", Jordan Journal of Civil Engineering, Vol. 4, No. 4.

88. Keshaw, L., and Mangaiar K., V., (2012), "Effect of Fly Ash on an Expansive Soil for Flexible Pavement Design", International Journal of Engineering and Innovative Technology (IJEIT), Vol. 2, Issue 3, September.

89. Kelly, E.F., (1939), "Application of Results of Research to the Structural Design of Concrete Pavements", Proc. Journal of ACI, Vol. 35, pp. 437 – 464.

90. Khadiranaikar, R.B., Lecture, (GSY 2010), "High Performance Concrete", BEC, Bagalkot.

91. Khan, M.I., (2010), "Chloride Ingress Resistant Concrete: High Performance Concrete Containing Supplementary Composite", International Journal of Civil and Environmental Engg., IJCEE-IJENS ,Vol. 10, No.4.

92. Khanna, S.K., and Justo, C.E.G., (2001), "Highway Engineering", Nem Chand and Brothers, Roorkee (U.A.)

93. Langan, B.W., Weng, K., and Ward, M.A., (2002), "Effect of Silica Fume and Fly Ash on Hydration of Portland Cement", Cement and Concrete Research 32, 1045 – 1051.

94. Laogan, B.T., and Elnashai, A.S., (1999), "Structural Performance and Economics of Tall High Strength RC Buildings in Seismic Regions", Structural Design Tall Building 8, 171 – 20.

95. Magudeawaran, and P., Eswaramoorthi, (2013), "Experimental Study on Durability Characteristics of High Performance Concrete", International Journal of Emerging Technology and Advanced Engineering, Vol. 3, Issue-1, January.

96. Maiti, S.C., Agrawal, R.K., and Kumar, R., (2006), "Concrete Mix Proportioning", Point of View, Indian Concrete Journal, December.

97. Mallick, R. B., Radzicki, M., Nanagiri Y. V., and Veeraragavan, A., (2013), "The Impact of Road Construction on Depletion of Natural Aggregates and Consequence of Delay in Recycling Pavements – Key Factors in Sustainable road Construction", Indian Highway, December, Vol. 41, ISSN 0376 – 7256.

98. Markstad, S.A., (1977), "An Investigation of Concrete in Regard to Permeability Problems and Factors influencing the Results of Permeability Tests", Report STF 65, A77027, FCB/SINTEF, The Norwayian Institute of Technology, Trondheim, Norway, June.

99. Marriaga, J.L., and Yepez, L.G.L., (2012), "Effect of Silica fume addition on the chloride – Related Transport Properties of High – Performance Concrete", Dyna, Year 79, No. 171, pp. 105 – 110, Medellin, February, ISSN 0012 – 7353.

100. Marthong, C., and Agrawal, T.P., (2012), "Effect of Fly Ash Additive on Concrete Properties", International Journal of Engineering Research and Applications, Vol. 2, Issue-4, July – August, pp. 1986 – 1991.

101. Mayerhof, G.G., (1962), "Load Carrying Capacity of Concrete Pavement", Journal of Soil Mechanics and Foundation Division, ASCE, SM3, Vol. 88.

102. McCarthy, M.J., Dhir, R.K., Newlands, M.D., and Singh, S.P., (2011), "Combining Durability and Sustainability in Material Selection for Concrete",

Proceedings of International UKIERI Concrete Congress – Concrete for High Performance Sustainable Infrastructure, March 8-10, I.I.T. New Delhi, pp. 277-291.

103. Mehta, P.K., (2004), "High – Performance, High – Volume Fly Ash Concrete for Sustainable Development", International Workshop on Sustainable Development and Concrete Technology, May 20 – 21, Beijing, China.

104. Mehta, P.K., (1997), "Durability: Critical Issues for the Future", Concrete International 19(7), pp. 69-76.

105. Mehta, P.K., and Aitcin, P.C., (1990), "Principles Underlying the Production of High-Performance Concrete", Cement Concrete and Aggregate Journal 12(2), pp. 70-78.

106. Mehta, P.K., and Barrow, R.W., (2001), "Building Durable Structures in the 21st Century", Concrete International 23(3), pp. 57-63.

107. Memon, F.A., Nuruddin, M.F., and Shafiq, N., (2013), "Effect of Silica Fume on Fresh and Hardened Properties of Fly Ash- Based Self - Compacting Geopolymer Concrete", International Journal of Minerals, Metallurgy and Materials, Vol. 20, No. 2, pp. 205, February.

108. Miller, B., (1991), "Microsilica Modified Concrete for Bridge Deck Overlays", First Year Interim Report, Material and Research Section, Highway Division, Oregon Department of Transportation, Salem, OR, iv, 27, pp. (OR-90-03/INTERIM-2).

109. Ministry of Road Transport and Highways, (1996) "Specification of Maximum Gross Vehicle Weight and the Maximum Safe Axle Weight", Notification S.O. 728 (E) dated 18th October, Government of India.

110. Moayed, R.Z., and Janbaz, M.,(2008), "Foundation Size Effect on Modulus of Subgrade Reaction in Clayey Soil", EJGE, Vol. 13, Bund E.

111. Moayed, R.Z., and Nacini, A., (2006), "Evaluation of Modulus of Subgrade Reaction (Ks) in Gravelly Soils Based on SPT Results", IA EG, Number 505.

112. Moreno, J., (1998), "High – Performance Concrete Economics Considerations", Concrete International, Vol. 20, No. 3, Mar.

113. Naik, T.R., Singh, S.S., and Hossain, M.M., (1995), "Abrasion Resistance of High- Strength Concrete Made with Class C Fly Ash", Centre for By-Products Utilization, University of Wisconsin – Milwaukee, Department of Civil Engineering and Mechanics, 3200 North Carmer Street, Milwaukee, WI 53211.

114. Nanda, P.K., Tiwari, Devesh, Jain, Sunil, and Sharma, B.M., (2006), "Optimization of Road Materials for Construction", International Seminar on Innovation in Construction and Maintenance of Flexible Pavements, IRC, PP 1-57-66, 2-4 September.

115. Nazeer, M., Narasimhan, M.C., and Rajeava, S.V., (2009), "Investigations on Chloride Diffusion of Silica Fume High Performance Concrete", International Journal of Earth Sciences and Engineering , ISSN 0974 – 5904, Vol. 02, No. 05, October, pp. 441 – 449.

116. Neville, A.M., (1975), "Properties of Concrete", Pitmen Publishing Ltd., London.

117. Nugroho, S.A., Hendri, A., and Ningsih, R., (2012), "Correlation between Index Properties and California Bearing Ratio Test of Pekanbaru Soils with and without Soaked", Canadian Journal on Environmental, Construction and Civil Engineering, Vol. 3, No. 1, January.

118. Osci, D.Y., and Jackson, E.N., (2012), "Compressive Strength and Workability of Concrete Using Natural Pozzolana as partial Replacement of Ordinary Portland Cement", Advances in Applied Science Research, 3(6): 3658 – 3662, Pelagia Research Library.

119. Ozyildirim, C., (1994), "A Field Investigation of Concrete Patches Containing Pyrament Blended Cement", Virginia Transportation Research Council, Charlottesville, VA, Jun, 16 pp. (FHA/VA-94-R26).

120. Pane, I., Will Hansen, and Mohamed, A.R., (1998), "Three Dimensional Finite Element Study on Effects of Non-Linear Temperature Gradients in Concrete Pavements", Transportation Research Record, Vol. 1629, pp. 58-66.

121. Panjehpour, M. Ali, A.A.A., and Demirboga, R., (2011), "A Review for Characterization of Silica Fume and its Effect on Concrete Properties",

International Journal of Sustainable Construction Engineering and Technology, ISSN: 2180 – 3242, Vol. 2, Issue-2, and December.

122. Parhizkar, T., Ghasemi, A.M.R., Pourkhorshidi, A.R., and Ramezanianpour, A.A., (2010), "Influence of Fly Ash and Dense Packing Method to Increase Durability of HPC Subjected to Acid Corrosion", Second International Conference on Sustainable Construction Materials and Technologies, June 28-June 30, UniversitaPolitenciaDelle Marche, Ancona, Italy.

123. Perumal, K., and Sundararajan, R., (2004), "Effect of Partial Replacement of Cement with Silica Fume on the Strength and Durability Characteristics of High – Performance Concrete", 29th Conference on Our World in Concrete and Structures, 25 – 26, August, Singapore.

124. Phung, V.D., (1985), "A Study of Load – Carrying Capacity of Rigid Pavements for Highways and Airfields", M.E. Thesis, University of Roorkee, Roorkee.

125. Pickett, G., Raville, M.E. Jones, W.C. McCormick F.J., (1951), "Deflections, Moments and Reactive Pressures for Concrete Pavements", Kansas State College Bulletin No. 65, Manhattan Kansas, Oct. 15.

126. Ping, W.V., and Sheng, B., (2013), "Evaluation of Resilient Modulus and Modulus of Subgrade Reaction for Florida Pavement Subgrade", The 26th International Chinese Transportation Professionals Association Conference, May 24-26, Tampa, FL.

127. Piyatrapoomi, N., Kumar, A., Robertson, N., and Welligamage, J., (2004), "Risk Assessment in Life Cycle Costing for Road Asset Management", Proceedings of the 1st CRC Construction Innovation Conference, Gold Coast, 24-27 October, Australia.

128. Portland Cement Association (PCA), (1984), "Thickness Design of Concrete Highways and Street Pavements".

129. Prasad, B., (2007) "Life Cycle Cost analysis of Cement Concrete Roads vs. Bituminous Roads", Indian Highway, Vol. 35, No. 9, Sept., pp. 19 – 25.

130. Pudhir, N.K.S., Grover, Shailendra, and Veeraragavan, A., (2010), "Cold Mix Design of Semi Dense Bituminous Concrete", Indian Highways, Vol. 38, ISSN 0376 – 7256.

131. Rajgopal, A.S., and George, K.P., (1990), "Pavement Maintenance Effectiveness", Transportation Research Record, 1276: 62 – 68.

132. Ram kumar, V.R., Murali, G., and Jayaganesh, K., (2012), "Flexural Behaviour of Concrete by Using Silica Fume as Partial Replacement of Cement", International Journal of Engineering Trends in Engineering and Development, Issue 2, May, Vol. 4, (DP).

133. Ramana, Jee, M., (2004), "Why Concrete Roads", Seminar on Design, Construction and Maintenance of Cement Concrete Pavements, October 8 – 10, New Delhi.

134. Rashid, M.A. and Mansur, M.A., (2009), "Considerations in Producing High Strength Concrete", Journal of Civil Engineer (JEB), 37 (1), pp. 53-63.

135. Rathnakara, K., Reddy, and Veeraragavan, A., (2004), "Life Cycle Cost Analysis of Flexible and Rigid Pavements Using (HDM-4)", Seminar on Design, Construction and Maintenance of Cement Concrete Pavements, October 8 – 10, New Delhi.

136. Reddy, K.S., and Pandey, B.B., (1992), "Lateral Placement of Commercial Vehicle on National Highways", HRB Bulletin No. 47, Indian Road Congress, New Delhi.

137. Reddy, M.V.S., Reddy, I.V.R., and Murthy, N.K., (2013), "Predicting the Strength Properties of High Performance Concrete Using Mineral and Chemical Admixtures", ARPN Journal of Science and Technology, Vol. 3, No. 1, Jan.

138. Reddy, M.V.S., Reddy, I.V.R., Reddy, K.M.M., Nataraja, M.C., and Murthy, K.N., (2012), "Durability Aspects of High Performance Concrete Containing Supplementary Cementing Material", International Journal of Structural and Civil Engineering Research, Vol. 1, No. 1, November.

139. Roy, T.K., Chattopadhyay, B.C., and Roy, S.K., (2010), "California Bearing Ratio and Estimation: A Case Study on Comparisons", Geotechnical Conference, December 16 – 18, India.

140. Russell, H.G., (1999), "ACI Defines High – Performance Concrete", ACI Concrete International, pp. 56-7, February.

141. Russell, H.G., (1999), "Why Use High – Performance Concrete", Concrete Products, Technical Talk, March.

142. Sabir, B.B., (1995), "High-Strength Condensed Silica Fume Concrete", Magazine of Concrete Research, 47, 172, 219-226.

143. Sabir, B.B., (1997), "Mechanical Properties and frost Resistance of Silica Fume Concrete", Cement Composites 19, 285-294 © 1997 Elsevier Science Ltd.

144. Scott, R., and Singh, S.P., (2011), "High Performance Silica Fume Concrete and Some Applications in India", Proceedings of the International UKIERI Concrete Congress – New Developments in Concrete Construction, March 8-10, IIT Delhi, pp. 217-238.

145. Seehra, S.S., Gupta, S., and Kumar, S., (1993), "Rapid Setting Magnesium Phosphate Cement for Quick Repair of Concrete Pavements Characterization and Durability Aspects", Cement and Concrete Research, Mar, Vol. 23, No. 2, pp. 254 – 286.

146. Shah, S.P., and Weiss, W.J., (2000), "High Performance Concrete Strength, Permeability, and Shrinkage Cracking", Proceedings of the PCI / FHWA International Symposium on High Performance Concretes, Orlands, Florida , pp. 331-340.

147. Shetty, M.S., (2008), "Concrete Technology Theory and Practices".

148. Shrivastava, Yash, and Bajaj, Ketem, (2012), "Performance of Fly Ash and High Volume Fly Ash Concrete in Pavement Design", IACSIT Coimbatore Conferences.

149. Singh, D., Reddy, K.S., and Yadu, L., (2011), "Moisture and Compaction Based Statistical Model for Estimating CBR of Fine Grained Subgrade Soil",

International Journal of Earth Sciences and Engineering, ISSN 0874-5904, Vol. 04, No. 06 SPL, October, pp. 100-103.

150. Singh, S.P., and Kaushik, S.K., (2001), "Flexural Fatigue Analysis of Steel Fibre Reinforced Concrete", ACI Materials Journal, American Concrete Institute, Vol. 98, No. 4.

151. Singh, Amrit, (1976), "Stresses and Deformation in a Layered System by Finite Element Method", M.E. Thesis, University of Roorkee, Roorkee.

152. Sinha, D.A., (2012), "Comparative Mechanical Properties of Different Ternary Blended Concrete", ISSN – 2250-1991, Vol. 1, Issue – 10, October.

153. Solanki, R.V., Mishra, C.B., Umrigar, F.S., and Sinha, D.P., (GSY 2010), "Use of Steel Fibre in Concrete Pavement: A Review", National Conference on Recent Trends in Engineering and Technology.

154. Sprinkel, M.M., (1993), "Polymer Concrete Bridge Overlays," Transportation Research Record, No. 1392, pp. 107-116.

155. Srinivas, T., Suresh, K., and Pandey, B.B., (2006), "Wheel Load and Temperature Stresses in Concrete Pavement", HRB Bulletin, Indian Road Congress.

156. Srivastava, Sanjay, Jain, S.S., and Chauhan, M.P.S., (2013), "Laboratory Investigations of High Performance Concrete for Highway Pavements", Innovations in Concrete Construction, Proceedings of the International UKIERI concrete Congress, March 5-8, NIIT, Jalandhar, India.

157. Sunkurwar, R.R., and Patil, S.P., (2011), "Flexural Strength Behaviour of High Strength Prestressed Concrete Beam by Using Silica Fume", International Journal of Science and Engineering, Vol. 4, No. 06 SPL, October, pp. 1047 – 1050.

158. Suresh, K.K.S., Kamala Kara, G.K., and Amarnath, M.S., (2012), "Fatigue Analysis of High Performance Cement Concrete for Pavements using the Probabilistic Approach", International Journal of Emerging Technology and Advanced Engineering, Vol. 2, Issue-II, November.

159. Suryawanshi, C.S., (2007), "Structural Significance of High Performance Concrete", The Indian Concrete Journal, March, pp. 13-16.

160. Tayabji, S., (2005), “Framework for the Design and Construction of Long – Life Concrete Pavements”, Proceedings of the Eight International Conference on Concrete Pavements, pp. 208-220.

161. Teller, C.H., and Sutherland, E.C., (1935), “The Structural Design of Concrete Pavements”, Public Roads, Vol. 17, No. 7.

162. Teller, L.W., and Sutherland, E.C. (1943), “The Structural Design of Concrete Pavements”, Public Roads, Vol. 23, No. 8.

163. Third Edition, (1970), “Road Note 29”, Department of the Environment Road Research Laboratory, HMSO.

164. Thomas, M.O.A, (2010), “Optimizing Fly Ash Content for Sustainability, Durability, and Constructability”, Second International Conference on Sustainable Construction Materials and Technologies, June 28 – 30, UniversitaPolitenciaDelle Marche, Ancona, Italy.

165. Thomlinson, J., (1940), “Temperature Variations and Consequent Stresses Produced by Daily and Seasonal Temperature Cycles in Concrete Slabs”, Concrete Constructional Engineering, London, U.K., 36(6), 298 – 307; 36(7), 352-360.

166. Tiwari, Devesh, Mishra, A.K., and Nanda, P.K. ,(2006), “HDM-4 Tool for Prioritizing Logical Life Cycle Maintenance / Improvement Practices for Roads”, Civil Engineering and Construction Review Journal, March,

167. Tiwari, Devesh, Nanda, P.K., and Kunal, Binod, (2006), “Non-Destructive Tests on Pavements”, Proceeding of International Seminar on Hands on Demo with Exhibition, Indian Chapter of American Conference Institute, pp. 83-94, January 27-28.

168. Tomar, S.,and Mallick, T.K.,(2011), A Thesis on, “A Study on Variation of Test Conditions on CBR Determination”, Department of Civil Engineering, National Institute of Technology, Rourkela.

169. Turk, K., Karatas, M., and Gonen, T., (2013), “Effect of Fly Ash and silica Fume on Compressive Strength, Sorptivity and Carbonation of SCC”, KSCE Journal of Civil Engineering, 17 (1): 202 – 209.

170. Turk, K., Tugat, P., Karatas, M., and Benli, A., (2010), "Mechanical Properties of Self Compacting Concrete with Silica Fume / Fly Ash", 9th International Congress on Advances in Civil Engineering, 27-30, September, Karadeniz Technical University, Trabzon, Turkey.

171. Turkel, S., and Altunas, Y., (2009), "The Effect of Lime-Stone Powder, Fly Ash and Silica Fume on the Properties of Self -Compacting Repair Mortars", Sadhana Vol. 34, Part-2, April, pp. 331-343.

172. Uddin, W., and Jaafar, Z.F.M., (2013), "Achieving Sustainability without Compromising Long-Term Pavement Performance for Road Infrastructure Assets", IJP-International Journal of Pavements, Vol. 12, Special Volume top Ranked 2013 IJPC Papers.

173. Uddin, W., Haas, R., and Hudson, W.R., (2013), "Pavement Design or Pavement Management? Good Design is not Enough", IJP – International Journal of Pavements, Vol. 12, Special Volume of Top Ranked 2013 IJPC Papers.

174. Uddin, W., Hackett, R.M., Joseph, A., Pan, Z., and Crawley, A.B., (1995), "Three dimensional Finite – Element Analysis of Jointed Concrete Pavement having Discontinuities", Transportation Research Record 1482, Journal of Transportation Research Board, Washington, D.C., pp. 26-32.

175. Uddin, W., Zhang, D., and Fernandez, F., (1994), "Finite Element Simulation of Pavement Discontinuities and Dynamic Load Response", Transportation Research Record 1448, Journal of Transportation Research Board, Washington, D.C., pp. 100-106.

176. Vasan, R.M., (1989), "Investigations of Steel Fibre Reinforced Concrete Pavements", Ph.D. Thesis, University of Roorkee, Roorkee.

177. Vasan, R.M., Chandra, S., and Chauhan, M.P.S., (1999),"Structural Behaviour of High Strength SFRC Pavements", Vol. 73, No. 11, Nov., The Indian Concrete Journal.

178. Vasan, R.M., Kaushik, S.K., Godbole, P.N., and Khanna, S.K., (1986), "Structural Behaviour of Steel Fibre Reinforced Concrete Pavements", Proc.

Third International Symposium on Developments in Fibre Reinforcement Cement and Concrete, University of Sheffield, Sheffield, England.

179. Vinayagam, P., (2012), "Experimental Investigation on High Performance Concrete Using Silica Fume and Super plasticizer", International Journal of Computer and Communication Engineering, Vol. 1, No. 2, July.

180. Vuong, B.T., and Kumar, A., (2000), "Improved Performance Based Material Specifications for Granular Pavement Materials", Proceedings 10th REAAA Conference, Tokyo, Japan, 4 to 7 September.

181. Vuong, B.T., and Kumar, A., (2002), "Development of Performance Based Material Specifications and Construction Standards for Unbound Granular Base Materials", Proceedings 4th International Conference on Road and Airfield Pavement Technology, Kunming P.R., China, Peoples Communications Publishing House, ISBN 7114 042019, pp. 801-817, 23-25 April.

182. Westergaard, H.M., (1925), "Computation of Stresses in Concrete Roads", Proc. H.R.B. Vol. 15.

183. Westergaard, H.M., (1926), "Stresses in Concrete Pavements computed by Theoretical Analysis", Public Roads, Vol. 7, No. 2 April.

184. www.rms.nsw.gov.au/heavyvehicles/down loads.

185. www.saaq.gou.qc.ca/en/heavy/definition.s

186. Yaqub, M., and Bukhari, I., (2006), "Effect of Size of Coarse Aggregate on Compressive Strength of High Strength Concrete", 31st Conference on Our World in Concrete & Structures, 16-17, August, Singapore.

187. Yaqub, M., and Bukhari, Imran, (2006), "Development of Mix Design for High Strength Concrete", 31st Conference on Our World in Concrete and Structure, August 16-17, Singapore.

188. Yazici, S., and Arel, H.S., (2012), "Effect of Fly Ash Fineness on the Mechanical Properties of Concrete" Sadhana, Vol. 37, Part-3, June, pp. 389 – 403, Indian Academy of Sciences.

189. Yijin, L., Shigiong, S. Jian, Y., and Yingli, G., (2004), "The Effect of Fly Ash on the Fluidity of Cement Paste, Mortar and Concrete", International

Workshop on Sustainable Development and Concrete Technology, Beijing, May 20 – 21.

190. Zhang, P., and Li, Q. F., (2012), "Combined Effect of Polypropylene Fibre and Silica Fume on Workability and Carbonation Resistance of Concrete Composite Containing Fly Ash", Proceedings of the Institution of Mechanical Engineers, Part L; Journal of Materials: Design and Applications, August 24.

191. Zhang, P., and Li, Q., (2013), "Fracture Properties of Polypropylene Fibre Reinforced Concrete Containing Fly Ash and Silica Fume", Research Journal of Applied Sciences, Engineering and Technology, 5 (2): 665 – 670.

192. Zhang, P., and Li, Q.F., (2013), "Freezing-Thawing Durability of Fly Ash Concrete Composites Containing silica Fume and Polypropylene Fibre", Proceedings of the Institution of Mechanical Engineers, Part L; Journal of Materials : Design and Applications, March 22,.

193. Zhang, P., and Li, S.E., (2012), "Effect of Silica Fume on Durability of Concrete Composites Containing Fly Ash", Science and Engineering of Composite Materials, Volume 20, Issue-1, pp. 57 – 65, November.

194. Zhang, P., Li, Q., and Zhang, H., (2012), "Fracture Properties of High-Performance Concrete Containing Fly-Ash", Proceedings of the Institution of Mechanical Engineer's, Part L: Journal of Material Design and Applications, January.

LIST OF PUBLICATIONS

Paper Published so Far

1. Srivastava, S., Jain, S.S., and Chauhan, M.P.S., "Laboratory Investigation of High-Performance High-Strength Concrete for Highway Pavements", Presented in International Conference, Innovations in Concrete Construction, Proceedings of the International UKIERI Concrete Congress, 5-8 March, 2013, NIIT, Jalandhar, India.

2. Srivastava, S., Jain, S.S., and Chauhan, M.P.S., "High-Strength Concrete of M60 Grade for Highway Pavements for Heavy Vehicles", International Journal of Scientific and Research Publications, vol. 4, Issue 11, Nov. 2014, ISSN 2250-3153.

3. Srivastava, S., Jain, S.S., and Chauhan, M.P.S., "Structural Behavior of High Strength High Performance Concrete Pavement under Heavy Loads", International Journal of Engineering Research and Technology, vol.3, Issue 10, Oct. 2014, ISSN-2278-0181.

Paper Sent for Publication

4. Srivastava, S., Jain, S.S., Chauhan, M.P.S., and Mandal, B., "Analysis and Design of Rigid Pavement for Heavy Vehicles by Finite Element Method", paper has been sent for publication in IRC.
5. Srivastava, S., Jain, S.S., and Chauhan, M.P.S., "High-Performance Concrete for Highway Pavements", Paper sent for publication.